# Chapter 1

# Sound Wave Propagation

## 1.1 INTRODUCTION

This book covers the propagation of acoustic waves in solids and liquids. We want to know what kinds of waves can propagate in various types of materials, how they are reflected from and transmitted through the boundaries between two materials, how they are excited, and how their properties are related to the mass, density, and elasticity of the materials involved.

We shall be particularly concerned with the properties of piezoelectric transducers, which are the most efficient, and hence most widely used ultrasonic transducers for converting electrical into mechanical energy. Therefore, we will have to derive formulas for their conversion efficiency and electrical impedance as a function of frequency, and for their pulse response characteristics. To do this, we need to know how waves propagate in piezoelectric and nonpiezoelectric materials. We start with the simpler case of nonpiezoelectric materials and then extend the analysis to piezoelectric materials.

In general, the treatment of acoustic wave propagation in solids is complicated by the fact that solids are not always isotropic. Thus the parameters of the acoustic wave must be expressed in terms of tensor quantities and the relations between them.

For simplicity, we shall assume that the waves of interest are either pure longitudinal or pure shear waves, and that all physical quantities (particle displacement, particle velocity, stress, strain, elasticity, and the piezoelectric coupling constant) can be expressed in one-dimensional form. In addition, we restrict our analysis in this chapter to plane wave propagation, which reduces the problem

from three dimensions to one. The results we obtain are identical in form to a general, more complete treatment for isotropic materials, and are valid even for propagation of waves along an axis of a crystalline material, provided that the elastic constants and coupling coefficients are defined correctly. The required formalism will be described briefly in Sec. 1.1.1; Sec. 1.5 has a more detailed treatment and Appendix A contains more rigorous derivations of some of the essential formulas. Later, in Sec. 2.2, we generalize the theory to account for propagation in an arbitrary direction in isotropic media; in Sec. 2.3 we deal with waves in materials of finite cross section.

### 1.1.1 Sound Waves in Nonpiezoelectric Materials: One-Dimensional Theory

We must first define the two basic types of waves that are important in acoustic wave propagation. The first is a *longitudinal wave*, in which the motion of a particle in the acoustic medium is only in the direction of propagation. Thus when a force is applied to the acoustic medium, the medium expands or contracts in the $z$ direction, as shown in Fig. 1.1.1(a). The second type of wave is a *shear wave*, in which the motion of a particle in the medium is transverse to the direction of propagation, as illustrated in Fig. 1.1.1(b). Shear waves are associated with the flexing or bending of a material (e.g., twisting a rod). There is no change in volume or density of the material in a shear wave mode, as shown in Fig. 1.1.1(b).

In general, the acoustic waves that can propagate through a solid medium may combine shear and longitudinal motion. However, in a crystalline medium

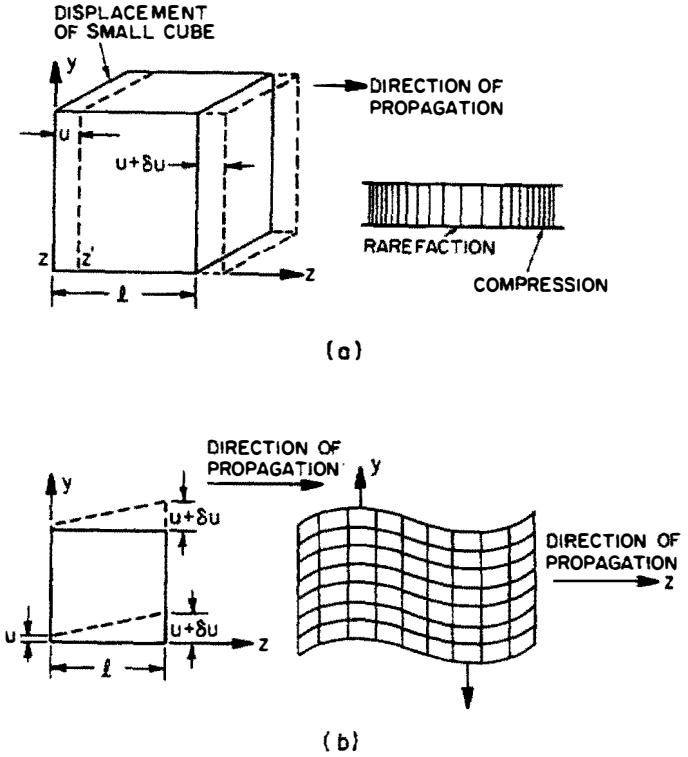


**Figure 1.1.1** (a) Longitudinal wave propagation; (b) shear wave propagation (full cube not shown).

with anisotropic elastic properties, the direction of propagation can be chosen to be along one of the principal axes of the crystal; in this case the basic modes can be purely longitudinal or purely shear waves. In acoustic transducers, microwave delay lines, amplifiers, and most other acoustic devices, propagation is usually chosen to be along one of the principal axes of the material.

We shall define the basic wave equation for acoustic propagation in the longitudinal case. The results obtained are identical in form to those for shear wave propagation. A more complicated treatment is needed only when considering propagation at an angle to one of the principal axes of the crystal. Therefore, we will carry out the initial derivations in a one-dimensional form. The reader is referred to Sec. 1.5, Chapter 2, and Appendix A for more general derivations of these relations with a tensor formalism [1].

**Stress.** The force per unit area applied to a solid is called the *stress*. In the one-dimensional case, we shall denote it by the symbol $T$. A force, applied to a solid, stretches or compresses it. We first consider a slab of material of infinitesimal length $l$, as shown in Fig. 1.1.2. Figure 1.1.2(a) illustrates the application of a longitudinal stress, and Fig. 1.1.2(b) illustrates the application of shear stress. The stress $T(z)$ is defined as the force per unit area on particles to the left of the plane $z$. We note that the longitudinal stress is defined as positive if the external stress applied to the right-hand side of the slab is in the $+z$ direction, while the external stress applied to the left-hand side of the slab is $-T$ in the $-z$ direction. If the stress is taken to be positive in the $+x$ or $+y$ directions, these

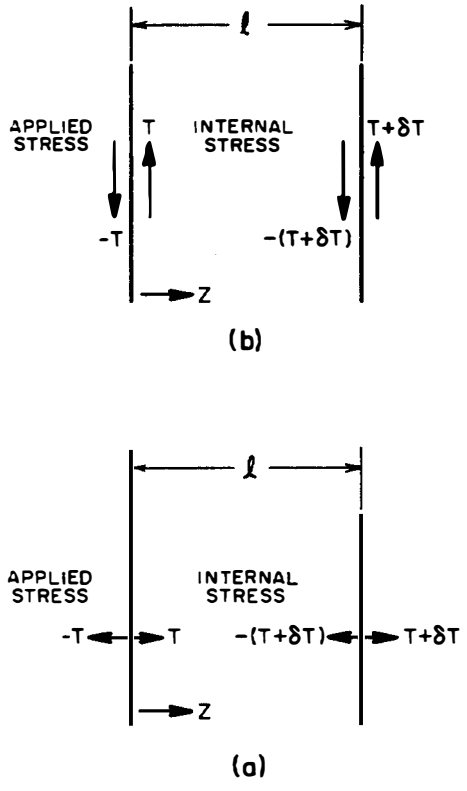


**Figure 1.1.2** (a) Stress in the longitudinal direction for a slab of length $l$; (b) stress in the shear direction.

definitions also apply to shear stress. The net difference between the external stresses applied to each side of the slab is $l(\partial T/\partial z)$. Thus the net force applied to move a unit volume of the material relative to its center of mass is $\partial T/\partial z$.

**Displacement and strain.** Suppose that in the one-dimensional case, the plane $z$ in the material is displaced in the $z$ direction by longitudinal stress to a plane $z' = z + u$, as shown in Fig. 1.1.1(a). The parameter $u$ is called the *displacement* of the material and in general is a function of $z$. At some other point in the material $z + l$, the displacement $u$ changes to $u + \delta u$. If the displacement $u$ is a constant throughout the entire material, the material has simply undergone a bulk translation. Such gross movements are of no interest to us here. We are interested in the variation of particle displacement as a function of $z$.

We can use a Taylor expansion to show that, to first order, the change in $u$ in a length $l$ is $\delta u$, where

$$\delta u = \frac{\partial u}{\partial z} l = Sl \tag{1.1.1}$$

The fractional extension of the material is defined as

$$S = \frac{\partial u}{\partial z} \tag{1.1.2}$$

The parameter $S$ is called the *strain*.

We may also consider the one-dimensional case of shear motion where the material is displaced in the $y$ direction by a wave propagating in the $z$ direction. Then, as shown in Fig. 1.1.1(b), a particle in the position $\mathbf{a}_z z$ is displaced to a point $\mathbf{a}_z z + \mathbf{a}_y u$, where $\mathbf{a}_y$ and $\mathbf{a}_z$ are unit vectors in the $y$ and $z$ directions, respectively. The same treatment used for longitudinal motion holds for the shear wave case. We define a shear strain as $S = \delta u/l = \delta u/\delta z$. Here the only difference is that the displacement $u$ is in the $y$ direction. The diagram shows that there is no change in the area of the rectangle as shear motion distorts it. Longitudinal motion, however, changes the cube volume by $\delta u A$, where $A$ is the area of the $x$, $y$ face. Thus the relative change in volume is $\delta u/l = S$. The reader is referred to Appendix A for a more general definition of strain.

**Hooke's law and elasticity.** Hooke's law states that for small stresses applied to a one-dimensional system, the stress is proportional to the strain, or

$$T = cS \tag{1.1.3}$$

where $c$ is the elastic constant of the material. The parameters $T$ and $c$ would be tensors in the general system, but can be represented by one component for one-dimensional longitudinal or shear wave propagation. Because it is easier to bend a solid than to stretch it, the shear elastic constant is normally smaller than the longitudinal elastic constant.

**Equation of motion.** Consider now the equation of motion of a point in the material when a small time-variable stress is applied to it. From Newton's

second law, the net translational force per unit area applied to the material is $l\,\partial T/\partial z$, so the equation of motion must be

$$\frac{\partial T}{\partial z} = \rho_{m0}\ddot{u} = \rho_{m0}\dot{v} \tag{1.1.4}$$

Here $v$ is defined as the particle velocity of the material and $\rho_{m0}$ is its mass density in the stationary state.

**Conservation of mass.** The particle velocity of the material is $v = \dot{u}$, so that in a small length $l$ in the one-dimensional case, the change in velocity is

$$\delta v = \frac{\partial v}{\partial z} l \tag{1.1.5}$$

However, from Eq. (1.1.1),

$$\delta v = \frac{\partial}{\partial t}\delta u = l\frac{\partial S}{\partial t} \tag{1.1.6}$$

We can therefore combine Eqs. (1.1.5) and (1.1.6) to show that

$$\frac{\partial S}{\partial t} = \frac{\partial v}{\partial z} \tag{1.1.7}$$

Equation (1.1.7) is essentially another way of writing the equation of conservation of mass of the material for longitudinal waves. The same equation holds for shear waves; however, as there is no change of density with shear motion, the equation of conservation of mass is not implied. Suppose that we write $\rho_m = \rho_{m0} + \rho_{m1}$, where $\rho_{m0}$ is the unperturbed density and $\rho_{m1}$ is the perturbation in the density. We can write the one-dimensional equation of conservation of mass for longitudinal waves in the form

$$\frac{\partial}{\partial z}\rho_m v + \frac{\partial \rho_m}{\partial t} = 0 \tag{1.1.8}$$

Assuming that $v$ and $\rho_{m1}$ are first-order perturbations, and keeping only first-order terms, it follows that

$$\rho_{m0}\frac{\partial v}{\partial z} + \frac{\partial \rho_{m1}}{\partial t} = 0 \tag{1.1.9}$$

where $\rho_m = \rho_{m0} + \rho_{m1} = \rho_{m0}/(1 + S) \approx \rho_{m0}(1 - S)$. Thus

$$\frac{\partial v}{\partial z} = -\frac{\partial}{\partial t}\left(\frac{\rho_{m1}}{\rho_{m0}}\right) = \frac{\partial S}{\partial t} \tag{1.1.10}$$

**The wave equation and definition of propagation constant.** We may now use Eqs. (1.1.3), (1.1.4), and (1.1.7), and put $v = \partial u/\partial t$, to obtain the small signal wave equation for sound wave propagation in the material:

$$\frac{\partial^2 T}{\partial z^2} = \rho_{m0}\frac{\partial^2 S}{\partial t^2} = \frac{\rho_{m0}}{c}\frac{\partial^2 T}{\partial t^2} \tag{1.1.11}$$

The solutions of this wave equation for the stress are of the form $F(t \pm z/V_a)$. For a wave of radian frequency $\omega$, with all field quantities varying as exp $(j\omega t)$, the solutions are of the form exp $[j(\omega t \pm \beta_a z)]$, where the negative sign in the exponential corresponds to a forward wave, the positive sign corresponds to a backward wave, and

$$\beta_a = \omega\left(\frac{\rho_{m0}}{c}\right)^{1/2} = \frac{\omega}{V_a} \tag{1.1.12}$$

and $V_a = (c/\rho_{m0})^{1/2}$ is the acoustic wave velocity. The parameter $\beta_a$ is called the *propagation constant* of the acoustic wave.

For propagation in the forward direction, it follows that

$$v = -V_a S = -\frac{V_a}{c} T \tag{1.1.13}$$

The magnitude of the strain $S$ is also the ratio of the particle velocity of the medium to the sound wave velocity of the medium.

Tables of the relevant parameters for longitudinal and shear wave propagation for various types of commonly used materials are given in Appendix B. A liquid such as water, for example, is relatively easy to compress and has a small mass density (1000 kg/m$^3$). Its elastic constant is $2.25 \times 10^9$ N/m$^2$, so the acoustic wave velocity in water is 1.5 km/s. Sapphire has a larger mass density than water (3990 kg/m$^3$), but it is a rigid material with a relatively large longitudinal elastic coefficient ($4.92 \times 10^{11}$ N/m$^2$). Therefore, it has a high longitudinal wave velocity along the $z$ axis of 11.1 km/s. Most metals have longitudinal wave velocities on the order of 5 km/s, with shear wave velocities approximately half this value. There are exceptions, such as beryllium, which is extremely light (1870 kg/m$^3$) and rigid and therefore has a longitudinal wave velocity of 12.9 km/s. Lead, which is very heavy (11,400 kg/m$^3$), has a low longitudinal wave velocity of 1.96 km/s. However, the acoustic wave velocity in a gas is small because it is relatively easy to compress. Thus the acoustic wave velocity in air is 330 m/s. As liquids and gases cannot support shear stresses, shear waves cannot propagate through them.

**Energy.** The total stored energy per unit volume in the medium is the sum of two components: (1) the elastic energy per unit volume due to the force applied to displace the material, $W_c = \frac{1}{2}TS$; and (2) the kinetic energy per unit volume due to the motion of the medium, $W_v = \frac{1}{2}\rho_{m0}v^2$. For a propagating plane wave whose components vary as exp $(j\omega t)$, following the analogy for electromagnetic (EM) waves, the average elastic energy per unit volume is

$$W_c = \tfrac{1}{4}\text{Re}\,(TS^*) = \tfrac{1}{4}\text{Re}\,(cSS^*) \tag{1.1.14}$$

and the average kinetic energy per unit volume is†

$$W_v = \tfrac{1}{4}\text{Re}\,(\rho_{m0} v v^*) \tag{1.1.15}$$

†Suppose that we put $A = A_0 \exp(j\omega t)$ and $B = B_0 \exp[j(\omega t + \phi)]$. Then Re $A \times$ Re $B$ is the average over one radio-frequency (RF) cycle of $\langle A_0 B_0 \cos\omega t \cos(\omega t + \phi)\rangle = \frac{1}{2}(A_0 B_0 \cos\phi)$. This quantity is just $\frac{1}{2}$Re $(AB^*)$.

It follows from Eqs. (1.1.12)–(1.1.15) that $W_c = W_v$ and that the total energy per unit volume in an acoustic wave is

$$W_a = \tfrac{1}{4}\mathrm{Re}\,(\rho_{m0} v v^* + TS^*) = \tfrac{1}{2}\mathrm{Re}\,(TS^*) \tag{1.1.16}$$

Similarly, the power flow per unit area in the acoustic wave may be defined as the product of the force per unit area $-T$ applied by the material on the left-hand side of the plane $z$, and the material velocity (i.e., the average value of $-vT$ during the RF cycle). The complex power flow through an area $A$ may therefore be defined as

$$P_a = -\tfrac{1}{2}(v^* T)A \tag{1.1.17}$$

For a propagating wave in a lossless medium, $v$ and $T$ are in phase, so $P_a$ is real and

$$P_a = V_a W_a A = -\tfrac{1}{2}(v^* T)A \tag{1.1.18}$$

**Poynting's theorem.** The power and energy in an acoustic wave obey conservation laws similar to those of Poynting's theorem in EM theory [1, 2]. To prove the conservation laws, we write Eq. (1.1.4) in the form

$$\frac{\partial T}{\partial z} = j\omega\rho_{m0} v \tag{1.1.19}$$

and Eq. (1.1.10) in the form

$$\frac{\partial v}{\partial z} = j\omega S = \frac{j\omega T}{c} \tag{1.1.20}$$

By multiplying Eq. (1.1.19) by $v^*$ and the complex conjugate of Eq. (1.1.20) by $T$, and adding the results, it follows that

$$-2\frac{\partial}{\partial z}\mathrm{Re}\,(P_a) = A\frac{\partial}{\partial z}\mathrm{Re}\,(Tv^*) = (j\omega\rho_{m0} v v^* - j\omega TS^*)A \tag{1.1.21}$$

Writing $T = cS$, and assuming that $c$ is real, we find that

$$-2\frac{\partial}{\partial z}\mathrm{Re}\,(P_a) = (j\omega\rho_{m0} v v^* - j\omega cSS^*)A \tag{1.1.22}$$

As both terms on the right-hand side of Eq. (1.1.22) are imaginary, it follows that

$$\frac{\partial}{\partial z}\mathrm{Re}\,(P_a) = 0 \tag{1.1.23}$$

This relation is entirely analogous to Poynting's theorem in EM theory and shows that Re $(P_a)$ is constant (i.e., the power in the wave is conserved). For a propagating wave, since $P_a$ itself is real, the average stored kinetic energy per unit volume is equal to the average elastic energy, or

$$\rho_{m0} v v^* = cSS^* \tag{1.1.24}$$

**Acoustic losses.** When the system can dissipate energy so that it is not purely elastic, and $c$ is complex, there is a loss term just like that due to conduction current in EM theory. The viscous forces between neighboring particles with different velocities are a major cause of acoustic wave attenuation in solids and liquids. These are additional viscous stresses $T_\eta$ on the particles in a medium through which a plane wave is propagating of the form

$$T_\eta = \eta \frac{\partial v}{\partial z} = \eta \frac{\partial S}{\partial t} \tag{1.1.25}$$

where the coefficient of viscosity is called $\eta$. It follows from Eqs. (1.1.3) and (1.1.25) that the total stress is

$$T = cS + \eta \frac{\partial S}{\partial t} \tag{1.1.26}$$

The equation of motion has the same form as for a lossless medium:

$$\frac{\partial T}{\partial z} = \rho_{m0} \frac{\partial v}{\partial t} \tag{1.1.27}$$

Just as in EM theory, the attenuation due to loss can be calculated approximately by using Poynting's theorem. Following the derivation of Eqs. (1.1.22) and (1.1.23), and assuming that all field quantities vary as exp ($j\omega t$), Poynting's theorem in the complex form now has an additional term associated with viscosity:

$$\frac{\partial}{\partial z} \text{Re}\,(P_a) = -\tfrac{1}{2}\eta\omega^2 SS^* A \tag{1.1.28}$$

where $A$ is the area of the beam. Thus viscosity gives rise to a loss term that varies as the square of the frequency. If we regard this loss term as small, it follows from Eqs. (1.1.16) and (1.1.18) that

$$\tfrac{1}{2}cSS^* \approx W_a \approx \frac{P_a}{V_a A} \tag{1.1.29}$$

Hence, after substitution in Eq. (1.1.28), writing $P_a$ for Re ($P_a$), we see that

$$\frac{1}{P_a}\frac{\partial P_a}{\partial z} \approx \frac{-\eta\omega^2}{V_a c} = \frac{-\eta\omega^2}{V_a^3 \rho_{m0}} \tag{1.1.30}$$

The solution of this equation is $P_a = P_0 \exp(-2\alpha z)$, where $\alpha$ is the attenuation constant of the wave and $P_0$ is a constant. The attenuation constant is given by the relation

$$\alpha = \frac{\eta\omega^2}{2V_a^3 \rho_{m0}} \tag{1.1.31}$$

Thus the attenuation of the wave due to viscous losses varies as the square of the frequency and inversely as the cube of the velocity. As shear waves typically have velocities of the order of half those of longitudinal waves in the same material, we might expect the shear wave attenuation per unit length to be considerably larger

than the longitudinal wave attenuation per unit length, although this is not always so in practice. In water at room temperature, the attenuation is 0.22 dB/m at 1 MHz; thus low-frequency waves can propagate over long distances in water. At 1 GHz, however, the attenuation is estimated to be $2.2 \times 10^5$ dB/m, or 0.22 dB/ μm. Therefore, for such applications as the acoustic microscope, it is important to limit the propagation path of the waves in water to the order of tens of micrometers.

There are many other sources of loss in real materials. One is thermal conduction. When a material is compressed adiabatically, its temperature increases; its temperature decreases when the material expands. Since thermal conduction causes the process to be nonadiabatic and contributes to a loss of energy, it tends to give higher attenuations in metals than in insulators. The attenuation due to thermal conduction also varies as the square of the frequency. In addition, attenuation may exist because waves have been scattered by finite-size grains or by dislocations in a solid; another cause of attenuation is the unequal thermal conduction and expansion of neighboring grains due to their axes being rotated with respect to each other. For these reasons, high-quality single-crystal materials exhibit much lower sound attenuation at high frequencies than do the same materials in a polycrystalline form.

Loss mechanisms also result from sound-induced changes of state in a solid or a liquid such as water. Water molecules are thought to exhibit a partial crystalline structure. A sound wave loses energy when it disturbs this structure, which creates a further loss mechanism. Such mechanisms can be a powerful tool for measuring chemical changes, and the relaxation times associated with them, in solids and liquids. A further discussion of grain scattering losses is given in Sec. 3.6.

The acoustic attenuation in common materials varies over a very wide range. Thus a hard, high-quality, single-crystalline material such as sapphire can be used for acoustic delay lines at frequencies up to 10 GHz. The attenuation at this frequency may be as much as 40 dB/cm. However, the wavelength at this frequency is of the order of 1 μm. Thus the attenuation per wavelength is $4 \times 10^{-3}$ dB, a lower loss than is typical for EM waves in a waveguide. On the other hand, viscous materials such as rubber, exhibit relatively high losses at frequencies greater than a few kilohertz, and thus make good sound absorbers.

**Acoustic impedance.** In analogy to EM theory or transmission line theory, we can define an acoustic impedance $Z$, which we more formally call the *specific acoustic impedance.* We write

$$Z = -\frac{T}{v} \tag{1.1.32}$$

For a plane wave traveling in the forward direction, which we denote by subscript $F$, we define the *characteristic impedance* $Z_0$ as

$$Z_0 = -\frac{T_F}{v_F} = (\rho_{m0} c)^{1/2} = V_a \rho_{m0} \tag{1.1.33}$$

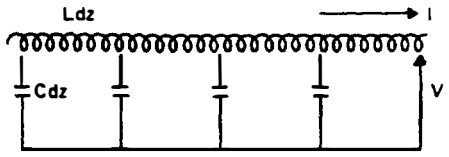


**Figure 1.1.3** Transmission line with a series inductance $L$ per unit length and shunt capacitance $C$ per unit length.

while the impedance $Z$ for a wave traveling in the backward direction, denoted by subscript $B$, (for which $\beta_a$ is negative) is defined as

$$Z = -\frac{T_B}{v_B} = -V_a \rho_{m0} = -Z_0 \tag{1.1.34}$$

Both the impedances defined here have the dimensions of

$$\frac{\text{pressure}}{\text{velocity}} = \frac{\text{N/m}^2}{\text{m/s}} = \frac{\text{N}}{\text{m}^3\text{/s}} = \frac{\text{kg}}{\text{m}^2\text{-s}}$$

With the use of Eq. (1.1.32), Eqs. (1.1.19) and (1.1.20) take the standard form of the transmission line equations and may be be used in the same way.

To see this result, we compare Eqs. (1.1.19) and (1.1.20) with the transmission-line equations for the voltage and current along a transmission line, which are

$$\frac{\partial V}{\partial z} = -j\omega LI \tag{1.1.35}$$

and

$$\frac{\partial I}{\partial z} = -j\omega CV \tag{1.1.36}$$

where $L$ is the series inductance per unit length and $C$ is the shunt capacitance per unit length, as illustrated in Fig. 1.1.3. A wave propagating along this line has a propagation constant $\beta = \omega\sqrt{LC}$ and an impedance $Z_0 = \sqrt{L/C}$.

Suppose that we replace $V$ by $-T$ and $I$ by $v$. Then Eqs. (1.1.19) and (1.1.20) are equivalent to Eqs. (1.1.35) and (1.1.36), respectively, provided that we replace $L$ with $\rho_{m0}$ and $C$ with $1/c$ and define a characteristic acoustic impedance as in Eq. (1.1.33). It follows that we can use these equations just as we did in EM theory [1, 2].

It is convenient to define the reflection coefficient of an acoustic wave in terms of the stress. This gives a relation exactly equivalent to the one used in electromagnetic theory. As we shall see, such relations are useful in defining equivalent circuits, because piezoelectric transducers convert electromagnetic energy to acoustic energy.

If we consider a wave reflected normally from the interface between two media of differing characteristic impedances $Z_{01}$ and $Z_{02}$, as shown in Fig. 1.1.4(a), then $T$ and $v$ will be continuous at the interface. We therefore write the stress $\hat{T}_1(z)$ and velocity $\hat{v}_1(z)$ of the left-hand side of the interface $z = 0$ as

$$\hat{T}_1 = T_{F1}e^{-j\beta_1 z} + T_{B1}e^{j\beta_1 z} \tag{1.1.37}$$

and

$$\hat{v}_1 = v_{F1}e^{-j\beta_1 z} + v_{B1}e^{j\beta_1 z} \tag{1.1.38}$$

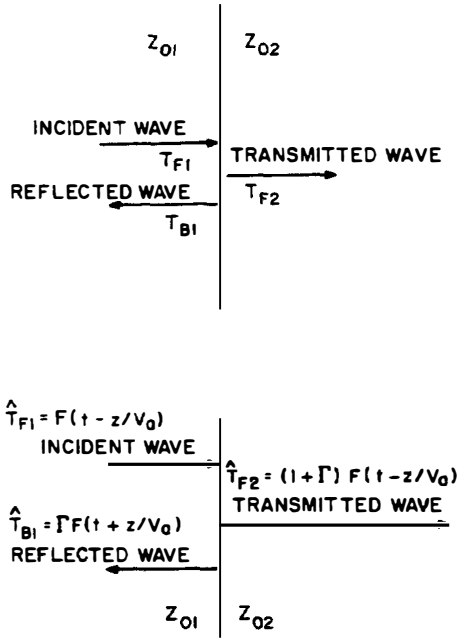


**Figure 1.1.4** (a) Reflection of a continuous wave at the interface between two boundaries; (b) reflection of a pulsed signal at the interface of the two boundaries. The symbol ˆ represents a quantity that varies with $z$.

where $T_{F1}$ and $T_{B1}$ are the amplitudes of the forward and backward waves on the left-hand side of $z = 0$, respectively, and the symbol ˆ denotes a quantity that varies with $z$. We may also define the reflection coefficient $\Gamma$ of the wave at the plane $z = 0$ as the ratio of the amplitude of the backward to the forward stress components, or as

$$\Gamma = \frac{T_{B1}}{T_{F1}} \tag{1.1.39}$$

Furthermore, using Eqs. (1.1.33) and (1.1.34) to write the velocities in terms of the stress, we can substitute into Eqs. (1.1.37) and (1.1.38) and write

$$\hat{T}_1 = T_{F1}(e^{-j\beta_1 z} + \Gamma e^{j\beta_1 z}) \tag{1.1.40}$$

and

$$\hat{v}_1 = -\frac{T_{F1}}{Z_{01}}(e^{-j\beta_1 z} - \Gamma e^{j\beta_1 z}) \tag{1.1.41}$$

respectively.

In the region to the right of the interface, there is only an excited wave propagating in the forward direction. Thus we can write

$$\hat{T}_2 = T_{F2} e^{-j\beta_2 z} \tag{1.1.42}$$

and

$$\hat{v}_2 = -\frac{T_{F2}}{Z_{02}} e^{-j\beta_2 z} \tag{1.1.43}$$

where $T_{F2}$ is the amplitude of the stress on the right-hand side of $z = 0$. The boundary condition at the plane $z = 0$ is that the stress $T$ and the velocity $v$ must

be continuous. This leads to the result

$$\Gamma = \frac{Z_{02} - Z_{01}}{Z_{02} + Z_{01}} \tag{1.1.44}$$

The stress transmission coefficient $\mathcal{T}_T$ is defined as

$$\mathcal{T}_T = \frac{T_{F2}}{T_{F1}} = 1 + \Gamma = \frac{2Z_{02}}{Z_{02} + Z_{01}} \tag{1.1.45}$$

and the power transmission coefficient $\mathcal{T}_P$ is defined as

$$\mathcal{T}_P = \frac{P_{F2}}{P_{F1}} = \frac{T_{F2}^2/Z_{02}}{T_{F1}^2/Z_{01}} = 1 - |\Gamma|^2 \tag{1.1.46}$$

This parameter determines how efficiently power is transmitted from one medium to another. Thus it is normally desirable to keep the reflection coefficient $\Gamma$ as small as possible.

Note that the mismatches that can occur between different acoustic media are generally much more severe than they are in the electromagnetic case. For example, a rigid material such as sapphire has an impedance of $Z_0 = 44.3 \times 10^6$ kg/m$^2$-s for longitudinal waves, while a heavy material such as lead, with a large mass density $\rho_{m0}$, also tends to have a relatively high impedance. On the other hand, water has an impedance of $Z_0 = 1.5 \times 10^6$ kg/m$^2$-s, and air has an extremely low impedance, which for our present purposes can be considered to be zero.

It is obviously important to provide good matches between different media. Quarter-wave matching sections can be used to match a material of one impedance to another, just as they are with optical lenses or microwave transmission lines.

Let us consider the general case when a layer of impedance $Z_0$, propagation constant $\beta$, and thickness $l$ is placed in contact with a medium that presents a load impedance $Z_L$. If this medium were semi-infinite, $Z_L$ would in fact be the impedance $Z_L = Z_{02}$ of the medium. It follows from Eqs. (1.1.40) and (1.1.41) that if the load $Z_L$ is at $z = 0$, the value of the input impedance $Z_{\text{in}} = -T(-l)/v(-l)$ of the layer of length $l$ is given by the expression

$$Z_{\text{in}} = Z_0 \frac{e^{j\beta l} + \Gamma e^{-j\beta l}}{e^{j\beta l} - \Gamma e^{-j\beta l}} \tag{1.1.47}$$

where $\beta$ is the propagation constant in the layer. It follows from Eqs. (1.1.44) and (1.1.47) that

$$Z_{\text{in}} = Z_0 \frac{Z_L \cos \beta l + jZ_0 \sin \beta l}{Z_0 \cos \beta l + jZ_L \sin \beta l} \tag{1.1.48}$$

By using an intermediate layer, the input impedance can be changed to a different value. In particular, if the matching layer is $\lambda/4$ thick (i.e., $\beta l = \pi/2$), then

$$Z_{\text{in}} = \frac{Z_0^2}{Z_L} \tag{1.1.49}$$

Thus matching can be obtained between two media of widely different impedances by choosing an intermediate matching layer properly, although perfect matching occurs only at one frequency. Typically, the larger the ratio of impedances $Z_{in}/Z_L$ or $Z_L/Z_{in}$, the narrower the bandwidth of the impedance match.

Techniques also exist for matching with multiple quarter-wavelength layers to improve the bandwidth. The reader is referred to the considerable literature on this subject which has been developed to deal with the problem of matching transmission lines [2–5].

Another important case is the reflection of an acoustic pulse by an interface. We consider a stress pulse of value $\hat{T}_{F1}(t, z) = F(t - z/V_a)$ incident on the interface $z = 0$, as illustrated in Fig. 1.1.4(b). This will give rise to a reflected pulse of the same form, $\hat{T}_{B1}(t, z) = \Gamma F(t + z/V_a)$. Thus we can write the total stress $T_1$ in medium 1 as

$$\hat{T}_1 = F\left(t - \frac{z}{V_a}\right) + \Gamma F\left(t + \frac{z}{V_a}\right) \tag{1.1.50}$$

with a corresponding velocity $v_1$ of value

$$\hat{v}_1 = -\frac{1}{Z_{01}}\left[F\left(t - \frac{z}{V_a}\right) - \Gamma F\left(t + \frac{z}{V_a}\right)\right] \tag{1.1.51}$$

By following exactly the same procedure as before, we arrive at the same value of the reflection coefficient given by Eq. (1.1.44).

Suppose that the incident stress is in the form of a square pulse, as illustrated in Fig. 1.1.5. If $Z_{01} > Z_{02}$, as illustrated in Fig. 1.1.5(a), the reflection coefficient is negative, so the reflected stress pulse has the opposite sign from that of the incident pulse. In particular, at an air interface with $Z_{02} = 0$, the total stress at the interface $z = 0$ will be zero, and $\Gamma = -1$. At all events, the total stress at the interface will be less than the incident stress if $Z_{01} > Z_{02}$. On the other hand, it follows from Eq. (1.1.34) that because the velocity associated with the return echo is of the same sign as the velocity of the stress, the total velocity at the interface $z = 0$ is increased and doubled at an air interface. In this case, the reflected velocity pulse then has the same sign as the incident velocity pulse. On the other hand, if $Z_{01} < Z_{02}$, as illustated in Fig. 1.1.5(b), the reflected stress pulse has the same sign as the incident pulse but the velocity is reversed in sign. Furthermore, as might be expected, the stress at the interface is larger than that of the incident wave; in fact, if the second layer is perfectly rigid so that $Z_{02} = \infty$, then $\Gamma = 1$ and the stress is doubled in value at the time the pulse reaches the interface.

**Shear waves.** The analysis for shear wave propagation is exactly the same as that for longitudinal waves. Now the stress may be taken to have components in both the $y$ and $z$ directions, with propagation in the $z$ direction. As an example, an isotropic material may be displaced in the $y$ direction, and the displacement $u_y$ will be a function of $z$. The shear motion of particles in the material is thus like a rotation about the $x$ axis. Now the shear strain $t$ is defined by the one-dimensional

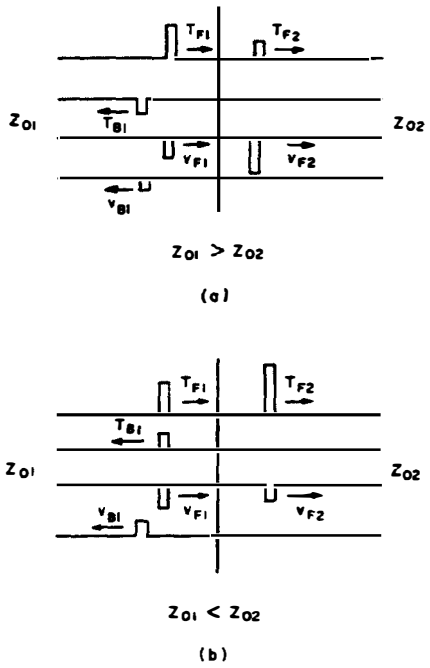


**Figure 1.1.5** Acoustic pulse incident on the interface between two media: (a) $Z_{01} > Z_{02}$; (b) $Z_{01} < Z_{02}$.

parameter $S = \partial u_y/dz$. The derivation of the wave equation for shear wave propagation follows as before, the only difference being that the appropriate elastic coefficient relating shear stress and strain must be used. This leads to sound wave velocities and wave impedances, which are typically smaller than for longitudinal waves in the same material, as discussed in Sec. 2.2. With these restrictions, the energy conservation theorem and expression for attenuation may be derived for shear waves and will have the same forms as the ones for longitudinal waves [1].

**Extensional waves.** Another type of wave of great practical importance, which can be treated by the simple one-dimensional theories given here, is the *extensional wave* in a thin rod. In this mode, illustrated in Fig. 1.1.6, it is assumed that the cross-sectional dimensions of the rod, or in the case of a cylindrical rod, its diameter, are much smaller than the wavelength of the wave of interest. In this case, the only stress component present is a longitudinal one in the direction of propagation along the rod. There can be no stress components within the rod perpendicular to its axis, because the normal stress must be zero at its surface. When a wave propagates along the rod, there is particle motion both along the rod and perpendicular to it, for the rod is free to expand its cross-sectional area when it is compressed in the $z$ direction, and vice versa. However, the component of strain $S = \partial u_z/\partial z$ associated with the motion in the $z$ direction is directly related by Hooke's law [Eq. (1.1.3)] to the stress $T$ in the $z$ direction, but with a different effective coefficient of elasticity. The relevant coefficient of elasticity is called *Young's modulus*, which we denote by the symbol $E$, thus writing $T = ES$. Young's modulus is the coefficient of elasticity normally measured when a long wire or rod is stretched by a static force. In all cases Young's modulus is smaller than the longitudinal coefficient of elasticity, because a larger force is required to stretch a

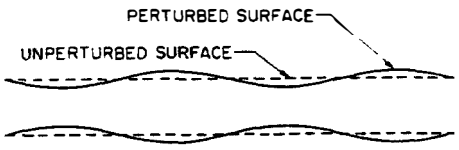


**Figure 1.1.6** Extensional wave in a rod or strip.

slab of material with the same strain $S$ when the slab is not free to expand or contract in the transverse direction.

The general case is far more complicated, for the stress and strain must be tensors of rank 2 and may contain both shear and longitudinal components. In general, the solution of acoustic problems tends to be more complicated than for the equivalent electromagnetic problems, because the stress and strain terms are tensors rather than vectors. The formalism required to deal with the general case of propagation of an acoustic wave in an arbitrary direction in an anisotropic material is given in Appendix A. The techniques developed there are applied to propagation of waves in finite isotropic media in Chapter 2. Fortunately, in isotropic materials, it is always possible to resolve any waves present into plane shear wave and longitudinal wave components. In a finite isotropic medium, however, both types of fields are required to satisfy the boundary conditions.

## PROBLEM SET 1.1

1. **(a)** The correct formula for attenuation due to viscosity in water was derived by Lord Rayleigh, who showed that the result in Eqs. (1.1.26) and (1.1.28) should have $\eta$ replaced by $\frac{4}{3}\eta_s$, where $\eta_s$ is the shear viscosity of water. Assuming that $\eta_s = 0.01$ poise (dyn-s/cm$^2$) for water at room temperature, calculate the attenuation at 1 MHz, and compare your result with the measured value of 0.0022 dB/cm at room temperature. Your results for power attenuation will be lower than the measured result because not all contributions to loss have been taken into account.

   **(b)** Suppose that we want to construct an acoustic microscope working at 1 GHz to examine a biological specimen suspended in water. Find the wavelength of sound in water ($V_a = 1.5$ km/s) at 1 GHz. From the experimental value of loss at 1 MHz, estimate the maximum path length that could be used at 1 GHz if the attenuation had to be less than 80 dB.

2. A longitudinal wave is excited in a sapphire rod that is immersed in water. Use the data of the tables in Appendix B. Assuming that the water is lossless, find the reflection coefficient at the sapphire–water interface. What proportion of the power is reflected and transmitted at the sapphire–water interface? Despite the mismatch, this combination of materials is convenient to use in an acoustic microscope. Suppose that you wanted to improve the efficiency by using a quarter-wavelength matching section of impedance $Z = (Z_{01}Z_{02})^{1/2}$, where $Z_{01}$ is the impedance of the sapphire and $Z_{02}$ is that of water. What would the impedance of this matching material have to be? As you will see from the tables in Appendix B, very few, if any, materials with this impedance exist. Can you suggest a compromise solution or solutions using two layers, one of the layers having a higher impedance than sapphire, that might at least improve the transmission efficiency? Basically, the lowest-impedance common material that can be deposited in the form of a thin film is glass, with an impedance of the order of $12 \times 10^6$

kg/m²-s. What are the advantages and disadvantages of such a two-layer solution compared to using a single matching layer of impedance $(Z_{01} Z_{02})^{1/2}$?

3. **(a)** We want to design an acoustic transducer that can emit a pulsed signal with as great a transmission efficiency as possible into water. Because the signal required is a short pulse, matching over a broad frequency band is desirable. Thus a single quarter-wavelength matching layer might not be the best choice. Another possible choice is to use a long buffer rod between the transducer and the water. Suppose that the transducer were made of PZT with an impedance of $34 \times 10^6$ kg/m²-s. Then the signal emitted from the transducer into the rod would suffer a certain transmission loss, and there would be further transmission loss from the rod to the water. What would be the best choice of impedance for optimum transmission efficiency from the transducer to the water? Ignore multiple echoes.

   **(b)** Consider a second situation where a matching layer a quarter-wavelength long at the center frequency is employed. In this case, assume that a short tone burst $A(t)$ sin $\omega t$, two RF cycles long, is employed [$A(t) = 0$ when $\omega t < 0$, $A(t) = 0$ when $\omega t > 4\pi$, and $A(t) = 1$ when $0 < \omega t < 4\pi$]. The return echoes from the two interfaces tend to cancel out if the RF frequency is chosen correctly. Sketch the form of the return echo for a sinusoidal pulse two RF cycles long, chosen with its frequency to be at the center frequency of the quarter-wavelength matching layer. Choose the impedance of the matching layer to be $Z_0 = (Z_{01} Z_{02})^{1/2}$, where $Z_{01}$ and $Z_{02}$ are the impedances of the transducer material and the load, which are both regarded as semi-infinite in extent.

4. **(a)** An acoustic transducer emits a power of 1 W/cm² into water at a frequency of 1 MHz. Determine the peak RF stress or pressure in the acoustic beam and the maximum displacement of the water. Consider what happens when the RF pressure is negative (i.e., during the negative half of the RF cycle). In this case, a vacancy or a bubble would form. Normally, this does not occur at low acoustic levels of power because of the finite pressure due to gravity and the atmosphere. Consider a laboratory water tank with a transducer located near its top surface, so that only atmospheric pressure need be considered. At what power density would this effect, known as *cavitation*, occur?

   *Note:* In comparison with experiments, your result will predict very low power for the onset of cavitation; neither will it vary with frequency, as it does in practice. This is because viscosity and surface tension have been neglected in this example.

   **(b)** Now consider sapphire, a solid material with an acoustic impedance of $44.3 \times 10^6$ kg/m²-s. Suppose that its breaking strain is $S = 5 \times 10^{-3}$. Estimate the power density required to fracture it. Your estimate in part (a) was really equivalent to the one for a liquid.

   *Note:* This effect can cause damage by a high-power laser beam passing through a transparent solid, due to the excitation of acoustic waves (phonons) by the laser beam (the Raman effect).

5. Consider the effect of a thin bond on the transmission of an acoustic wave between two identical materials of impedance $Z_0$. Work out an approximate formula for the reflection coefficient through a bond material of impedance $Z_1$ and length $l$ such that $\beta l << 1$. Show that if $Z_1 << Z_0$, even though $\beta l << 1$, there can be a serious reflection due to the bond. As an example, consider two layers of PZT-5A with $Z_0 = 34 \times 10^6$ kg/m²-s, bonded with an epoxy layer of impedance $Z_1 = 3.24 \times 10^6$ kg/m²-s and $V_a = 2.67$ km/s that is 2 μm thick. At what frequency does the magnitude of the reflection coefficient become 0.5? What is the ratio of the bond length to the wavelength in the bond at this frequency?

6. Suppose that a uniform, static tensile stress of 300 MPa (1 MPa = $10^6$ N/m$^2$-s) were applied to an aluminum rod. What would be the strain? How much does the effective density of the material decrease? Assuming that there is no change in the elastic constant, estimate the relative change in acoustic wave velocity along the rod. Suppose that the rod were 5 cm long. What would be the relative change in phase? How much phase change would there be in a 10-MHz wave passing through the total expanded length of the rod? This idea forms the basis of an acoustic technique for measuring stress, although the relative change of the effective elastic constant may be two or three times larger than the relative change in density.

## 1.2 PIEZOELECTRIC MATERIALS

### 1.2.1 Constitutive Relations

A piezoelectric material has an asymmetric atomic lattice. When an electric field is applied to such a material, it changes its mechanical dimensions. Conversely, an electric field is generated in a piezoelectric material that is strained. All ferroelectric materials are piezoelectric. In the ferroelectric state, the center of positive charge of the crystal does not coincide with its center of negative charge, as illustrated in Fig. 1.2.1. In such a material two neighboring atoms that are not identical will not move the same distances in an applied electric field. Therefore, the dimensions of a ferroelectric material will change (i.e., the material will be strained when an electric field is applied to it).

Consider the periodic atomic system illustrated in Fig. 1.2.1, in which the equilibrium spacings between neighboring rows of atoms in the $z$ direction are $a_1$ and $a_2$, and the spacings between neighboring rows of atoms in the $x$ and $y$ directions

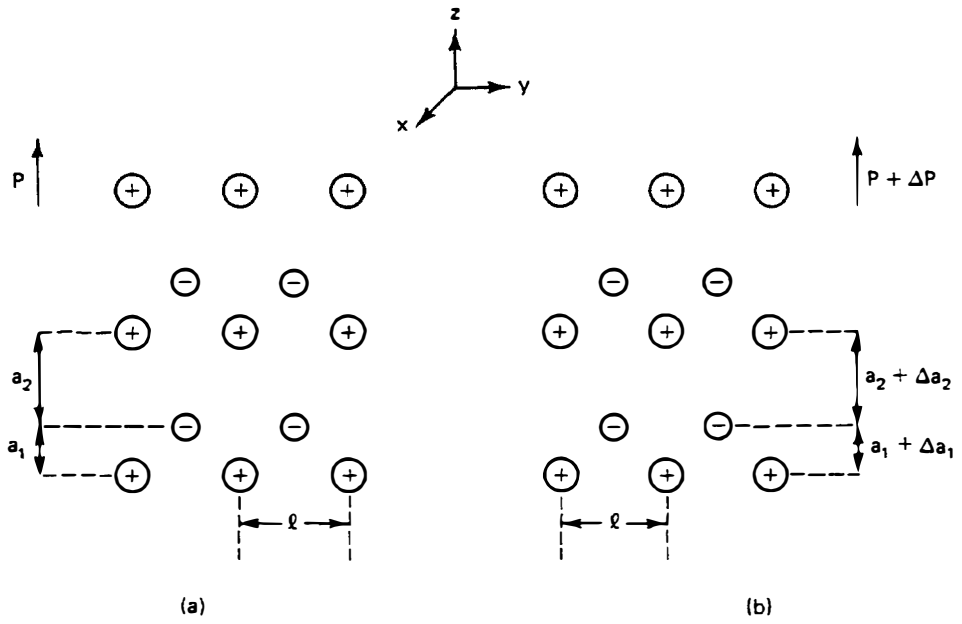


**Figure 1.2.1** Ferroelectric crystals: (a) unstrained; (b) strained.

is $l$. The dipole moment per unit volume of these atoms is

$$P = \frac{q(a_2 - a_1)}{l^2(a_2 + a_1)} = \frac{\text{dipole strength of unit cell}}{\text{volume of unit cell}} \tag{1.2.1}$$

where the charges on the atoms are $q$ and $-q$, respectively.

We now consider the effect of strain on the polarization of the material. When $a_1$ changes to $a_1 + \Delta a_1$ and $a_2$ changes to $a_2 + \Delta a_2$, the polarization changes by $\Delta P$, and we can write $\Delta a_1 = a_1 S$ and $\Delta a_2 = a_2 S$. It follows from Eq. (1.2.1) that to first order in strain,

$$\Delta P = PS = eS \tag{1.2.2}$$

where the parameter $e$ is called the piezoelectric stress constant, and $S$ is the macroscopic strain in the material.

The total change in electric displacement in the presence of an electric field is

$$D = \varepsilon E + \Delta P \tag{1.2.3}$$

We can also write

$$D = \varepsilon^S E + eS \tag{1.2.4}$$

where the dielectric constant is the permittivity with zero or constant strain and is thus denoted by $\varepsilon^S$. The electric displacement in a piezoelectric material depends on the strain as well as the electric field.

We shall now determine the stress in a piezoelectric medium due to an electric field $E$. The forces per unit area on the positive and negative atoms are $qE/l^2$ and $-qE/l^2$, respectively. The stresses in the regions of length $a_2$ and $a_1$ are therefore

$$T_2 = \frac{qE}{l^2} \tag{1.2.5}$$

and

$$T_1 = \frac{-qE}{l^2} \tag{1.2.6}$$

respectively. Therefore, the average stress in the medium due to the electric field is

$$T_E = \frac{a_1 T_1 + a_2 T_2}{a_1 + a_2} = eE \tag{1.2.7}$$

The total stress applied to the medium is the sum of the externally applied stress $T$ and the internal stress $T_E$ due to the electric field. The application of Hooke's law leads to the result

$$T + T_E = c^E S \tag{1.2.8}$$

or

$$T = c^E S - eE \tag{1.2.9}$$

where we have defined the elastic constant in the presence of a constant or zero $E$ field to be $c^E$. Equations (1.2.4) and (1.2.9) are known as the *piezoelectric constitutive relations*.

We can estimate the value of $e$ by taking $a_1 = 2$ Å, $a_2 = 4$ Å, and $l = 3$ Å, and taking $q$ to be the charge of a single electron; these assumptions yield a value of $e = 0.6$ C/m$^2$. Because the atoms can have multiple charges, this figure is considerably lower than the largest measured values of $e$ in strongly piezoelectric materials such as the lead zirconium titanate (PZT) ceramics ($e_{z3} = 23.3$ C/m$^2$ in PZT-5H) or lithium niobate crystals, but it is comparable to the values observed in many other piezoelectric materials.

**Poling and domains in ferroelectric materials.** Ferroelectric materials such as the PZT ceramics and lithium niobate, which are important piezoelectric materials, exhibit a dipole moment. Above a certain temperature, known as the *Curie point*, the dipole directions have random orientations. The dipoles may be aligned by applying a strong electric field at a temperature near the Curie point; this process is known as *poling*. As illustrated in Fig. 1.2.2, an unpoled ferroelectric material is normally divided into macroscopic regions, called *domains*, in which the dipoles are aligned. The alignment of the dipoles in these separate domains is, however, random with respect to those in the other domains. Ideally, after poling, all the domains are aligned with each other.

A crystal such as quartz can be piezoelectric without being ferroelectric. For example, a crystal with a threefold symmetry axis, as illustrated in Fig. 1.2.3, represents three dipoles aligned at 120° to each other. The sum of the dipole moments at each vertex is zero. When an electric field is applied in the $z$ direction, the three dipoles tend to expand or contract by different distances in the $z$ direction; thus the crystal can develop a net stress. Similarly, when the material is strained in the $z$ direction, it can develop a net dipole moment, so it is a piezoelectric

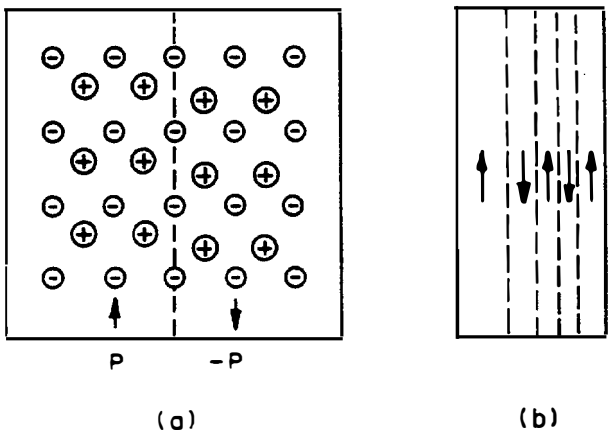


**Figure 1.2.2** Displacement of the atoms on either side of a domain boundary: (a) unpolarized medium with domains on either side of the boundary polarized in opposite directions; (b) domain structure showing neighboring domains polarized in opposite directions.

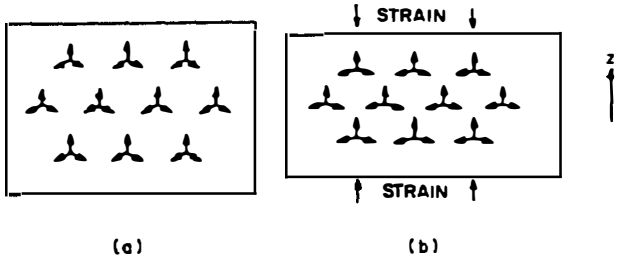


**Figure 1.2.3** Piezoelectric crystal that is not ferroelectric. (a) The unstressed crystal has a threefold symmetry axis. The three arrows represent a planar group of ions with a triple charge, a positive charge at each vertex, and single negative charges at the arrowheads. The sum of the three dipole moments is zero. (b) When the sample is stressed, so that the sum of the three dipole moments is finite, there is no longer threefold symmetry.

material. Such piezoelectric materials have much smaller piezoelectric stress constants than do ferroelectric materials.

The argument we have given here also applies in the presence of shear strain, which means that an electric field applied in the $x$ or $y$ directions would create shear stress. We shall see in Sec. 1.5 that it is possible to generalize the definitions of the elastic constants and piezoelectric coupling parameters to take both longitudinal and shear stress and strain components into account.

There are other possible ways in which an electric field can generate stress. In any dielectric, there is an electrostrictive stress applied to the material. In a liquid, its value is $\frac{1}{2}(\varepsilon - \varepsilon_0 + S\,\partial\varepsilon/\partial S)E^2$ [6]. For simplicity, we shall neglect the third term in this expression. When a dc field $E_0$ is applied to a dielectric, a first-order perturbing field $E_1$ yields $E^2 = (E_0 + E_1)^2 \approx E_0^2 + 2E_0E_1$. So a small first-order component of stress will be generated, of value $T_1 \approx (\varepsilon - \varepsilon_0)E_0E_1$. Taking fused quartz as an example, if we use fields comparable to the breakdown strength of quartz (i.e., $10^8$ V/m), by comparing the electrostrictive component of stress to Eq. (1.2.9), we find the effective value of $e$ to be $5 \times 10^{-3}$ C/m$^2$. In an unpoled ferroelectric material such as barium titanate, with a relative permittivity of 5000 and $E_0 = 10^6$ V/m, the effective value of $e$ can be quite large, of the order of 0.1 C/m. Thus in most materials, except those with a very high dielectric constant, electrostriction is a very weak effect in comparison to the piezoelectric effect. This is basically because the internal fields resulting from the asymmetry of the lattice are many orders of magnitude larger than the fields that can be applied externally. The same arguments applied to deduce the electrostrictive effect lead us to this conclusion.

Note that for one-dimensional shear or longitudinal wave propagation, the **E** field must be along the direction of propagation, at least to the limit of the assumption that $\mathbf{E} = -\nabla\phi$, because the only variation of potential is in this direction. Because of symmetry, this usually implies that **D**, if finite, is also in this direction.

### 1.2.2 Effect of Piezoelectric Coupling on Wave Propagation in a Medium of Infinite Extent

We can now consider wave propagation in a piezoelectric medium. If the medium is infinite in extent, the wave motion is one-dimensional, there is no free charge within the medium, and **D** is in the $z$ direction, then

$$\frac{\partial D_z}{\partial z} = 0 \tag{1.2.10}$$

This implies that $D_z$ = constant (i.e., $D$ does not vary with $z$), although it may vary with time. So the total displacement current density in the medium is

$$i_D = \frac{\partial D}{\partial t} \tag{1.2.11}$$

The current $i_D$ must either be uniform with $z$ or zero. In a piezoelectric transducer with metal electrodes on each surface, a displacement current passes between the electrodes, as it does in any capacitor. In a piezoelectric medium of infinite extent, however, we would expect the displacement current to be zero; hence $D = 0$ in the medium.

**Piezoelectrically stiffened elastic constant.** Let us now solve for the effective value of the elastic constant $c$ with $D = 0$, or $c^D$, and determine the propagation constant of a wave in the infinite piezoelectric medium. Writing $D = 0$ in Eq. (1.2.4) and substituting the result in Eq. (1.2.9), we find that

$$E = -\frac{eS}{\varepsilon^S} \tag{1.2.12}$$

and

$$T = c^E\left(1 + \frac{e^2}{c^E\varepsilon^S}\right)S = c^D S \tag{1.2.13}$$

Thus it is as if the piezoelectric medium has an effective elasticity

$$c^D = c^E(1 + K^2) \tag{1.2.14}$$

where we define the parameter $c^D$ as the *stiffened elastic constant*, and call the parameter $K$, defined by the relation

$$K^2 = \frac{e^2}{c^E\varepsilon^S} \tag{1.2.15}$$

the *piezoelectric coupling constant*. Values of $K^2$ and the acoustic wave velocity in some of the more common piezoelectric materials are given in Appendix B. The energy definition for $K^2$ will be discussed in Sec. 1.3. Section 1.5 gives various definitions of $K^2$ for wave fields applied in arbitrary directions in anisotropic piezoelectric materials.

Now it is easy to define the propagation constant in the piezoelectric medium for a wave of frequency $\omega$. Using the notations $\bar{\beta}_a$ for the stiffened propagation constant and $\bar{V}_a$ for the stiffened acoustic velocity, we see that

$$\bar{\beta}_a = \omega\left(\frac{c^D}{\rho_{m0}}\right)^{-1/2} = \frac{\omega}{\bar{V}_a} \tag{1.2.16}$$

and

$$\bar{V}_a = V_a(1 + K^2)^{1/2} \tag{1.2.17}$$

The piezoelectrically stiffened velocity is always larger than the equivalent velocity in a nonpiezoelectric medium or a piezoelectric medium with $E = 0$ (i.e., a perfectly conducting medium). In materials such as indium antimonide or gallium arsenide, $K^2$ can have values of the order of $10^{-4}$; in a piezoelectric ceramic such as PZT, or a crystal such as lithium niobate, it can be as large as 0.5.

**Stress-free dielectric constant.** Let us consider the properties of a finite-length medium of infinite cross section. In this case, $D$ may be finite and we can define an effective dielectric constant of the medium. We have seen that if the strain is zero, the ratio $D/E$ is $\varepsilon^S$, the strain-free dielectric constant. In the same way, we define an effective permittivity under stress-free conditions $\varepsilon^T$. Putting $T = 0$ in Eq. (1.2.9), we see that

$$S = \frac{e}{c^E}E \tag{1.2.18}$$

Thus, on substituting Eq. (1.2.18) into Eq. (1.2.4), we find that

$$D = \varepsilon^T E = \varepsilon^S(1 + K^2)E \tag{1.2.19}$$

Therefore,

$$\varepsilon^T = \varepsilon^S(1 + K^2) \tag{1.2.20}$$

Thus the stress-free dielectric constant is larger than the strain-free dielectric constant.

The definitions given here can and must be generalized to define $\varepsilon^T$ correctly. In using our definitions, we must know whether all components of $T$ or $D$ in a finite piezoelectric medium are zero, or whether only one of them is.

## PROBLEM SET 1.2

**1.** **(a)** A simple piezoelectric transducer consists of a thin piezoelectric layer, of thickness $l$, with thin metal film electrodes. The transducer is backed by a material of the same acoustic impedance $\bar{Z}_0$, and placed against a material of impedance $Z_1$, as illustrated below. Assume that $l \ll \lambda$, the acoustic wavelength, so that the RF field $E$ and the strain $S$ are essentially uniform within the transducer.

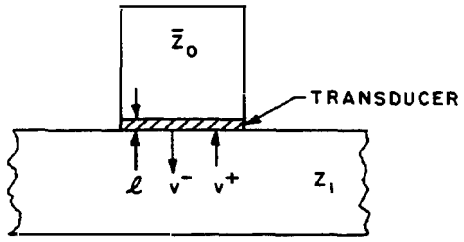


Suppose that a wave with an RF velocity $v^+$ is incident from the material of impedance $Z_1$ on the transducer, and passes through the transducer. Taking the transducer to be open-circuited ($i_D = j\omega D = 0$), use Eq. (1.2.4) to find the voltage induced across the transducer.

**(b)** Find the minimum detectable velocity $v$ and displacement $u$ at the front surface of a 100-μm-thick PZT-5H transducer, at center frequencies of 100 kHz and 1 MHz, respectively, when the usable sensitivity of the input amplifier is $5 \times 10^{-4}$ V. Assume that the transducer is thin compared to a wavelength. Over this frequency range, assume that the induced fields in the material are uniform. Assume that the transducer has the same impedance as the material with which it is in contact, and that it is terminated on its other side with a matched impedance. Use $e_{z3}$ for $e$.

**2. (a)** Consider a capacitive transducer consisting of two metal electrodes spaced by an air gap of width $l$. Assume that a dc field $E_0$ is applied to the transducer and induces charges $\rho_{s0}$ and $-\rho_{s0}$ per unit area on each electrode. Show that if the charge on the electrodes is kept constant, the induced transducer voltage is proportional to the RF displacement $u$ at its front surface.

**(b)** Suppose that a capacitive transducer is used to detect the emission of acoustic waves incident on a metal surface. In this case, the metal surface is one of the capacitor plates. Such acoustic emissions occur when a crack spreads under stress, the way wood creaks as it is strained. Take the air gap $l$ to be 2 μm and the applied static potential to be 50 V. Assume that a forward wave of displacement amplitude $u^+$ and velocity $v^+$ is normally incident at the surface. Suppose that the detector has a usable sensitivity of $5 \times 10^{-4}$ V. Find the minimum detectable displacement $u^+$ and the minimum detectable RF velocity at 100 kHz and 1 MHz. Take account of the reflection of the wave at the metal surface to find the total displacement $u$, which excites the transducer.

**(c)** Compare this result to your result for Prob. 1.

**3. (a)** Consider the propagation of an acoustic wave in a conducting piezoelectric medium with a conductivity $\sigma$, such as cadmium sulfide. In this case, Eq. (1.2.11) becomes $i = \partial D/\partial t + \sigma E = 0$. Work out an expression for the propagation constant of waves in this medium. Assume that $K^2 << 1$. Show that for very low frequencies, the attenuation varies as the square of the frequency, but for very high frequencies, reaches a constant value.

**(b)** Taking $K = 0.15$, $\varepsilon^S/\varepsilon_0 = 9.5$, and $\bar{V}_a = 4.45$ km/s, find the value of resistivity of the material for which the attenuation is a maximum at 50 MHz. Find the value of resistivity when the attenuation is a maximum at 1 GHz. Find the attenuation per unit length in each case.

**4.** Consider what occurs when a dc field is applied to a piezoelectric semiconductor such as the one described in Prob. 1, so that the carriers drift with a velocity $v_0$. The conduction

current density associated with the carriers is

$$i_C = qn\mu E$$

We put

$$i_C = i_{C0} + i_{C1}$$

$$v_0 = \mu E_0$$

$$E = E_0 + E_1$$

and

$$n = n_0 + n_1$$

where $E_0$ is the applied dc field, $E_1$ is the RF field, $\mu$ is the carrier mobility, $q$ is the carrier charge (the conductivity $\sigma = \mu q n_0$), $n_0$ is the static carrier density, $n_1$ is the RF carrier density, and it is assumed that $E_1 \ll E_0$ (i.e., $i_{C1} \ll i_{C0}$). Then

$$i_{C1} = q(n_1 v_0 + \mu n_0 E_1)$$

to first order in the RF quantities, with

$$v_0 = \mu E_0$$

The carriers obey the equation of continuity of charge

$$\frac{\partial i_{C1}}{\partial z} + q\frac{\partial n_1}{\partial t} = 0$$

The total first-order current density is

$$i = i_{C1} + \frac{\partial D}{\partial t} = 0$$

Following the method of Prob. 3, solve for the propagation constant $\beta$ of the wave. Find a simple formula for $\beta$ by writing $\beta = \beta_0 + K^2\beta_1 + K^4\beta_2 \cdots$, and keep only the first-order terms in $K^2$. Show that when $K^2 \ll 1$, the wave grows with distance if $\overline{V}_a < v_0$, and is attenuated if $v_0 < \overline{V}_a$. This is the basic theory of the acoustoelectric amplifier. In practice, the gain or growth rate of the device does not remain large at very high frequencies because carrier diffusion effects at such levels cause it to decrease.

## 1.3 ENERGY CONSERVATION IN PIEZOELECTRIC MEDIA

It is possible to obtain the equivalent of Poynting's theorem for piezoelectric media by generalizing the derivation of Eq. (1.1.22), the Poynting's theorem for nonpiezoelectric media. This is done for the general case in Appendix C.

For a plane wave of frequency $\omega$, like the one treated in Sec. 1.2, it follows from Eq. (C.11) that the generalized one-dimensional Poynting's theorem can be written in the form

$$\frac{\partial}{\partial z}[(-v^*T) + (\mathbf{E} \times \mathbf{H}^*)_z]$$

$$= j\omega c^E SS^* + j\omega\varepsilon^S \mathbf{E} \cdot \mathbf{E}^* - j\omega p_{m0}\mathbf{v} \cdot \mathbf{v}^* - j\omega\mu\mathbf{H} \cdot \mathbf{H}^* - \mathbf{i}_C^* \cdot \mathbf{E} \qquad (1.3.1)$$

where $\mathbf{i}_C$ is the conduction current in the medium.

The left-hand side of Eq. (1.3.1) is associated with the total power flow density in the medium. If the permittivity, elasticity, and permeability are real, then

$$\frac{\partial}{\partial z} \operatorname{Re}\,(P_a + P_e) = -\tfrac{1}{2} \operatorname{Re} \int_A \mathbf{i}_C^* \cdot \mathbf{E}\, ds \tag{1.3.2}$$

where the integral is taken over the cross section $A$ of the system. Thus we have generalized the usual complex Poynting's theorem to find that the only change required is that the total power must now include the electromagnetic power flow

$$P_e = \tfrac{1}{2} \operatorname{Re} \int_A (\mathbf{E} \times \mathbf{H}^*) \cdot d\mathbf{s} \tag{1.3.3}$$

Equation (1.3.1) shows that in addition to the stored elastic energy $W_S$ per unit volume, defined as

$$W_S = \tfrac{1}{4} S^* c^E S \tag{1.3.4}$$

and the stored kinetic energy $W_v$ per unit volume, defined as

$$W_v = \tfrac{1}{4} \rho_{m0} \mathbf{v} \cdot \mathbf{v}^* \tag{1.3.5}$$

there is stored magnetic energy $W_H$ per unit volume, defined as

$$W_H = \tfrac{1}{4} \mu \mathbf{H} \cdot \mathbf{H}^* \tag{1.3.6}$$

The stored magnetic energy is usually negligible for an acoustic wave. The stored electric energy $W_E$ per unit volume is

$$W_E = \tfrac{1}{4} \varepsilon^S \mathbf{E} \cdot \mathbf{E}^* \tag{1.3.7}$$

Let us consider the ratio of the electrical energy to the acoustic energy, defined as $W_E/(W_S + W_v) = W_E/W_a$, where we have taken the acoustic energy per unit volume to be

$$W_a = W_S + W_v \tag{1.3.8}$$

In the one-dimensional case, as $D \approx 0$, it follows from Eq. (1.2.12) that

$$E = \frac{-eS}{\varepsilon^S} \tag{1.3.9}$$

The electrical energy per unit volume is

$$\begin{aligned} W_E &= \frac{1}{4} \varepsilon^S |E|^2 \\ &= \frac{1}{4} \frac{e^2 |S|^2}{\varepsilon^S} \\ &= \frac{1}{4} \frac{e^2}{c^E \varepsilon^S} TS = K^2 W_S \end{aligned} \tag{1.3.10}$$

Thus $K^2$ can be defined as the ratio of the stored electrical energy to the stored elastic energy. This ratio is usually much less than unity. It also follows from

Eq. (1.3.1), with $\mathbf{i}_C = 0$ and $\mathbf{H} = 0$ (the magnetic field can usually be neglected), that

$$W_E + W_S - W_v = 0 \tag{1.3.11}$$

Therefore, Eqs. (1.3.10) and (1.3.11) lead to the result

$$W_v = (1 + K^2)W_S = \frac{1 + K^2}{K^2} W_E \tag{1.3.12}$$

or

$$\frac{W_E}{W} = \frac{K^2}{2(1 + K^2)} \tag{1.3.13}$$

where the total stored energy per unit volume is $W = W_S + W_v + W_E$. Because the square of the piezoelectric coupling constant $K^2$ is normally small, the stored electrical energy is usually much less than the total stored energy in a piezoelectric medium.

The same results also follow simply from the one-dimensional static equations. If we consider a material in which the electric field is zero, then under static conditions, the stored elastic energy $W_S$ is

$$W_S = \tfrac{1}{2}TS = \tfrac{1}{2}cS^2 \text{ per unit volume} \tag{1.3.14}$$

Suppose that the electric field is finite and $D = 0$ (i.e., no charge flows into the system). The stored energy is now

$$\begin{aligned} W &= \tfrac{1}{2}TS = \tfrac{1}{2}c^E S^2 + \tfrac{1}{2}\varepsilon^s E^2 \\ &= \tfrac{1}{2}c^E(1 + K^2)S^2 \text{ per unit volume} \end{aligned} \tag{1.3.15}$$

Thus the increase in stored energy due to the piezoelectric effect is $K^2 W_S$.

To put it another way, it follows from Eq. (1.2.9) that the static energy per unit volume is

$$\tfrac{1}{2}TS = \tfrac{1}{2}c^E S^2 - \tfrac{1}{2}eES \tag{1.3.16}$$

The elastic energy is $\frac{1}{2}c^E S^2$ per unit volume, and the energy resulting from coupling between electrical and mechanical quantities is $\frac{1}{2}eES$ per unit volume. The ratio of the mutual coupling to the self-energy term is $-eE/c^E S$. If $D = 0$, this quantity is equal to $K^2$. Thus $K^2$ is also the ratio of the mutual coupling energy to the stored energy.

## PROBLEM SET 1.3

1. Consider the effect of resistive loss in a piezoelectric medium. Suppose that the conductivity of the material is $\sigma$. Using Poynting's theorem [Eq. (1.3.2)] and the Maxwell equation

$$\nabla \times \mathbf{H}^* = -j\omega\mathbf{D}^* + \mathbf{i}_C^*$$

and assuming that for an acoustic beam of area $A$ with no attenuation, the power in the acoustic beam is $P_a = W\bar{V}_a A$, find the attenuation of a plane wave due to resistive loss. Carry out a treatment such as the one to derive viscous losses in Sec. 1.1 and the derivation leading to Eq. (1.1.31), and use the values of $E$, $S$, $T$, and $P_a$ for the perfectly insulating medium.

2. Derive the one-dimensional form of Poynting's theorem, using the one-dimensional piezoelectric constitutive relations and the one-dimensional equation of motion for a plane wave.

## 1.4 PIEZOELECTRIC TRANSDUCERS

### 1.4.1 Introduction

Electromechanical transducers convert electrical energy into mechanical energy, and vice versa, in low-frequency applications; microphones and loudspeakers are well-known examples of such transducers used at frequencies below 20 kHz. But for higher-frequency applications, piezoelectric transducers are useful. Their high $Q$ as mechanical resonators means that they can be used at medium frequencies (1 to 50 MHz) in quartz crystal resonators and filters, and also at much higher frequencies as bulk and surface wave electromechanical transducers, from a few kilohertz up into the microwave range.

A simple configuration for a delay line operating at frequencies above 100 MHz, which might be made of sapphire, for example, is shown in Fig. 1.4.1(a). A metal film is deposited on either end of the delay-line rod to create two metal counter electrodes, one at each end. Then a film of a piezoelectric material, such as zinc oxide, is deposited on each counter electrode by sputtering or evaporation in a vacuum; typically, this layer is chosen to be between a quarter- and a half-wavelength thick. Finally, a metal film is laid down on the surface of the piezoelectric material to form a metal top electrode; this second metal electrode is normally a small fraction of a wavelength thick. We now have a transducer at either end of the rod, comprised of a metal counter electrode, a piezoelectric film, and a metal top electrode. At one end of the rod, a potential is applied between the two metal electrodes on either side of the piezoelectric film to excite a longitudinal acoustic wave in the delay line. After the wave has traveled through the delay line, it is detected on the transducer at the end of the rod. The electrical impedance at the input terminals will depend on the thickness and acoustic impedance of the electrodes and the piezoelectric material, and on the nature of the substrate material. To make a broadband UHF delay line, it is often necessary to use a quarter-wavelength-thick matching layer of material between the counter electrode and the delay-line rod, to match the impedance of the piezoelectric material to the impedance of the delay line.

Another type of application, illustrated in Fig. 1.4.1(b), uses an air-backed piezoelectric transducer to excite a wave in water. In a low-frequency device, using a PZT transducer ($Z_0 = 34 \times 10^6$ kg/m$^2$-s) to excite a wave in water ($Z_0 = 1.5 \times 10^6$ kg/m$^2$-s), there is a 22-to-1 mismatch in impedance. This leads to a resonant characteristic with an acoustic $Q$ of the order of 30. But using a quarter-

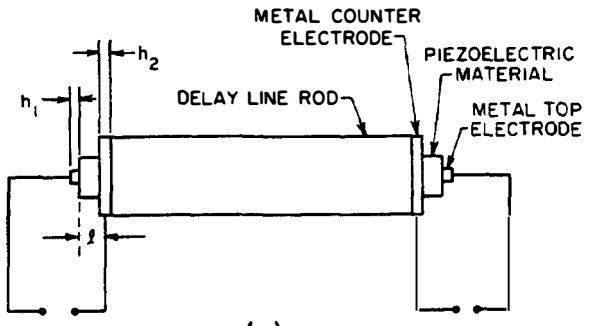


(a)

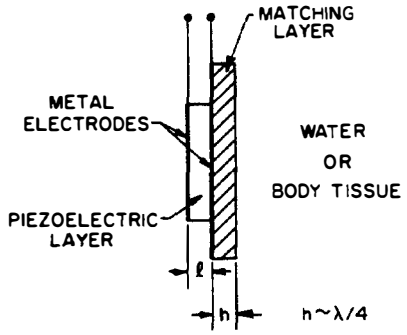


(b)

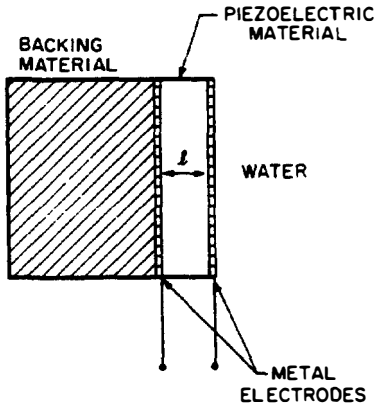


(c)

**Figure 1.4.1** (a) Delay line used at UHF frequencies. All materials are typically deposited by vacuum deposition on the delay-line rod. (b) Air-backed piezoelectric transducer with a matching layer on its front surface, for exciting a wave in water or body tissue. (c) Piezoelectric transducer loaded on its back surface, for exciting a wave in water.

wavelength-thick intermediate layer, with an impedance $Z_0 \sim \sqrt{34 \times 1.5} \times 10^6 = 7.1 \times 10^6$ kg/m$^2$-s, between the ceramic and the water will yield a broader-band characteristic with better power transmission. The resonance can also be broadened by using acoustically lossy material with an impedance comparable to that of the PZT ($Z_0 = 34 \times 10^6$ kg/m$^2$-s) bonded to the other side of the transducer, as illustrated in Fig. 1.4.1(c).

First we will carry out a general derivation to determine the properties of a transducer with arbitrary acoustic impedances at each surface. The piezoelectric transducer can be regarded as a "black box" having one or more mechanical ports and one electrical port.

### 1.4.2 The Transducer as a Three-Port Network

We shall consider a uniform transducer or resonator with cross-sectional dimensions of many wavelengths, and electrodes on opposite surfaces normal to the $z$ direction, as shown in Figs. 1.4.1 and 1.4.2. Because the electrodes short out the field, it is reasonable to assume that $E_x = 0$ and $E_y = 0$. The symmetry means that if the transducer is designed to operate with longitudinal waves, there will be no motion in the $x$ and $y$ directions. In this case, the parameters $S$, $E$, $D$, $v$, $u$, and $T$ have components only in the $z$ direction, and Eqs. (1.2.4) and (1.2.9) are the natural ones to use with the appropriate values of $c^E$, $e$, and $\varepsilon^S$. Similarly, for shear wave resonators or transducers in which $S$, $E$, $D$, $v$, $u$, and $T$ have only one component, Eqs. (1.2.4) and (1.2.9) can be used with the appropriate shear wave constants $c^E$ and $e$. The definitions of these parameters are discussed in more detail in Sec. 1.5.

We now regard the transducer as a three-port black box. We define the force $F$ at the surface of the transducer as we do voltage in electrical circuits, and the particle velocity $v$ as we do current in electrical circuits. Using the notation shown in Fig. 1.4.3(a) for the three-port network, and that shown in Fig. 1.4.3(b) for the physical transducer, we can find an equivalent circuit for this black box.

The external force applied to the piezoelectric material at the surface of the resonator is

$$F = -AT \tag{1.4.1}$$

where $A$ is the area of the transducer and $T$ is the internal stress.

The equivalent circuit definitions used in the theory of the piezoelectric transducer are based on the idea that particle velocity is equivalent to current and

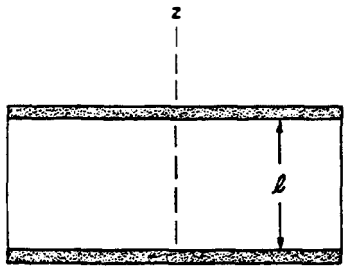


**Figure 1.4.2** Piezoelectric resonator of length $l$ with electrodes on opposite surfaces.

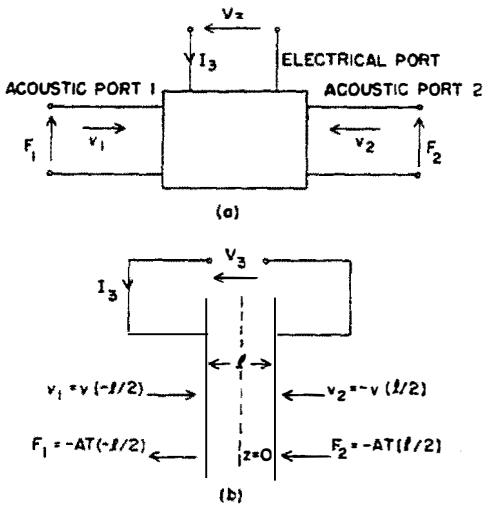


**Figure 1.4.3** (a) Transducer, regarded as a three-port black box; (b) relation of three-port notation to the physical parameters of the transducer.

stress is equivalent to voltage, as we discussed in the transmission-line analogy in Sec. 1.1.

The definition for velocity, as it applies to the two acoustic ports or terminals, follows the definition for current at the ports of an electrical two-port network. Thus the particle velocity is positive *inward* to the piezoelectric material. It follows that the boundary conditions at the acoustic ports are

$$\begin{aligned} F_1 &= -AT\left(\frac{-l}{2}\right) \\ F_2 &= -AT\left(\frac{l}{2}\right) \\ v_1 &= v\left(\frac{-l}{2}\right) \\ v_2 &= -v\left(\frac{l}{2}\right) \end{aligned} \tag{1.4.2}$$

respectively, where $v(-l/2)$ and $v(l/2)$ are the velocity components at the surface of the piezoelectric material.

The relation between $T$ and $v$ within the material of the transducer is

$$\frac{dT}{dz} = j\omega\rho_{m0}v \tag{1.4.3}$$

and

$$\frac{dv}{dz} = j\omega S \tag{1.4.4}$$

The total current through the transducer is

$$I_3 = j\omega AD \tag{1.4.5}$$

With the sign convention shown in Fig. 1.4.3, the voltage across the transducer is

$$V_3 = \int_{-l/2}^{l/2} E\, dz \tag{1.4.6}$$

Since current is conserved, $D$ must be uniform with $z$. Eliminating $E$ from Eqs. (1.2.4) and (1.2.9), the generalization of Eq. (1.2.13) with $D$ finite is

$$T = c^D S - hD \tag{1.4.7}$$

where $h$ is known as the *transmitting constant*, defined as

$$h = \frac{e}{\varepsilon^S} \tag{1.4.8}$$

with

$$c^D = c^E\left(1 + \frac{e^2}{c^E \varepsilon^S}\right) = c^E(1 + K^2) \tag{1.4.9}$$

If we eliminate $T$ and $S$ from Eqs. (1.4.3), (1.4.5), and (1.4.7), then $v$ obeys the wave equation

$$\frac{d^2v}{dz^2} + \frac{\omega^2 \rho_{m0}}{c^D} v = 0 \tag{1.4.10}$$

This has the solutions

$$v = v_F e^{-j\bar{\beta}_a z} + v_B e^{j\bar{\beta}_a z} \tag{1.4.11}$$

and

$$T = T_F e^{-j\bar{\beta}_a z} + T_B e^{j\bar{\beta}_a z} - hD \tag{1.4.12}$$

where the subscripts $F$ and $B$ denote forward and backward propagating waves, respectively. We define the following parameters:

$$\bar{\beta}_a = \omega\left(\frac{\rho_{m0}}{c^D}\right)^{1/2} \tag{1.4.13}$$

and

$$\bar{Z}_0 = (\rho_{m0} c^D)^{1/2} \tag{1.4.14}$$

with

$$T_F = -\bar{Z}_0 v_F \tag{1.4.15}$$

and

$$T_B = \bar{Z}_0 v_B \tag{1.4.16}$$

Using the boundary conditions of Eq. (1.4.2) in Eq. (1.4.11), we see that

$$v = \frac{-v_2 \sin[\bar{\beta}_a(z + l/2)] + v_1 \sin[\bar{\beta}_a(l/2 - z)]}{\sin \bar{\beta}_a l} \tag{1.4.17}$$

Substituting this result in Eqs. (1.4.2) and (1.4.4)–(1.4.7), it follows, after some algebra, that

$$\begin{bmatrix} F_1 \\ F_2 \\ V_3 \end{bmatrix} = -j \begin{bmatrix} Z_C \cot \bar{\beta}_a l & Z_C \operatorname{cosec} \bar{\beta}_a l & \frac{h}{\omega} \\ Z_C \operatorname{cosec} \bar{\beta}_a l & Z_C \cot \bar{\beta}_a l & \frac{h}{\omega} \\ \frac{h}{\omega} & \frac{h}{\omega} & \frac{1}{\omega C_0} \end{bmatrix} \begin{bmatrix} v_1 \\ v_2 \\ I_3 \end{bmatrix} \tag{1.4.18}$$

where the clamped (zero strain) capacitance of the transducer is

$$C_0 = \frac{\varepsilon^S A}{l} \tag{1.4.19}$$

Consistent with our definition of electrical impedance, we define the acoustic impedance of an area $A$ of piezoelectric material as

$$Z_C = \bar{Z}_0 A \tag{1.4.20}$$

where the parameter $Z_C$ has the dimensions force/velocity or kg/s and $\bar{Z}_0$ has the dimensions pressure/velocity or kg/m$^2$-s. Impedances with the dimensions of force/velocity are sometimes called *radiation impedances*.

**Example: Electrical Input Impedance of a Transducer**

We can determine the electrical input impedance of a transducer terminated by acoustic load impedances $Z_1$ and $Z_2$ by using the matrix formula (1.4.18). We define the radiation impedances of the loads (looking outward from the transducer) as

$$Z_1 = -\frac{F_1}{v_1} = \frac{AT(-l/2)}{v(-l/2)} \tag{1.4.21}$$

and

$$Z_2 = -\frac{F_2}{v_2} = \frac{-AT(l/2)}{v(l/2)} \tag{1.4.22}$$

Using these relations in Eq. (1.4.18) yields the electrical input impedance of the transducer in the form

$$Z_3 = \frac{V_3}{I_3} = \frac{1}{j\omega C_0}\left[1 + k_T^2 \frac{j(Z_1 + Z_2)Z_C \sin \bar{\beta}_a l - 2Z_C^2(1 - \cos \bar{\beta}_a l)}{[(Z_C^2 + Z_1 Z_2) \sin \bar{\beta}_a l - j(Z_1 + Z_2)Z_C \cos \beta_a l]\bar{\beta}_a l}\right] \tag{1.4.23}$$

where

$$k_T^2 = \frac{K^2}{1 + K^2} \tag{1.4.24}$$

and

$$\frac{c^D}{c^E} = 1 + K^2 = \frac{1}{1 - k_T^2} \tag{1.4.25}$$

For longitudinal waves, the parameter $k_T$ is often defined as the piezoelectric coupling constant for a transversely clamped material, for it is the effective piezoelectric constant used when there is no motion transverse to the electric field. For $K^2 << 1$, $k_T^2$ and $K^2$ are essentially identical. For materials such as quartz, cadmium sulfide, and zinc oxide, this assumption is adequate. It tends to break down, however, with piezoelectric ceramics; with PZT-5A, for instance, $K^2 = 0.5$ and $k_T^2 = 0.33$.

The definitions of $K^2$ and $k_T^2$ are useful only if the material can be regarded as being transversely clamped. A piezoelectric transducer with a cross section of many wavelengths has very little transverse motion, so $k_T$ is the effective coupling constant. Such transducers are commonly employed in UHF applications, where the wavelengths are less than 100 μm, and often in low-frequency applications, where the wavelengths are of the order of 1 mm and the cross-sectional dimensions of the transducer are 1 or more centimeters. Similar relations hold for a shear wave transducer with a cross section of many wavelengths.

### 1.4.3 Mason Equivalent Circuit

We show here that the matrix formula (1.4.18) results in the Mason equivalent circuit of Fig. 1.4.4. First we consider the value of $F_1$:

$$F_1 = -jZ_C v_1 \cot \bar{\beta}_a l - jZ_C v_2 \operatorname{cosec} \bar{\beta}_a l + \frac{hI_3}{j\omega} \tag{1.4.26}$$

When $I_3 = 0$, the first two terms can be written in the form of an impedance matrix of the type shown in Fig. 1.4.5(b), where

$$Z_{11} = -jZ_C \cot \bar{\beta}_a l \tag{1.4.27}$$

$$Z_{12} = -jZ_C \operatorname{cosec} \bar{\beta}_a l \tag{1.4.28}$$

and

$$Z_{11} - Z_{12} = jZ_C(\operatorname{cosec} \bar{\beta}_a l - \cot \bar{\beta}_a l) = jZ_C \tan \frac{\bar{\beta}_a l}{2} \tag{1.4.29}$$

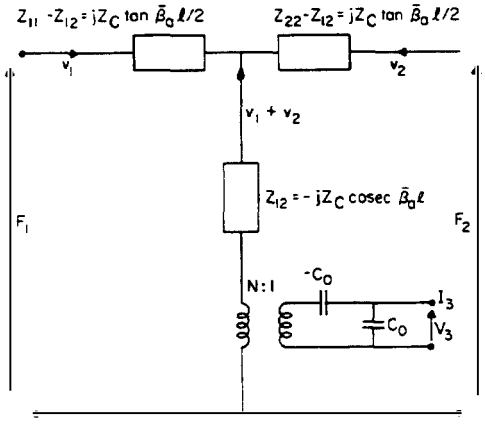


**Figure 1.4.4** Mason series equivalent circuit for the in-line transducer with the $E$ field in the same direction as the material velocity. In this circuit the transformer ratio is $N = hC_0 = eC_0/\varepsilon^S = eA/l$, and $Z_C = \bar{Z}_0 A$.

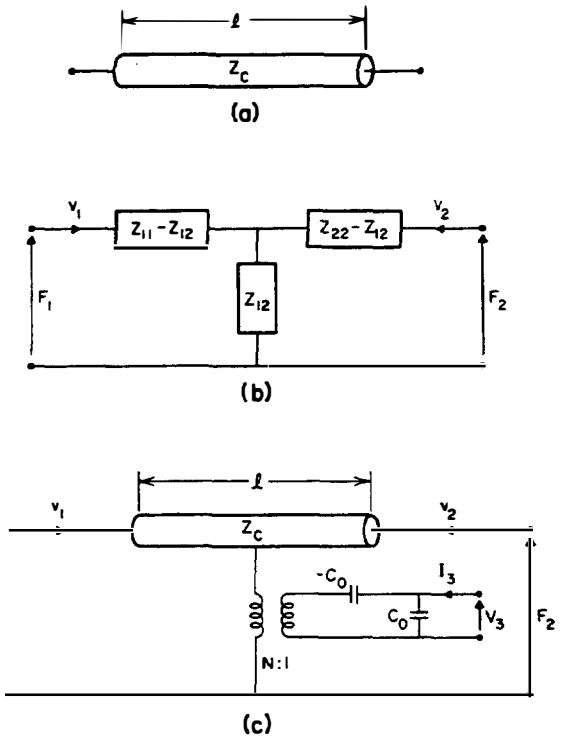


**Figure 1.4.5** Redwood equivalent circuit. (a) Coaxial transmission line of impedance $Z_C$. In this circuit, $Z_{11} - Z_{12} = Z_{22} - Z_{12} = jZ_C \tan \bar{\beta}_a l/2$, $Z_{12} = -jZ_C \operatorname{cosec} \bar{\beta}_a l$. (b) $T$ network equivalent of the coaxial line. (c) Redwood equivalent circuit, derived from the Mason model of Fig. 1.4.4. In this circuit the transformer ratio is $N = hC_0 = eC_0/\varepsilon^S = eA/l$, and $Z_C = \sqrt{Z_0 A}$.

The right-hand side of the network has the same form as the left-hand side. In general, there is an extra potential of value $hI_3/j\omega$ in series with the potentials generated by $v_1$ and $v_2$. Before treating this source, let us consider the value of $V_3$:

$$V_3 = \frac{h}{j\omega}(v_1 + v_2) + \frac{I_3}{j\omega C_0} \tag{1.4.30}$$

The last term in this equation is merely a voltage across the capacitor $C_0$. The first term is a voltage proportional to the total equivalent current $v_1 + v_2$ flowing into the transformer. A perfect transformer of value $N$ to 1, where $N = hC_0 = eC_0/\varepsilon^S = eA/l$, would introduce a current of value $(v_1 + v_2)N$ into the right-hand side of the circuit, and the current would then develop a potential $(h/j\omega)(v_1 + v_2)$ across the capacitor $C_0$.

The transformed potential $V_3$ does not appear across terminals 1 or 2. A potential $-(h/j\omega)/(v_1 + v_2)$ is developed across the negative capacitor $-C_0$ in the circuit of Fig. 1.4.4, which just cancels out the potential across $C_0$. This equivalent circuit also gives the last term in the expression for $F_1$. Thus the final Mason equivalent circuit is the one shown in Fig. 1.4.4.

**Example: Clamped Transducer**

If the transducer is rigidly held (clamped) so that $v_1 = v_2 = 0$, the mechanical terminating impedances are infinite and it follows from Eq. (1.4.18), or the Mason equivalent circuit of Fig. 1.4.4, that

$$\frac{F_1}{V_3} = \frac{F_2}{V_3} = N = \frac{eA}{l} \tag{1.4.31}$$

There is no motion in a rigidly clamped system. Thus with $v(z) = 0$ and $S = 0$, it follows from Eqs. (1.2.4) and (1.2.9) that $T = -eE$ and $D = \varepsilon^S E$. So if $F = -AT$ and $V_3 = El$, then $F_1/V_3 = F_2/V_3 = eA/l$, which is the result of Eq. (1.4.31).

### 1.4.4 Redwood Equivalent Circuit

An alternative equivalent circuit, the *Redwood equivalent circuit* [7], can be derived from the Mason model of Fig. 1.4.4. The $T$ network $Z_{11}$, $Z_{12}$, $Z_{22}$ of the Mason equivalent circuit can be represented by a transmission line of impedance $Z_C$, as illustrated in Fig. 1.4.5(a) and (b). This means that we can write the Mason model in the form shown in Fig. 1.4.5(c), which is the Redwood equivalent circuit. The transmission line in this new circuit can be regarded as a coaxial line whose outer shield is connected to the transformer. The Redwood equivalent circuit is particularly useful for dealing with a short pulse excitation of the transducer, especially when the pulse length is less than the delay time of an acoustic wave passing through the transducer. In this case, the input impedance of the coaxial line appears to be $Z_C$, and it is very easy to determine the pulse response of the system.

**Example: Open-Circuited Pulse-Excited Acoustically Matched Receiving Transducer**

We assume that the transducer is electrically open-circuited (i.e., $I_3 = 0$). In this case, the voltage across the transformer is zero because the two capacitors $C_0$ and $-C_0$, in series, form a short circuit. Suppose that the transducer is excited at its left-hand side with a velocity pulse $v_1(t)$. The pulse propagates along the transmission line and gives rise to a pulse $v_2(t)$, where

$$v_2(t) = -v_1(t - T) \tag{1.4.32}$$

and $T = l/\bar{V}_a$ is its transit time along the line.

The current flowing into the capacitor $C_0$ is

$$\begin{aligned} I &= N(v_1 + v_1) \\ &= N[v_1(t) - v_1(t - T)] \end{aligned} \tag{1.4.33}$$

Thus the output voltage $V_3$ is defined as

$$V_3 = \frac{N}{C_0} \int_0^t [v_1(t) - v_1(t - T)]\, dt \tag{1.4.34}$$

or

$$V_3 = h \int_0^t [v_1(t) - v_1(t - T)]\, dt \tag{1.4.35}$$

If $v_1(t)$ has the form of a $\delta$ function velocity pulse (a very short pulse), $V_3(t)$ will be a square-topped pulse of length $T$, as illustrated in Fig. 1.4.6.

### 1.4.5 Impedance of an Unloaded Transducer

First we consider an unloaded transducer in air (e.g., a ceramic or quartz plate with thin electrodes). In this case, $F_1 = F_2 = 0$ or $Z_1 = Z_2 = 0$.

From Eq. (1.4.23) we find that the RF input impedance $Z_3 = V_3/I_3$ of the

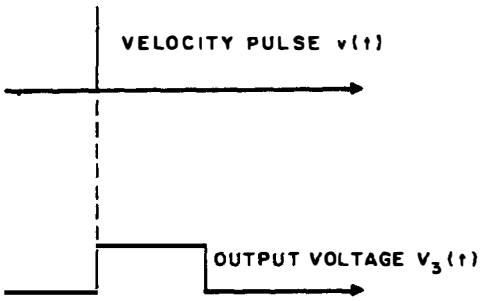


**Figure 1.4.6** Output voltage of an open-circuited receiving transducer, terminated in a matching acoustic impedance when excited by a δ-function velocity pulse.

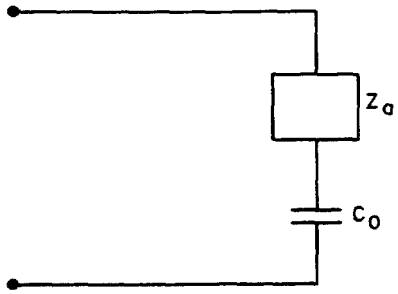


**Figure 1.4.7** Equivalent circuit of a piezoelectric transducer.

transducer is

$$Z_3 = \frac{V_3}{I_3} = \frac{1}{j\omega C_0}\left(1 - k_T^2 \frac{\tan \bar{\beta}_a l/2}{\bar{\beta}_a l/2}\right) \tag{1.4.36}$$

Equation (1.4.36) shows that the equivalent circuit of the transducer shown in Fig. 1.4.7 can be represented by the clamped capacity of the transducer in series with the *motional impedance* $Z_a$ (i.e., where $Z_a$ is the acoustic contribution to the electrical impedance), defined by the relation

$$Z_a = -\frac{k_T^2}{j\omega C_0} \frac{\tan \bar{\beta}_a l/2}{\bar{\beta}_a l/2} \tag{1.4.37}$$

The transducer exhibits a parallel resonance with an infinite electrical impedance. Thus the transducer impedance is like that of an inductance and capacitance in parallel, at frequencies where the transducer is an odd number of half-wavelengths long [i.e., where $\beta_a l = (2n + 1)\pi$]. The corresponding resonant frequencies $\omega_{0n}$ are given by the relation

$$\omega_{0n} = \frac{\pi(2n + 1)\bar{V}_a}{l} \tag{1.4.38}$$

For simplicity, we shall call the lowest-order parallel resonance ($n = 0$) $\omega_0$. Resonances also exist when the transducer length is an even multiple of a half-wavelength, but because the RF electric field associated with these modes has an odd symmetry about the center of the resonator, there is no net potential across the resonance. Thus there is no electrical coupling to even modes.

The transducer exhibits zero electrical impedance at a frequency $\omega_1$ near the $n = 0$ parallel resonance. Near this frequency $\omega_1$, the transducer behaves like an inductance and capacitance in series, and so exhibits a series resonance. At this frequency $\omega_1$, the transducer impedance is $Z_3 = 0$, where

$$\frac{\tan \bar{\beta}_a l/2}{\bar{\beta}_a l/2} = \frac{1}{k_T^2} \tag{1.4.39}$$

It follows from Eqs. (1.4.38) and (1.4.39) that

$$\frac{\tan\,(\pi\omega_1/2\omega_0)}{\pi\omega_1/2\omega_0} = \frac{1}{k_T^2} \tag{1.4.40}$$

We can, in principle, determine $k_T$ from Eq. (1.4.40) by measuring $\omega_1$ and $\omega_0$.

**Equivalent circuit of an unloaded transducer.** It is convenient to express the impedance $Z_a$ in the form of equivalent lumped circuits that correspond to the fundamental resonance and higher-order resonances of the resonator. The function tan $x$ has poles at $x = (2n + 1)\pi/2$. This allows us to obtain a partial fraction, or a Mittag Leffler expansion, for tan $x$ in the form [2]

$$\tan x = \sum_{n=0}^{\infty} \frac{2x}{[(2n + 1)\pi/2]^2 - x^2} \tag{1.4.41}$$

We can express the motional impedance $Z_a$ in a similar form, as

$$Z_a = -\frac{1}{j\omega C_0} \sum_n \frac{k_{\text{eff},n}^2}{1 - \omega^2/\omega_{0n}^2} \tag{1.4.42}$$

where $k_{\text{eff},n}$ is an effective coupling coefficient for the $n$th mode, defined by the relation

$$k_{\text{eff},n}^2 = \frac{8}{[(2n + 1)\pi]^2} k_T^2 \tag{1.4.43}$$

The coupling coefficients to the higher-order modes of the resonator $k_{\text{eff},n}$ fall off with $n$. The value of $\int_{-l/2}^{l/2} E\,dz$ falls off with $n$ for a given maximum value of $E$, because the negative contributions to the integral tend to cancel out the positive contributions. This implies that it is possible to excite a resonator at an odd harmonic of its fundamental resonant frequency, although the effective coupling coefficient for this higher-order mode is smaller than for the fundamental mode. Coupling to higher-order modes is often very convenient; for example, quartz or lithium niobate resonators are often used as narrowband transducers at frequencies many times their fundamental resonant frequency. This makes it possible, for instance, to work at a frequency of 200 MHz with a quartz or lithium niobate resonator whose fundamental frequency is in the 20-MHz range. In this case, the transducer material has a thickness on the order of 0.1 to 0.2 mm, making it easier to handle than a fundamental mode resonator, which would be only 15 μm thick. This technique also tends to give a higher $Q$ or a narrower bandwidth than a thin fundamental mode resonator, whose lapped surfaces might contribute some power loss.

Let us derive a lumped equivalent circuit for the transducer. Using Eq. (1.4.42), we write the impedance $Z_3$ of the resonator as

$$Z_3 = \frac{1}{j\omega C_0}\left[1 - \sum_n \frac{k_{\text{eff},n}^2}{1 - \omega^2/\omega_{0n}^2}\right] \tag{1.4.44}$$

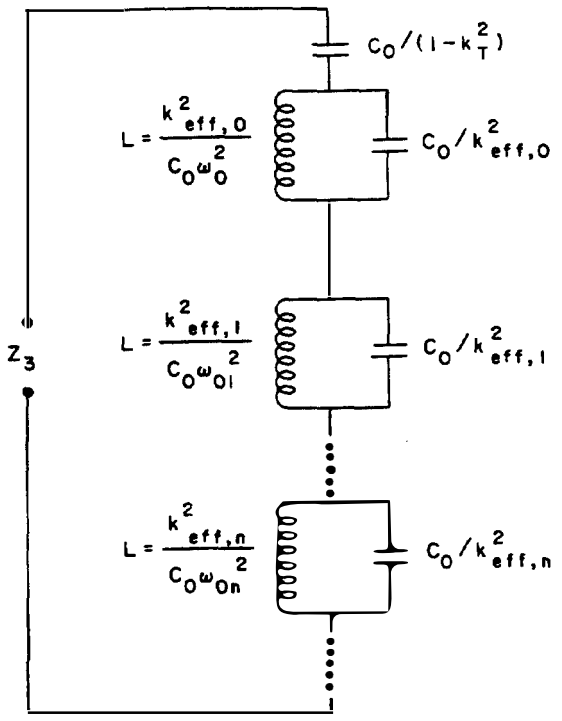


**Figure 1.4.8** Complete series equivalent circuit including all resonances. Each parallel inductance–capacitance combination has a resonant frequency $\omega_{0n}$, and the total series capacitance is $C_0/(1 - k_T^2)$, the unclamped parallel-plate capacitance. A similar parallel equivalent circuit can also be found.

It is convenient to write this relation in the form

$$\begin{aligned} Z_3 &= \frac{1}{j\omega C_0}\left[1 - \sum_n k^2_{\text{eff},n} + \sum_n \frac{j\omega k^2_{\text{eff},n}}{(\omega_{0n}^2 - \omega^2)C_0}\right] \\ &= \frac{1 - k_T^2}{j\omega C_0} + \sum_n \frac{j\omega k^2_{\text{eff},n}}{(\omega_{0n}^2 - \omega^2)C_0} \end{aligned} \tag{1.4.45}$$

This impedance can be represented exactly by the equivalent circuit shown in Fig. 1.4.8. It may be approximated by ignoring the higher-order terms and taking only the fundamental resonance into account, which leads us to the equivalent circuit shown in Fig. 1.4.9(a), with

$$Z_3 \approx \frac{1 - k_T^2}{j\omega C_0} + \frac{8}{\pi^2}\frac{j\omega k_T^2/C_0}{\omega_0^2 - \omega^2} \tag{1.4.46}$$

This equivalent circuit has both a series resonance at $\omega_1$ and a parallel resonance at $\omega_0$. The ratio of these frequencies is given by the relation

$$\frac{\omega_1}{\omega_0} = \left(1 + \frac{8}{\pi^2}\frac{k_T^2}{1 - k_T^2}\right)^{-1/2} = \left(1 + \frac{8K^2}{\pi}\right)^{-1/2} \tag{1.4.47}$$

To second order in $k_T^2$, it follows that

$$\frac{\omega_1}{\omega_0} \approx \left(1 - \frac{8k_T^2}{\pi^2}\right)^{1/2} \tag{1.4.48}$$

When $k_T^2 = 0.5$, the approximate formula of Eq. (1.4.47) has an error of only 0.15% from the exact formula of Eq. (1.4.40). Figure 1.4.10 shows that even the

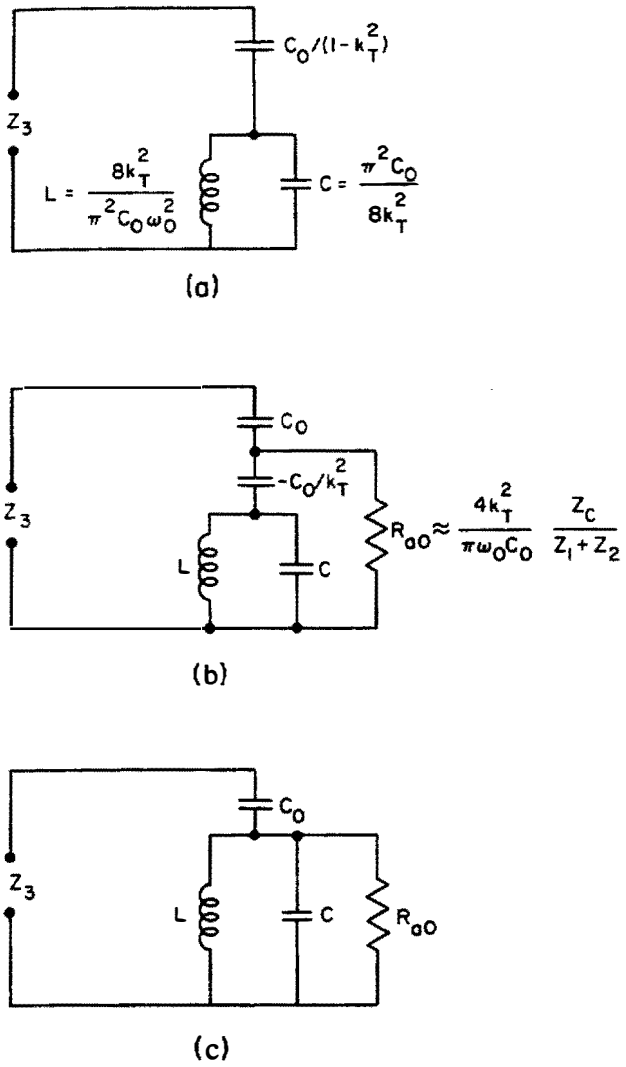


**Figure 1.4.9** (a) Series equivalent circuit for $Z_3$. The paralllel inductance–capacitance combination has a resonant frequency $\omega_0$. (b) Transducer loaded by impedances $Z_1$ and $Z_2$. It is assumed that $|(Z_1 + Z_2)| \ll Z_C$. (c) Usually, in the neighborhood of resonance, the reactance $-C_0/k_T^2$ can be ignored in comparison to the impedance of the shunt resonant circuit.

approximate formula of Eq. (1.4.48) agrees with the exact formula Eq. (1.4.40) for all reasonable values of $k_T^2$. For example, the piezoelectric ceramic PZT-5H has a relatively large $k_T^2$ value of 0.25, while a material such as zinc oxide has a $k_T^2$ value of 0.078. In both cases the errors in either of the approximate formulas (1.4.47) and (1.4.48) are negligible.

Let us estimate the effect on $Z_a$, at the shunt resonance frequency $\omega = \omega_0$, of load impedances $Z_1$ and $Z_2$ at each end of the transducer. We use Eq. (1.4.23) with $Z_1$ and $Z_2$ finite to show that

$$Z_a = R_{a0} = \frac{4k_T^2 Z_C}{(Z_1 + Z_2)\pi\omega_0 C_0} \tag{1.4.49}$$

Thus it is as if a capacity $C_0$ is placed in series with a resistance $R_{a0} = 4k_T^2 Z_C/(Z_1 + Z_2)\pi\omega_0 C_0$; $R_{a0}$ itself is placed in parallel with the lumped resonant circuit. The reactance of the capacitor $-C_0/k_T^2$ is small compared to that of the shunt resonator in the neighborhood of resonance. We will discuss the implications of this circuit

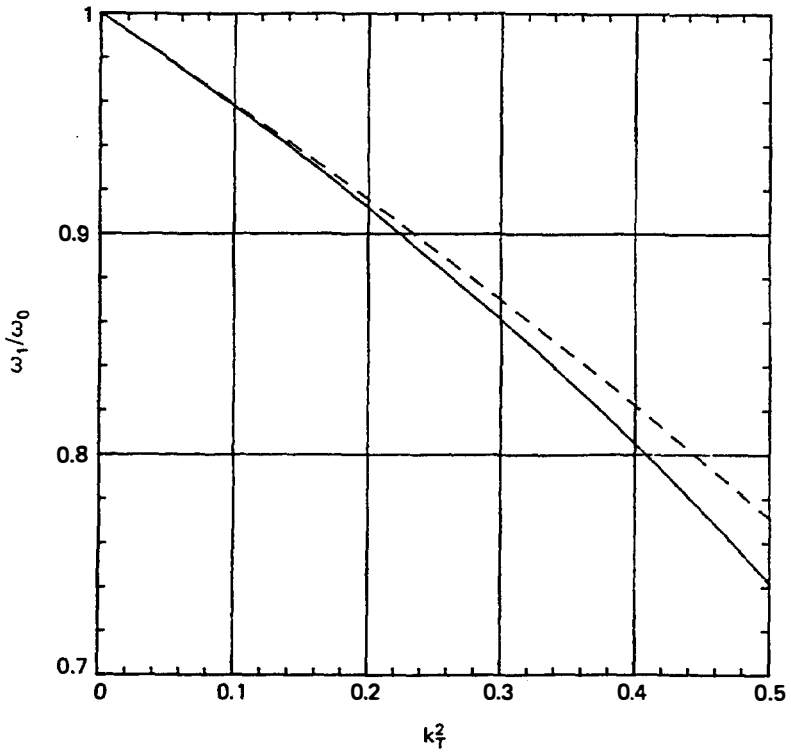


**Figure 1.4.10** Plot of $\omega_1/\omega_0$ as a function of $k_T^2$: solid line, plot of Eq. (1.4.40) or Eq. (1.4.47); dashed line, plot of Eq. (1.4.48). The results of Eqs. (1.4.40) and (1.4.47) are within 0.15% at $k_T^2 = 0.5$.

on matching to an external electrical source and to bandwidth throughout this section.

We can also use Eq. (1.4.46), or the Mason equivalent circuit of Fig. 1.4.4, to derive an alternative parallel equivalent circuit for the admittance $Y_3 = 1/Z_3$. This circuit is convenient for cases where we need to operate near the series resonance into a real input impedance that is relatively small compared to the impedance at shunt resonance. The result obtained is shown in Fig. 1.4.11(a). The series and parallel resonances are at frequencies $\omega_1$ and $\omega_0$, respectively, as we might expect.

A similar derivation from the Mason equivalent circuit, which takes account of the loads $Z_1$ and $Z_2$, can be used to derive the equivalent circuit shown in Fig. 1.4.11(b). Here the direct use of the Mason equivalent circuit is the most convenient approach (see Prob. 10). Such a circuit is most accurate when $(Z_1 + Z_2) << Z_C$. Using the series resonance is helpful if an input circuit with a relatively low input impedance is required.

We have seen that the value $k_T^2$ of a piezoelectric material can, in principle, be measured by determining the frequencies $\omega_0$ and $\omega_1$ of the parallel and series resonances of an unloaded piezoelectric resonator. This technique of measurement works well, again in principle, with a plate of piezoelectric material on which thin electrodes have been deposited. With piezoelectric ceramics, however, other resonances may be associated with shear waves, and with other transverse modes in which stress and strain variations occur in directions parallel, as well as perpen-

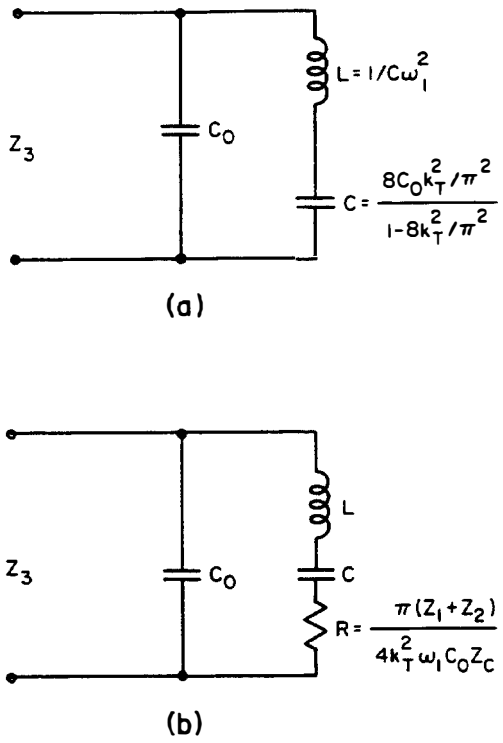


**Figure 1.4.11** (a) Equivalent circuit for an unloaded resonator with an inductance and capacitance in series, and a series resonance at $\omega = \omega_1$. Note that $C$ is equal in value to a capacity $-C_0$ in series with a capacity $8C_0k_T^2/\pi^2$. (b) Equivalent circuit for a resonator loaded with impedances $Z_1$ and $Z_2$ at each end.

dicular, to the electrodes. Such resonances can sometimes hinder good readings of $\omega_1$, making it difficult to determine $k_T^2$ accurately. However, Onoe et al. [8] have shown that measurement of the points where the conductance of a transducer goes through maxima and minima will normally give accurate readings of $\omega_1$ and $\omega_0$, respectively. Furthermore, difficulties in determining the resonant frequency $\omega_0$, due to the presence of other modes, can often be circumvented by using a higher-order resonance, usually the third harmonic.

### 1.4.6 Broadband Operation of Transducers into an Acoustic Medium: The KLM Model

We now consider the operation of a transducer used to excite a wave in an acoustic medium. Normally, it is difficult to design transducers for broadband operation and predict their behavior without resorting to numerical computation. But we can obtain some physical insight into the behavior of such transducers by deducing yet another equivalent circuit, due to Krimholtz, Leedom, and Matthaei [9], which we shall refer to as the *KLM model.*

We regard the piezoelectric material as capable of propagating two waves or modes, one in the forward direction, denoted by a subscript $F$, the other in the backward direction, denoted by a subscript $B$. These modes are continually excited along the length of the transducer by the displacement current $j\omega DA$ that passes through it.

In the Redwood model of Fig. 1.4.5, the continuous excitation is replaced by two electrical sources, one at each end of the transmission line. In the KLM model, a more conventional circuit is derived, which has an electrical source at the

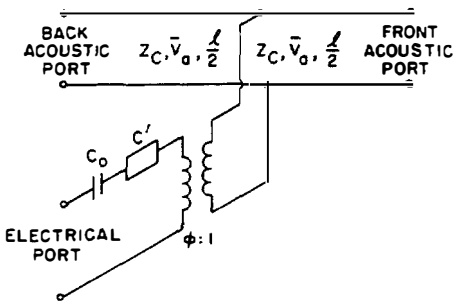


**Figure 1.4.12** KLM model of a piezoelectric transducer: $\phi = k_T(\pi/\omega_0 C_0 Z_C)^{1/2}$ sinc $(\omega/2\omega_0)$ and $C' = -C_0/[k_T^2 \text{ sinc } (\omega/\omega_0)]$. (From Krimholtz et al. [9].)

center of a transmission line. Its disadvantage is that the ratio of the required transformer varies with frequency.

The KLM model is represented by the three-port network shown in Fig. 1.4.12. This equivalent circuit relates the voltage $V_3$ and the current $I_3$ at the electrical port to the forces $F_1 = -AT(-l/2)$ and $F_2 = -AT(l/2)$ and the velocities $v_1 = v(-l/2)$ and $v_2 = -v(l/2)$. It is convenient because it expresses the acoustic parameters in terms of an equivalent transmission line, regarding the stress $T$ as equivalent to a voltage $-V$, and the velocity $v$ as equivalent to a current $I$. This makes it easier to design multiple matching layers [10]. On the other hand, the electrical terminal parameters are expressed in terms of an equivalent lumped circuit, which is convenient for the design of electrical matching networks at commonly used freque $\quad \bar{}_a = (c^D/\rho_{m0})^{1/2}$, $\bar{Z}_0 = (c^D\rho_{m0})^{1/2}$, $Z_C = A$ (1.4.7) in Eq. (1.4.4), then Eqs. (1.4.3) a

$$\qquad (1.4.50)$$

and

$$\frac{dv}{dz} - j\left(\frac{\bar{\beta}_a}{\bar{Z}_0}\right)T = \frac{hI_3}{Z_C\bar{V}_a} \qquad (1.4.51)$$

To obtain a transmission-line representation, it is convenient to define parameters proportional to the amplitudes of the forward and backward waves. Again, we denote these forward and backward waves propagating in the transducer by subscripts $F$ and $B$, respectively. Thus the total stress is

$$T = T_F(z) + T_B(z) \qquad (1.4.52)$$

and the total velocity

$$v = v_F(z) + v_B(z) \qquad (1.4.53)$$

We write $T_F(z) = -\bar{Z}_0 v_F(z)$ for the forward wave and $T_B(z) = \bar{Z}_0 v_B(z)$ for the backward wave. (This concept of forward and backward waves is slightly different to the one described in Sec. 1.4.1.) We substitute Eqs. (1.4.52) and (1.4.53) into Eqs. (1.4.50) and (1.4.51). After performing the necessary addition and subtrac-

tion, and leaving the $z$ dependences of $v_F(z)$ and $v_B(z)$ implicit, $v_F$ and $v_B$ obey the following relations:

$$\frac{dv_F}{dz} + j\bar{\beta}_a v_F = \frac{hI_3}{2Z_C\bar{V}_a} \tag{1.4.54}$$

and

$$\frac{dv_B}{dz} - j\bar{\beta}_a v_B = \frac{hI_3}{2Z_C\bar{V}_a} \tag{1.4.55}$$

When $I_3 = 0$ and there is no external excitation, the solutions of Eqs. (1.4.54) and (1.4.55) are the normal modes or propagating waves in the piezoelectric medium: thus these two equations vary as $v_F \sim \exp(-j\beta_a z)$ and $v_B \sim \exp(j\beta_a z)$, respectively. More generally, Eqs. (1.4.54) and (1.4.55) express the excitation of the modes of the system by external signals. As we shall see in Sec. 2.5, this normal-mode method can be generalized fairly easily and used in the same form for systems of finite cross section. We show in Sec. 2.5 that the normal-mode formulation is particularly useful for surface acoustic wave interdigital and wedge transducers.

If the center of the transducer is at $z = 0$, we can integrate Eq. (1.4.54) to yield the result

$$v_F(z) = v_F\left(\frac{-l}{2}\right)e^{-j\bar{\beta}_a(z+l/2)} + \frac{h}{2Z_C\bar{V}_a}e^{-j\bar{\beta}_a z}\int_{-l/2}^{z} e^{j\bar{\beta}_a z}I_3\,dz \tag{1.4.56}$$

Equation (1.4.56) shows that the amplitude of the forward wave at the plane $z$ depends on the wave initially propagating through the medium from the plane $z = -l/2$ and on an additional term due to the cumulative excitation by the current $I_3$ along the transducer. A similar result can be obtained for the excitation of the wave propagating in the $-z$ direction.

When $I_3$ is uniform, as it is in the transducer considered here, Eq. (1.4.56) can be integrated and written in the form

$$v_F\left(\frac{l}{2}\right) = v_F\left(\frac{-l}{2}\right)e^{-j\bar{\beta}_a l} + \frac{hI_3}{Z_C\omega}e^{-j\bar{\beta}_a l/2}\sin\frac{\bar{\beta}_a l}{2} \tag{1.4.57}$$

with

$$v_B\left(\frac{-l}{2}\right) = v_B\left(\frac{l}{2}\right)e^{-j\bar{\beta}_a l} - \frac{hI_3}{Z_C\omega}e^{-j\bar{\beta}_a l/2}\sin\frac{\beta_a l}{2} \tag{1.4.58}$$

The first term of Eq. (1.4.57) corresponds to the wave that is excited at the left-hand side of the transducer and propagates through it. The second term indicates that the current $I_3$ behaves as though it is exciting waves at the center of the transducer. These waves propagate along the transducer with amplitudes varying as $\exp(-j\bar{\beta}_a|z|)$ and reach the ends $z = \pm l/2$ with a phase delay $\bar{\beta}_a l/2$. We can formalize this concept by defining the velocities just to the right of the center of the transducer as $v_F^+$ and $v_B^+$, and the velocities just to the left of its

center as $v_F^-$ and $v_B^-$. Hence we write

$$\begin{aligned} v_F\left(\frac{l}{2}\right) &= v_F^+ e^{-j\bar{\beta}_a l/2} \\ v_B\left(\frac{l}{2}\right) &= v_B^+ e^{j\bar{\beta}_a l/2} \\ v_F\left(\frac{-l}{2}\right) &= v_F^- e^{j\bar{\beta}_a l/2} \\ v_B\left(\frac{-l}{2}\right) &= v_B^- e^{-j\bar{\beta}_a l/2} \end{aligned} \tag{1.4.59}$$

It follows from Eqs. (1.4.57)–(1.4.59) that if $I_3 = 0$, then $v_F^+ = v_F^-$ and $v_B^+ = v_B^-$. When $I_3$ is finite, then

$$v_B^+ - v_B^- = v_F^+ - v_F^- = \frac{hI_3}{Z_C\omega} \sin \frac{\bar{\beta}_a l}{2} \tag{1.4.60}$$

The total change in velocity induced by the current at the center of the transducer is therefore

$$v^+ - v^- = (v_F^+ + v_B^+) - (v_F^- + v_B^-) = \frac{2hI_3}{Z_C\omega} \sin \frac{\bar{\beta}_a l}{2} \tag{1.4.61}$$

The electrical current $I_3$ flowing into the transducer excites the backward and forward waves equally, so the ratio of induced acoustic velocity (or equivalent current) to the electrical current can be represented by a perfect transformer with a ratio 1 to $\phi$, defined on

$$\phi = \frac{\bar{\beta}_a l/2}{Z_C\omega} = k_T\left(\frac{\pi}{\omega_0 C_0 Z_C}\right)^{1/2} \operatorname{sinc} \frac{\omega}{2\omega_0} \tag{1.4.62}$$

where $\operatorname{sinc} x = \sin \pi x/\pi x$ and the center frequency of the transducer $\omega_0$ is defined from the relation $\bar{\beta}_a l = \pi$. When $\omega = n\omega_0$ and $n$ is even, the transformer ratio is zero, resulting in zero excitation. At these frequencies, the transducer is an integral number of wavelengths thick and the generated waves cancel exactly at the output terminals. As $\omega \to 0$, $\phi$ increases by $\pi/2$ from its value at $\omega = \omega_0$.

To complete the equivalent circuit, we also need to know the relationship between $T_F$, $T_B$, and $V_3$. It follows from Eq. (1.4.18) or Eq. (1.4.30) that

$$V_3 = \frac{I_3}{j\omega C_0} - \frac{h}{j\omega}\left[v\left(\frac{l}{2}\right) - v\left(\frac{-l}{2}\right)\right] \tag{1.4.63}$$

Substituting Eq. (1.4.59) into Eq. (1.4.63), we write

$$V_3 = \frac{h}{j\omega C_0}\left[(v_F^+ - v_F^- + v_B^+ - v_B^-) \cos \frac{\bar{\beta}_a l}{2} - j(v_F^+ + v_F^- - v_B^+ - v_B^-) \sin \frac{\bar{\beta}_a l}{2}\right] \tag{1.4.64}$$

From Eq. (1.4.60), we see that

$$v_F^+ - v_B^+ = v_F^- - v_B^- \tag{1.4.65}$$

Because we can write

$$T = T_F^+ + T_B^+ = T_F^- + T_B^- = (v_B^+ - v_F^+)\bar{Z}_0 = (v_B^- - v_F^-)\bar{Z}_0 \tag{1.4.66}$$

it follows that the input stress $T$ is continuous through the center terminal and is analogous to voltage. Therefore,

$$V_3 = \frac{I_3}{j\omega C_0} \cdot \frac{h^2 I_3}{j\omega^2 Z_C} \sin \bar{\beta}_a l - \frac{2hT}{\omega Z_C} \sin \frac{\bar{\beta}_a l}{2} \tag{1.4.67}$$

The first term of Eq. (1.4.67) is identified with the clamped capacitance of the transducer. The second and third terms are associated with acoustic wave excitation. The second term is a reactance $X = (h^2/\omega^2 Z_C) \sin \bar{\beta}_a l$, that is, a capacitance of value

$$C' = -\frac{C_0}{k_T^2} \frac{1}{\operatorname{sinc}(\omega/\omega_0)} \tag{1.4.68}$$

This capacitor is in series with the transducer capacity $C_0$; it is negative for frequencies where $\omega < \omega_0$ and is normally much larger than $C_0$. At resonance when $\omega = \omega_0$, $C' = \infty$; when $\omega \to 0$, then $C' \to -C_0/k_T^2$. The last term of Eq. (1.4.67) contains the transformer ratio already derived from the relationship between the electric and the equivalent acoustic currents. Thus the model is consistent for both voltage and current.

The KLM model of Fig. 1.4.12 retains close ties with the actual physical processes in an acoustic transducer. Its advantage is the use of a single central coupling point between electrical and acoustic quantities, gained at the cost of a variable series reactance and a variable transformer ratio.

**Effect of reflections on the response of a transducer to a sinusoidal signal.** We shall now use the KLM model of Fig. 1.4.12 to consider the effect of different terminations at the acoustic ports when the transducer is excited by a sinusoidal signal of frequency $\omega$. We see from Eq. (1.4.57), or from the KLM equivalent circuit, that the forward wave reaching $z = l/2$ has stress and velocity components

$$\begin{aligned} -Z_0 v_F\left(\frac{l}{2}\right) = T_F\left(\frac{l}{2}\right) &= -\frac{hI}{\omega} \qquad e^{-j\bar{\beta}_a l/2} \\ &= \frac{jhI_3}{\omega A} \qquad \frac{}{2} \end{aligned} \tag{1.4.69}$$

In Sec. 1.4.7 we show that it is better to use the second form of this equation when considering the pulse response of the transducer. But here, as there is no external acoustic excitation, we have assumed that $v_F(-l/2) = 0$.

We have written the expression for $v_F(l/2)$ on the first line of Eq. (1.4.69) as if the current $I_3$ generates a wave at the center of the transducer ($z = 0$), which

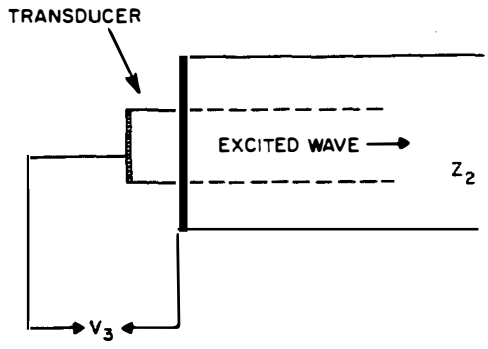


**Figure 1.4.13** Transducer used to excite a wave in a medium of impedance $Z_2$. The metal electrodes are regarded as being infinitesimally thin.

is delayed in phase by $\bar{\beta}_a l/2$ by the time it reaches $z = l/2$. This form is more convenient than, although equivalent to, writing $v_F(l/2) \propto I_3[1 - \exp(-j\bar{\beta}_a l)]$ and assuming that the wave is generated at two points, $z = -l/2$ and $z = l/2$, as it is in the Redwood model of Fig. 1.4.5.

We now consider what happens if the terminations are imperfect. In this case, it is as if the waves are produced at the center of the transducer and suffer reflections at $z = -l/2$ and $z = l/2$; thus the total stress or velocity depends on the reflection coefficients at each surface.

Suppose that we consider a transducer of the type shown in Fig. 1.4.13, with the surface $z = -l/2$ open to air (i.e., $Z_1 = 0$ at $z = -l/2$). In this case, two waves appear to be generated *at the center of the transducer* $z = 0$, as shown in Fig. 1.4.14. The velocity and stress components of the forward wave reaching $z = l/2$ are given by Eq. (1.4.69). The velocity and stress components of the backward wave reaching $z = -l/2$ are

$$Z_0 v_B\left(\frac{-l}{2}\right) = T_B\left(\frac{-l}{2}\right) = -\frac{hI_3}{\omega A}\sin\frac{\bar{\beta}_a l}{2}\, e^{-j\bar{\beta}_a l/2} \tag{1.4.70}$$

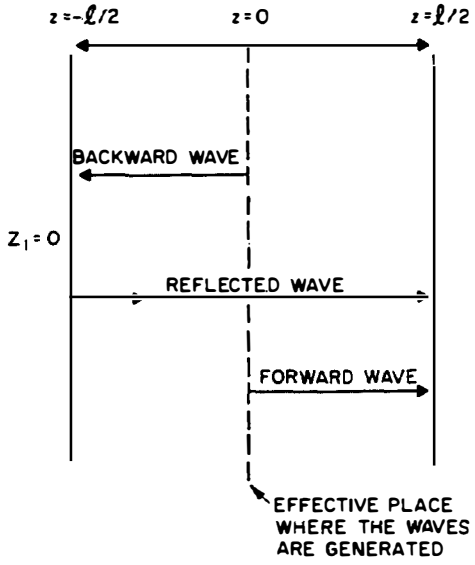


**Figure 1.4.14** Waves generated in a transducer with $Z_1 = 0$ at $z = -l/2$.

The wave is reflected at $z = -l/2$. Because of the zero-impedance boundary condition, the reflected wave has its stress $T$ of opposite sign to the incident wave. This wave suffers a further phase change $\bar{\beta}_a l$ by the time it reaches $z = l/2$. This implies that the wave suffers a total phase delay of $3\bar{\beta}_a l/2 + \pi$ from its effective point of generation to the output plane $z = l$. We therefore expect that when both waves add in phase, the output stress will be double the stress of a transducer that is perfectly matched at both ends. This occurs at $\bar{\beta}_a l = \pi$. On the other hand, because the reflected wave changes phase with frequency more rapidly than the forward wave, the bandwidth will tend to be narrower than for a transducer that is perfectly matched at both ends.

We can obtain this result in a more mathematical form by evaluating the amplitude and phase of the backward wave, after reflection and a total phase delay of $3\beta_a l/2$. In accordance with the sign convention used (where $T$ reverses in sign after reflection at $z = -l/2$), Eq. (1.4.70) yields the result

$$T_B\left(\frac{l}{2}\right) = \frac{hI_3}{\omega A} \sin \frac{\bar{\beta}_a l}{2} e^{-3j\bar{\beta}_a l/2} \tag{1.4.71}$$

Adding Eqs. (1.4.69) and (1.4.71), we see that the total stress at $z = l/2$ is

$$T\left(\frac{l}{2}\right) = -2j\frac{hI_3}{\omega A} e^{-j\bar{\beta}_a l} \sin^2 \frac{\bar{\beta}_a l}{2} \tag{1.4.72}$$

Thus $|T(l/2)|$ varies as $(\omega_0/\omega) \sin^2 (\pi\omega/2\omega_0)$. This result should be compared with Eq. (1.4.57), where $|v_F(l/2)|$ and hence $|T_F(l/2)|$ vary as $(\omega_0/\omega) |\sin (\pi\omega/2\omega_0)|$, that is, less rapidly than when the wave reflected at $z = -l/2$ is added to the forward wave component.

**Half-wave and quarter-wave resonators.** In general, if there are reflections at both surfaces of the transducer, then $T$, $v$, and $E$ will tend to be maximum when the forward and reflected waves add constructively. This occurs near a resonant condition. If $Z_1 << Z_C$ and $Z_2 << Z_C$, then $v$ and $T$ build up in amplitude when $l \approx (2n + 1)\lambda/2$, so for the strongest excitation, the resonator should be approximately a half-wavelength long. Similarly, if $Z_1 >> Z_C$ and $Z_2 << Z_C$, or if $Z_1 << Z_C$ and $Z_2 >> Z_C$, the reflections add up when $l \approx \lambda/4$; this implies that a rigidly backed resonator will show the strongest excitation near a frequency where $l \approx \lambda/4$. Thus by carefully choosing the backing and matching impedance into the medium of interest, the frequency response of the transducer can be varied and optimized at particular frequencies.

### 1.4.7 Pulse Response of a Transducer with Arbitrary Terminations

We can also consider what occurs when a pulse rather than a continuous-wave (CW) RF signal is injected into the transducer. We shall first assume that the transducer is perfectly terminated at both acoustic ports. In this case,

$v_F(-l/2) = 0$, and we can write Eq. (1.4.57) in the form

$$v_F\left(\omega, \frac{l}{2}\right) = \frac{hI_3}{2jZ_C\omega}\left(1 - e^{-j\bar{\beta}_a l}\right) \tag{1.4.73}$$

If the signal varies as exp $(j\omega t)$, the charge on the right-hand electrode is $Q = I_3/j\omega$ and that on the left-hand electrode, $-Q$. Thus, in the frequency domain, we can write

$$\frac{-T_F(\omega, l/2)}{\bar{Z}_0} = v_F\left(\ddot{\omega}, \frac{l}{2}\right) = \frac{hQ}{2Z_C}\left(1 - e^{-j\bar{\beta}_a l}\right) \tag{1.4.74}$$

We put $\bar{\beta}_a l = \omega l/\bar{V}_a = \omega T$, where $T$ is the transit time of an acoustic wave through the transducer. Then, taking the Fourier transform of Eq. (1.4.74), we see that the stress or velocity, as a function of time at $z = l/2$, is

$$\frac{_F(t,}{\bar{Z}_0} = v_F\left(t, \frac{l}{2}\right) = \frac{h}{2Z_C}\left[Q(t) - Q(t - T)\right] \tag{1.4.75}$$

This equation leads to an equally valid viewpoint of transducer operation in the time domain. A stress or velocity component proportional to the charge on the right-hand electrode is excited. The charge on the left-hand electrode excites a signal of opposite sign, which suffers a time delay $T$ before reaching $z = l/2$. If we assume in this model that $k_T^2 << 1$, the transducer behaves like a capacitor with a voltage source $V(t)$ across it. This voltage $V(t)$ is linearly proportional to the charges $Q(t)$ and $-Q(t)$ at each electrode; the transducer therefore emits signals proportional to $V(t)$. We can write

$$\frac{-T_F(t, l/2)}{\bar{Z}_0} = v_F\left(t, \frac{l}{2}\right) \approx \frac{hC_0}{2Z_C}\left[V(t) - V(t - T)\right] \tag{1.4.76}$$

or

$$T_F\left(t, \frac{l}{2}\right) = -\frac{hC_0}{2A}\left[V(t) - V(t - T)\right] \tag{1.4.77}$$

It is instructive to obtain this same result using the Redwood model of Fig. 1.4.5 for the equivalent circuit. If the transducer is terminated at each end, the Redwood circuit becomes the one shown in Fig. 1.4.15. When the coupling coefficient is sufficiently small (i.e., when $h$ is small), very little current flows through the negative capacitor. Thus we can ignore its presence. In this case, the equivalent voltage developed across the output of the transformer is $hC_0V$, and it is divided

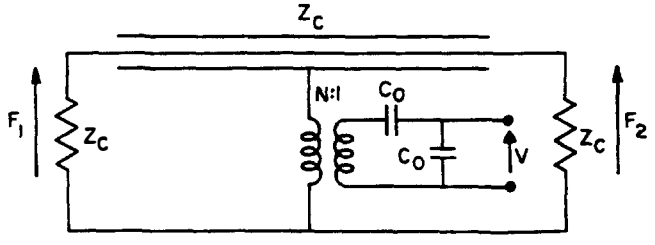


**Figure 1.4.15** Redwood circuit with terminations $Z_C$ and $N = hC_0$.

equally between the load impedance $Z_C$ and the impedance $Z_C$ of the coaxial line. Consequently, the equivalent voltages initially developed across the two loads (i.e., the forces in acoustic terms) are given by the simple relation

$$F_1(t) = F_2(t) = \frac{hC_0V(t)}{2} \tag{1.4.78}$$

The voltages developed across the coaxial line and the load are of opposite sign, as defined in Fig. 1.4.15. Consequently, the induced voltage or stress at the left-hand end of the coaxial line will propagate along it, giving rise to a stress pulse, of opposite sign to the initial stress pulse and at a later time $T$, across the right-hand load impedance $Z_C$. Using the relations $F_1 = -AT(-l/2)$ and $F_2 = -AT(l/2)$, the Redwood equivalent circuit results in Eq. (1.4.77). Thus the Redwood model demonstrates clearly that pulsed excitation makes the transducer behave as if excited by equal sources of opposite sign at each end, as shown in Fig. 1.4.16(a) and (b).

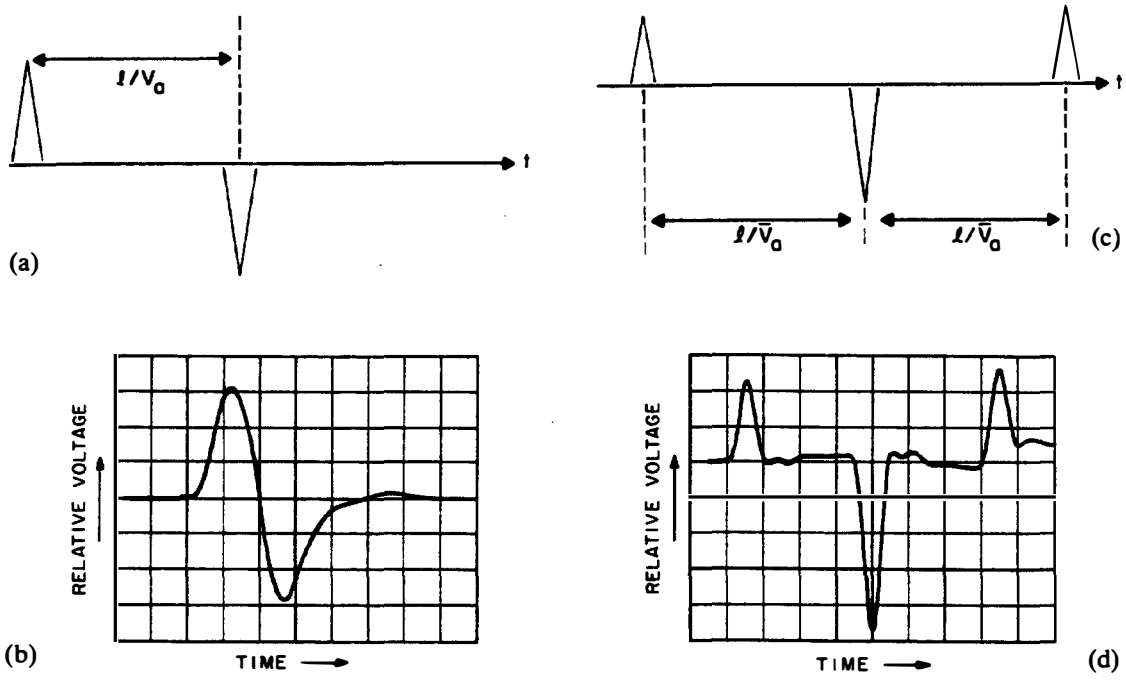


**Figure 1.4.16** Pulses generated by a transducer excited by a voltage spike. The signals are detected by a long transducer working into a low-impedance electrical load [see Eq. (1.4.63), which yields $I_3 = -hC_0v(-l/2)$ for the initial signal]. (a) Transducer terminated by a matched load at $z = 0$. (b) Corresponding experimental result obtained in the author's laboratory for a 5-MHz commercial transducer with a matched backing (Panametrics) excited by a short pulse. (c) Transducer terminated by a matched load at $z = l$ and with zero impedance at $z = 0$. (d) Corresponding result obtained in the author's laboratory with an unbacked, 2-mm-thick PZT-5A transducer excited by a short electrical pulse. Note that the experimental results tend to give pulses that are somewhat less sharp than indicated by simple theory. This is because the theory neglects finite coupling, and hence loading.

**Air-backed transducer and unmatched front surface.** An air-backed transducer terminated with an impedance $Z_2 = Z_C$ at $z = l/2$ will emit a series of three pulses, as illustrated in Fig. 1.4.16(c) and (d). The first pulse comes from the plane $z = l/2$. The second pulse has twice the amplitude of the first and is emitted from $z = -l/2$, arriving at a time $T = l/\bar{V}_a$. It is doubled in size because it corresponds to the sum of the forward and backward waves excited at the left-hand electrode. The third pulse is emitted in the backward direction from $z = l/2$; it arrives back at $z = l/2$ at a time $2l/\bar{V}_a$ after the first pulse.

Terminating the back surface of the transducer with a matched load $Z_1 = Z_C$ is a good technique for obtaining the shortest possible pulse because there is no reflection of a wave from the back surface. This is true even if the front surface of the transducer is not terminated with a matched load ($Z_2 \neq Z_C$). In this case, the Redwood equivalent circuit of Fig. 1.4.5 shows that

$$T_F(t) = -\frac{h}{A}\frac{Z_2/Z_C}{1 + Z_2/Z_C}[Q(t) - Q(t - T)] \tag{1.4.79}$$

Thus if a short voltage pulse is applied to the transducer, the output will be similar to the one shown in Fig. 1.4.16(a) and (b), differing only in amplitude from the situation when $Z_2 = Z_C$.

In practice, because the impedance of the transducer is not purely real, the transducer cannot be driven with a simple voltage spike. However, the stress excited by a transducer that is perfectly terminated at its back surface can approximate a single cycle of a sinusoidal wave when it is driven by a short pulse of current or voltage. In the same way, a transducer that is well terminated at its front surface ($Z_2 = Z_C$), but unmatched at the back surface, will give an output much like that of Fig. 1.4.16(c) and (d), although the relative amplitudes and signs of the three spikes may differ.

Matching at the back surface of the transducer tends to give a broader bandwidth but not the best efficiency. In this case, even if the front surface of the transducer is matched, half the power is lost at $z = -l/2$, and there is at least a 3-dB power loss in converting electrical to mechanical energy, or vice versa. Worse still, if the back surface is terminated with an impedance $Z_C$ and the front surface is badly mismatched, most of the electrical power entering the transducer will be dissipated in the backing. The Redwood or KLM equivalent circuits (Figs. 1.4.5 and 1.4.12, respectively) show that when a transducer is excited at the center frequency ($\omega = \omega_0$), where each half of the transducer is $\lambda/4$ long, the fraction of the input power $f$ reaching the acoustic load $Z_2$ is

$$f = \frac{Z_2}{Z_2 + Z_1} \tag{1.4.80}$$

**Example: PZT Transducer**

As an example, a PZT transducer of unit area with a matched backing ($Z_1 = Z_C = 34 \times 10^6$ kg/m$^2$-s), radiating into water, gives a fractional efficiency of $f = 0.042$, or $-13.7$ dB, when the electrical terminal is perfectly matched. If the backing impedance is reduced to $17 \times 10^6$ kg/m$^2$-s, the bandwidth decreases, and the efficiency increases to $f = 0.08$, or $-10.9$ dB.

More generally, if there are reflections at both surfaces of the transducer, it will "ring" with an output that looks like a decaying sinusoidal wave, with a period $2l/V_a$, whose decay rate depends on the acoustic mismatch and electrical loading of the transducer.

### 1.4.8 Electrical Input Impedance of a Loaded Transducer

We now consider the input impedance of a transducer used to excite a wave in a medium of impedance $Z_2$. When such a transducer is employed at UHF frequencies for a delay line, it is typically used in the configuration shown in Fig. 1.4.1(a). More generally, the back surface loading by the electrode and the backing materials, and the front surface loading by the impedances of intermediate layers between the transducer and the medium in which a wave is being excited, must be taken into account. Careful choice of these layers can optimize the bandwidth and efficiency of the transducer, although numerical calculations are normally required for a complete design of an optimized broadband transducer.

**Constructional techniques.** The transducers used in ultrahigh-frequency (UHF) delay lines (i.e., for frequencies over 100 MHz) are typically 1 to 30 μm thick. Therefore, a piezoelectric layer is normally deposited on the delay-line substrate; at the moment, the method of deposition most commonly used is sputter deposition of a material such as zinc oxide. Because the basic zinc oxide crystals have hexagonal symmetry, the individual crystallites deposited by this process need have only their $z$ axes aligned normal to the surface of the substrate to obtain strong longitudinal wave coupling. Rotation of the individual crystallites about their axes makes no difference. In practice, with a value of $k_T^2$, at least 90% of the value for a single crystal can be obtained in high-quality deposited layers. This means that the substrate must be chosen carefully and that its surface conditions must be well controlled.

Electrodes must of course be employed on either side of the piezoelectric layer. Unless the substrate is itself a conductor, a metal film such as gold, typically 1000 Å thick, is deposited on the substrate before the deposition of the piezoelectric layer. A similar film is deposited through a mask on the top surface of the transducer to form a top dot electrode, typically with a diameter of less than 1 mm. This top dot defines the effective diameter of the transducer and hence of the emitted acoustic beam.

Broadband impedance matching considerations may require that additional layers of materials, such as various metals or glasses, be deposited on the substrate before the electrode is deposited on the substrate side of the transducer. In practice, multiple layers of matching materials have only in rare instances been deposited on UHF transducers. But it is important to take account of the effect of the metal electrode on the acoustic matching.

Low-frequency broadband transducers used in the frequency range from 0.1 to 10 MHz are often made of high dielectric ($\varepsilon^S > 500\varepsilon_0$) and high-coupling-constant PZT ceramics so that they can be designed with electrical impedances of the order of 50 Ω. The full diameter of the ceramic is electroded. To obtain broadband

or short-pulse operation, the back side may be bonded to a lossy high-impedance material such as epoxy filled with tungsten, as illustrated in Fig. 1.4.1(b). Because tungsten has a very high impedance ($Z_0 = 103 \times 10^6$ kg/m$^2$-s for longitudinal waves) and epoxy has a low impedance ($Z_0 = 3.4 \times 10^6$ kg/m$^2$-s), the impedance of the composite material can be varied from $3.5 \times 10^6$ to $40 \times 10^6$ kg/m$^2$-s by changing the proportions of tungsten and epoxy. At the same time, such composites have relatively high attenuation coefficients, due to acoustic scattering by the tungsten powder and the high viscosity of the medium. Rubber-like media, such as urethane or vinyl filled with tungsten powder, provide still higher losses.

Such transducers have an excellent pulse response but are inefficient for exciting waves in a low-impedance medium such as water. To obtain high efficiency, however, it is better to use multiple quarter-wave matching layers between a PZT ceramic ($\overline{Z}_0 = 34 \times 10^6$ kg/m$^2$-s) and water ($Z_0 = 1.5 \times 10^6$ kg/m$^2$-s), employing for the layers such materials as glass ($Z_0 = 9$ to $13 \times 10^6$ kg/m$^2$-s), epoxy ($Z_0 = 3.4 \times 10^6$ kg/m$^2$-s), or filled epoxies ($Z_0 = 3$ to $12 \times 10^6$ kg/m$^2$-s). Either no backing or a low-impedance backing is used. These materials are either epoxy-bonded to each other or cast in place.

**Electrical impedance at resonance.** The impedance of the transducer at its center frequency $\omega_0$ can be found easily using the KLM equivalent circuit of Fig. 1.4.12. When $\omega = \omega_0$, the KLM circuit becomes a half-wavelength-long transmission line terminated by the impedances $Z_1$ and $Z_2$ at each end. We take $Z_1$ and $Z_2$ to be real. The effective impedance at the center point is calculated by transforming $Z_1$ and $Z_2$ through the two quarter-wavelength-long transmission lines to the center tap. At the center frequency $\omega_0$, as follows from Eq. (1.1.49), their effective values are $Z_C^2/Z_1$ and $Z_C^2/Z_2$, respectively, yielding a total shunt resistance of $R = Z_C^2/(Z_1 + Z_2)$.

The electrical radiation resistance of the transducer at its center frequency is determined by finding the electrical resistance seen on the other side of the transformer. This is

$$R_{a0} = [\phi(\omega_0)]^2 \frac{Z_C}{Z_1 + Z_2} = \frac{4k_T^2}{\pi\omega_0 C_0} \frac{Z_C^2}{Z_1 + Z_2} \tag{1.4.81}$$

This result can also be obtained directly from Eq. (1.4.23), with $\omega = \omega_0$ and $\overline{\beta}_a l = \pi$.

Because of the quarter-wavelength transformation along the transmission lines, the electrical radiation resistance $R_{a0}$ increases as $Z_1$ and $Z_2$ are decreased. When the ends are short-circuited, the radiation resistance becomes infinite, as we would expect for an unloaded loss-free transducer at the center frequency.

**Terminated transducer ($Z_1 = Z_2 = Z_C$) or $Z_1 = 0, Z_2 = Z_C$.** When the transducer is perfectly terminated at each end, the radiation resistance is $R_{a0} = 2k_T^2/\pi\omega_0 C_0$. Thus when $k_T$ is small, the radiation resistance typically is less than the series reactance $X = 1/\omega_0 C_0$ of the transducer. When the left-hand side of

the transducer is air-backed ($Z_1 = 0$), the input resistance at resonance becomes

$$R_{a0} = \frac{4k_T^2}{\pi\omega_0 C_0}\frac{Z_C}{Z_2} \tag{1.4.82}$$

Thus with $Z_2 = Z_C$, the input resistance is double that of a transducer terminated on both sides ($Z_1 = Z_2 = Z_C$) and the total input power, as opposed to half the input power, goes into the acoustic load. As we have seen, however, the bandwidth is narrower in this case.

### 1.4.9 Efficiency of Power Transfer to Transducer

We now consider frequency response and efficiency, and how matching is affected by the impedance variation of the transducer. When a transducer is terminated by a matched load $Z_2 = \overline{Z}_0$, for example, and air-backed by an impedance $Z_1 = 0$, all the electrical power entering it must appear as acoustic power in the acoustic load, which is the only resistive load present. At the center frequency $\omega = \omega_0$, it follows from Eq. (1.4.23) that the transducer exhibits zero motional reactive impedance. If $k_T << 1$, however, the electrical radiation resistance $R_{a0}$ presented by the transducer is much less than the capacitive reactance $1/\omega C_0$ in series with $R_{a0}$. Thus the transducer tends to present a highly reactive load to the input source. Typically, for most efficient operation, the series capacitance can be tuned out with an inductance, in which case the main source of loss is the resistance of the contacts, while the bandwidth may be seriously limited by the $Q$ of this tuning circuit. Often, because the timing inductance may itself be lossy, it is better to choose the source impedance to obtain maximum power into the acoustic load with a given input voltage, instead of tuning the transducer electrically. Typically, this means that the resistance of the source is chosen to equal the reactive impedance of the load.

We can derive the result by considering the equivalent circuit shown in Fig. 1.4.17. If we take the impedance of the power supply to be $R_0$, then the maximum power $P_{in}$ available from the power supply of voltage $V$, when terminated by an impedance $R_0$, is

$$P_{in} = \frac{V^2}{8R_0} \tag{1.4.83}$$

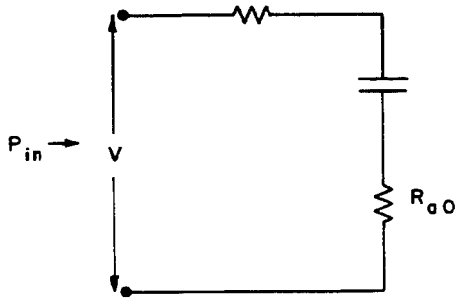


**Figure 1.4.17** Equivalent circuit of a piezoelectric transducer at its resonant frequency $\omega_0$.

The power delivered to the transducer with the same input voltage $V$ is that developed across the load $R_{a0}$. This is $P_L = R_{a0}I^2/2$, where $I$ is the current flowing in the circuit, or

$$P_L = \frac{V^2 R_{a0}}{2[(R_0 + R_{a0})^2 + (1/\omega C_0)^2]} \tag{1.4.84}$$

Thus the available input power is $P_{in}$, and the power dissipated in the radiation resistance is $P_L$. The efficiency $\eta_T$ is

$$\eta_T = \frac{P_L}{P_{in}} = \frac{4R_0 R_{a0}}{(R_0 + R_{a0})^2 + (1/\omega C_0)^2} \tag{1.4.85}$$

If we differentiate Eq. (1.4.85) with respect to $R_0$, then $\eta_T$ is maximum when $R_0 = \sqrt{R_{a0}^2 + 1/(\omega C_0)^2}$. When $R_{a0} << (1/\omega C_0)^2$, as it is when $k_T^2 << 1$, then $\eta_T$ is maximum when $R_0 \approx 1/\omega C_0$.

The maximum power transfer is

$$\begin{aligned} \eta_T(\max) &= \frac{2R_{a0}}{R_{a0} + R_0} = \frac{2R_{a0}}{R_{a0} + \sqrt{R_{a0}^2 + 1/(\omega C_0)^2}} \\ &\approx 2R_{a0}\omega C_0 \qquad \left(R_{a0} << \frac{1}{\omega C_0}\right) \end{aligned} \tag{1.4.86}$$

The mismatch is severe, however, with $R_{a0} << 1/\omega C_0$ and $R_0 \approx 1/\omega C_0$, the maximum efficiency condition when $k_T^2 << 1$.

**Example: Zinc Oxide Transducer on Sapphire**

These considerations apply to both transmitting and receiving transducers in microwave systems. As an example, we consider a half-wavelength-thick, 1-GHz zinc oxide transducer on a sapphire substrate. For longitudinal waves, $Z_C = 36 \times 10^6 A$ kg/m²-s and $Z_2 = 44.3 \times 10^6 A$ kg/m²-s, where $A$ is the area of the transducer. In this case, $l = 3.1$ μm. If the transducer is designed to have a 50-Ω reactive impedance so that it gives best efficiency with a 50-Ω source, its capacity must be 3.2 pF. With a permittivity of $\varepsilon^S = 8.8\varepsilon_0$, the area of the transducer or the metal top dot electrode is 0.13 mm², and the diameter of the circular dot is 0.4 mm. Thus the beam diameter must be fairly small, although still many wavelengths in diameter ($\lambda = 11$ μm in sapphire). The radiation resistance of the transducer at this frequency is given by Eq. (1.4.82). When $k_T = 0.28$, $R_{a0} = 4\ \Omega$ and $P_L/P_{in} = 0.16$ (i.e., there is an 8-dB input loss).

Series inductance tuning of the transducer using a lossless inductance, which is equivalent to removing the $1/\omega C_0$ term in Eq. (1.4.85), improves its acoustic conversion efficiency by 3 dB. Efficiency may be improved further by using more complicated tuning circuits or transformers. However, if the radiation resistance is only a few ohms, there will always tend to be some loss associated with the resistance of the metal films and leads. It is important to realize that in this example, $Z_2 > Z_C$. Hence, as we have already discussed in Sec. 1.4.6 and will discuss further in Sec. 1.4.11, the value of $R_a$ will tend to peak at a lower frequency, where the piezoelectric layer is a quarter-wavelength thick.

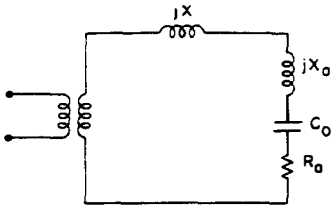


**Figure 1.4.18** Matching circuit for an acoustic transducer.

### 1.4.10 Electrical Matching of a Loaded Transducer for Optimum Bandwidth and Efficiency

We shall consider placing the transducer in an inductive circuit that can tune out its series capacity at the center frequency. In addition, we shall consider the situation when a transformer is employed for impedance matching, that is, to match $R_{a0}$ to the impedance of the input or output circuit, as shown in Fig. 1.4.18. Under these circumstances, the ratio of the electrical power transferred to the transducer to the available input power is

$$\eta_T = \frac{4R_0R_a}{(R_0 + R_a)^2 + (X + X_a - 1/\omega C_0)^2} \tag{1.4.87}$$

where $X$ is the reactance of the inductor, $R_0$ is the transformed value of the input resistance, and $Z_a = R_a + jX_a$ is the motional impedance of the transducer at an arbitrary frequency.

We first consider how the bandwidth is determined by the acoustic response of the circuit (i.e., how $R_a$ varies with frequency). In the simplest case, when $R_0 >>$ _ _ $<< 1/\omega C_0$, as occurs when the coupling coefficient $k_T^2$ is small and no electrical matching is used, then

$$\eta_T = \frac{4R_0R_a}{R_0^2 + (1/\omega C_0)^2} \tag{1.4.88}$$

Here the acoustic output of the transducer is proportional only to $R_a(\omega)$, that is, it depends only on the acoustic response as a function of frequency.

We now consider the response of a transducer placed in a matching circuit, such as the one shown with the equivalent circuit (impedance $jX_a$, $R_a$, and $1/j\omega C_0$ in series) of the transducer in Fig. 1.4.18. Its bandwidth will be limited for two reasons. First, the value of $R_a$, the radiation resistance, varies with frequency due to the acoustic properties of the transducer. This gives rise to an effective acoustic $Q$, defined as $Q = f_0/\Delta f$, where $f_0$ is the center frequency of the response and $\Delta f$ is the 3-dB bandwidth. We call the acoustic $Q$, $Q_a$. A transducer with poor acoustic matching at each end has a high value of $Q_a$; one that is well matched at each end has a low $Q_a$. The value of $Q_a$ is derived below for various types of acoustic loads. Second, the circuit used to tune out the transducer capacity, usually a series or parallel inductance, has an effective circuit $Q$ called $Q_e$ (the electrical $Q$) of value $Q_e \approx 1/\omega_0 C_0 R_{a0}$. Thus $Q_e$ tends to be small if $R_{a0} \sim 1/\omega_0 C_0$ (i.e., if the coupling coefficient $k_T$ is large).

These considerations make the PZT ceramics good choices for broadband, high-efficiency, low-frequency transducers. As a class they have a very high $k_T^2$, approximately 0.25, which makes $R_{a0}$ relatively high. They also have high dielectric constants ($\varepsilon^S = 1300\varepsilon_0$). Thus transducers designed to operate at frequencies of a few megaherz with diameters of the order of 1 cm can have capacitive reactances and input resistances of the order of 50 Ω. As this impedance is typical for most power sources, such a design leads to a system that can be reasonably well matched over a wide frequency range.

We shall now use the KLM circuit model of Fig. 1.4.12 to obtain a physical understanding of the matching problem. In Sec. 1.4.11 we shall also deal with a technique known as the Reeder–Winslow mathematical design method, illustrating it, for simplicity, only by reference to air-backed transducers [11]. The powerful and simple Reeder–Winslow formalism provides further insight into the design criteria for optimum efficiency and bandwidth.

**Transducer acoustically matched at each end, $Z_1 = Z_2 = Z_C$.** As a simple example of the KLM model, we consider both sides of the transducer to be terminated with a matching load so that $Z_1 = Z_2 = Z_C$. In this case, the acoustic response of the circuit is due only to the response of the transformer. It therefore follows from Eq. (1.4.23), or from the KLM model, that we can define a normalized radiation resistance $M_r(f)$ ($f = \omega/2\pi$ and $f_0 = \omega_0/2\pi$) as

$$M_r(f) = \frac{R_a}{R_{a0}} = \left(\frac{f_0}{f}\right)^2 \sin^2 \frac{\pi f}{2f_0} = \left(\frac{\pi}{2} \operatorname{sinc} \frac{f}{f_0}\right)^2 \tag{1.4.89}$$

where $\operatorname{sinc} x = (\sin \pi x)/\pi x$, and

$$R_{a0} = \frac{k_T^2}{\pi^2 f_0 C_0} \tag{1.4.90}$$

This function is plotted in Fig. 1.4.19. From the solid-line plot, we see that $M_r(0) = 2.47$ and $M_r(0.89\ f_0) = 1.23$. Hence the 3-dB acoustic bandwidth of the transducer lies in the frequency range from zero to $0.89f_0$, and the transducer acoustic response is like that of a low-pass filter because of the $(f_0/f)^2$ term in $M_r(f)$.

A transducer terminated by finite impedances on both sides has a finite response down to zero frequency. Physically, this is because the back of the transducer can push against an infinitely long backing, even at zero frequency, and thus move its front surface. An air-backed transducer cannot do this; thus at zero frequency, it cannot deliver power into the medium at its front surface. In practice, with a finite-length backing held in a rigid mount that is attached to the load, there will be a finite response at zero frequency.

**Air-backed transducer matched at output, $Z_1 = 0$, $Z_2 = Z_C$.** In this case, the KLM model of Fig. 1.4.12, or the use of Eq. (1.4.23), indicates that the

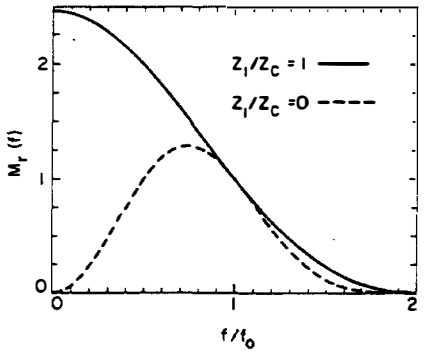


**Figure 1.4.19** Plots of $M_r(f)$ for a transducer matched at its front surface ($Z_2 = Z_C$). Solid line: transducer with a matched backing ($Z_1 = Z_C$); dashed line: the real part of the normalized input radiation resistance for an air-backed transducer ($Z_1 = 0$).

real part of the normalized input radiation resistance is

$$M_r(f) = \frac{R_a}{R_{a0}} = \left(\frac{f_0}{f}\right)^2 \sin^4 \frac{\pi f}{2f_0} \tag{1.4.91}$$

where

$$R_{a0} = \frac{2k_T^2}{\pi^2 f_0 C_0} \tag{1.4.92}$$

This normalized function is plotted as the dashed line in Fig. 1.4.19. Note that an air-backed transducer has twice the value of $R_{a0}$ of a transducer with $Z_1 = Z_C$.

The $(f_0/f)^2$ term makes the response maximum with a value of $R_a = 1.30R_{a0}$ at $f = 0.74f_0$. The response drops to $R_a = 0.65R_{a0}$ where $f = 0.365f_0$ and $f = 1.16f_0$. Thus the bandwidth is 107% of the frequency of maximum response. (*Note:* In both examples we have ignored the series reactance of the transducer.)

**Example: Acoustic Emission Transducer**

These results have important implications for the design of transducers with a broad frequency response. A good example is an acoustic emission receiving transducer. When solid materials are highly stressed, small cracks and defects develop. As these defects appear, they emit sound. Creaking wood is a familiar example of this phenomenon. Such acoustic emission occurs over a very wide frequency range and can be detected by a small transducer placed in contact with the cracked material. A wideband transducer is obviously desirable. Therefore, a transducer with a solid rather than an air backing must be used to give an almost constant response down to very low frequencies. The large series reactance of the transducer at low frequencies requires an extremely high impedance electrical load on the transducer.

**$Z_1 < Z_C$ and $Z_2 < Z_C$.** We now consider the situation where $Z_1$ and $Z_2$ are smaller than $Z_C$ and purely resistive, and the input circuit is inductively tuned. The KLM equivalent circuit of Fig. 1.4.12 becomes a center-tapped transmission line terminated by a load $Z_1$ at one end and a load $Z_2$ at the other. When $Z_1$ and $Z_2 < Z_C$, the transmission line has a resonance close to $\omega_0$. The approximate acoustic $Q$ of the resonator, which we call $Q_a$, can be calculated by transforming the impedances $Z_1$ and $Z_2$ through quarter-wave transmission lines to the center tap, where they have effective values of $Z_C^2/Z_1$ and $Z_C^2/Z_2$, respectively, at the center frequency. The total resistance is $R_{sh} = Z_C^2/(Z_1 + Z_2)$. Two shorted

quarter-wave transmission lines, with a total reactive impedance $X = (Z_C/2) \tan (\pi f/2f_0)$, are placed in parallel with this resistance. Thus the shunt reactance is infinite at $f = f_0$. The resistive load due to this parallel circuit is

$$R = \frac{R_{sh}}{1 + R_{sh}^2/X^2} \tag{1.4.93}$$

We can define the effective values of $Q$ and $Q_a$ by the 3-dB bandwidth of these points (i.e., the points where $X = R_{sh}$) to yield the result for $(Z_1 + Z_2) \ll Z_C$ that

$$Q_a \approx \frac{\pi}{2} \frac{Z_C}{} \tag{1.4.94}$$

When $Z_1 \approx Z_C$ and $Z_2 \approx Z_C$, the value of the acoustic $Q$, $Q_a$, is lower than this approximate formula implies, as we have already seen for the extreme cases of transducers with $Z_1 = 0$, $Z_2 = Z_C$, and $Z_1 = Z_2 = Z_C$.

A more rigorous treatment follows along similar lines to the derivation used to obtain the equivalent circuits of Figs. 1.4.8 and 1.4.9. Equation (1.4.23) gives the exact impedance of the transducer; this reduces to the model where $(Z_1 + Z_2) \ll Z_C$ and $|f - f_0| \ll f_0$, which we have already derived from the KLM equivalent circuit of Fig. 1.4.12. The negative series capacity $C'$ in the KLM equivalent circuit varies with frequency; it must therefore be treated as a variable reactance $X$, which we write as $X = -(k_T^2/j\omega C_0) \operatorname{sinc} (\omega/\omega_0)$. This reactance can be expressed in the form of a series resonator, using the relation

$$\operatorname{sinc} z = \frac{\sin \pi z}{\pi z} = \prod_1^\infty \left(1 - \frac{z^2}{n^2}\right) \tag{1.4.95}$$

and keeping only the $n = 1$ term. The properties of the transmission line can be represented by a series expansion, as we did in Sec. 1.4.3. Keeping only one term, the transmission line is replaced by a parallel resonant circuit with a shunt resistance $R_{sh}$ across it. If we ignore the variation with frequency of the turns ratio of the transformer, we obtain the equivalent circuit for the parameters on the input side of the transformer, shown in Fig. 1.4.20(a).†

When $k_T^2$ is small, the series resonant circuit can usually be ignored and the equivalent circuit reduces to that of Fig. 1.4.20(b). This equivalent circuit is identical to the one derived earlier shown in Fig. 1.4.9(c).

**Optimum value of the acoustic load with the source resistance $R_0 = 0$.** The electrical $Q$, $Q_e$, of the tuning circuit increases as the acoustic load of a transducer is decreased, while the acoustic $Q$, $Q_a$, decreases. Therefore, there is an optimum acoustic load for maximum bandwidth, which we shall derive here.

As we have seen, the electrical radiation resistance of the air-backed trans-

†If the variation of the transformer turns ratio with frequency in the KLM model is taken into account, the effective value of $R_a$ is multiplied by $(\omega_0/\omega)^2$ near the center frequency. This makes the maximum value of $R_a$ occur at a frequency lower than $\omega_0$.

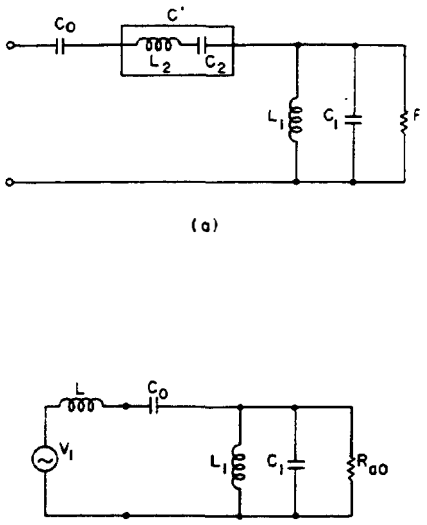


**Figure 1.4.20** (a) Equivalent circuit for a loaded transducer. A similar circuit is shown in Fig. 1.4.9(b). $C_1 = C_0\pi^2/8k_T^2$, $L_1 = 1/\omega_0^2 C_1$, $C_2 = -C_0/k_T^2$, $L_2 = 1/\omega_0^2 C_2$, and $R_{a0} = (4k_T^2/\pi\omega_0 C_0)[Z_C/(Z_1 + Z_2)]$. (b) Simplified form of the equivalent circuit shown in part (a), which is identical to the one shown in Fig. 1.4.9(c). It is illustrated with an external series tuning inductance $L$.

ducer at its center frequency is

$$R_{a0} = \frac{4k_T^2}{\pi\omega_0 C_0}\frac{Z_C}{Z_1 + Z_2} \tag{1.4.96}$$

Suppose that the circuit is supplied by a constant voltage source ($R_0 = 0$) through an inductance $L$, as illustrated in Fig. 1.4.20(b). Then, near the center frequency, the series resonant circuit has zero impedance, the parallel resonant circuit has infinite impedance, and $R_a = R_{a0}$. Thus the electrical $Q$ at the center frequency of the transducer (i.e., of the series part of the circuit) is $Q = Q_e$, where

$$Q_e = \frac{1}{\omega_0 C_0 R_{a0}} = \frac{\pi}{4k_T^2}\frac{Z_1 + Z_2}{Z_C} \tag{1.4.97}$$

We note from Eq. (1.4.94) that as $Z_1 + Z_2$ is decreased, the acoustic $Q$, $Q_a$, increases and the electrical $Q$, $Q_e$, decreases. Thus the optimum bandwidth of the transducer is obtained with $Q_e = Q_a$. This yields the relations

$$\frac{Z_1 + Z_2}{Z_C} = k_T\sqrt{2} \tag{1.4.98}$$

and

$$Q_e = Q_a = \frac{\pi}{2\sqrt{2}k_T} \tag{1.4.99}$$

The effective $Q$ of the tuned system is approximately $Q_e\sqrt{2}$. Thus

$$\frac{\Delta f\,(3\text{ dB})}{f_0} \approx \frac{2k_T}{\pi} \tag{1.4.100}$$

So for a low value of $k_T$, an optimum bandwidth with the highest efficiency possible can be obtained with a low value of $(Z_1 + Z_2)/Z_C$.

**Optimum value of the acoustic load with electrical tuning and source impedance $R_0 = R_{a0}$.** In this case, the electrical $Q$, $Q_e$, is half the value given by Eq. (1.4.97), or

$$Q_e = \frac{\pi}{8k_T^2}\frac{Z_1 + Z_2}{Z_C} \tag{1.4.101}$$

Putting $Q_e = Q_a$, it follows that

$$\frac{\Delta f\,(3\text{ dB})}{f_0} \approx \frac{4k_T}{\pi} \tag{1.4.102}$$

with the optimum value of $Z_1 + Z_2$ increased by a factor of $\sqrt{2}$ from that given in Eq. (1.4.98). Thus the bandwidth of the transducer, under optimum matching conditions for high-efficiency operation, is controlled by the coupling coefficient $k_T$. For low-efficiency operation with a mismatched electrical circuit, we can obtain the largest bandwidth by using a low value for the acoustic $Q$, $Q_a$, and hence relatively large values for $(Z_1 + Z_2)/Z_C$. On the other hand, with a tuned input circuit, we can use high-coupling-coefficient materials, such as PZT or lithium niobate, that have $k_T = 0.5$. Then the optimum load is given by the condition $(Z_1 + Z_2)/Z_C = 0.7$, and we can obtain bandwidths of nearly one octave with high efficiency.

**Tuned and untuned transducer, $Z_1 = Z_2 = Z_C$.** As we have seen in Sec. 1.4.9, if the device is untuned, the minimum power loss will occur with a generator impedance of $R_0 \approx \sqrt{R_{a0}^2 + (1/\omega C_0)^2}$. For $Z_1 = Z_2 = Z_C$, it follows from Eqs. (1.4.86) and (1.4.90) that this condition corresponds to a power transfer efficiency $\eta$ from the generator to the load at the center frequency $f_0$ of

$$\eta = \frac{1}{1 + (1 + \pi^2/4k_T^4)^{1/2}} \tag{1.4.103}$$

This formula takes into account the 3-dB loss due to power being emitted from both acoustic ports. Therefore, to obtain high efficiency with an untuned transducer, we must use as high a coupling coefficient $k_T$ as possible. In such a case, the best one-way efficiency we can expect from a PZT ceramic with $k_T^2 = 0.25$ is 13.6%; this transducer has a minimum round-trip insertion loss of 17.3 dB and a low-pass bandwidth characteristic.

Tuning further lowers the minimum round-trip loss, ideally to 6 dB. With $k_T^2 = 0.25$, it follows from Eqs. (1.4.94) and (1.4.97) that when $Z_1 + Z_2 = Z_C$, the resultant electrical bandwidth of 32% is the controlling factor. From Eq. (1.4.101), a constant voltage source lowers the bandwidth to 16%. Therefore, we want as large a coupling coefficient as possible, to increase $R\omega_0 C_0$ and thus lower the electrical $Q$ of the tuning circuit.

**Tuned and untuned air-backed transducer with $Z_2 = Z_C$.** We can make the transducer more efficient by leaving its left-hand side air-backed, that is, short-circuiting the left-hand transmission line in the KLM model of Fig. 1.4.12. In this

case, if the right-hand transmission line is terminated by an impedance $Z_2 = Z_C$, the effective resistance at the center terminals of the KLM circuit is doubled and the one-way optimized untuned efficiency at the center frequency is

$$\frac{2}{1 + (1 + \pi^2/16k_T^4)^{1/2}} \tag{1.4.104}$$

For $k_T^2 = 0.25$, this corresponds to 46.5% efficiency. The electrical bandwidth of the untuned system is now approximately 100%. The series-tuned system with $R_0 = R_{a0}$ will have an electrical bandwidth (the controlling bandwidth) of approximately 64%.

### 1.4.11 Reeder–Winslow Design Method for Air-Backed Transducers

A more direct mathematical formulation for piezoelectric transducer design has been given by Reeder and Winslow [11]. Their technique has been used extensively as a guide to designing very high frequency transducers laid down on a solid substrate. It involves calculating the real and imaginary parts of the input impedance of an air-backed piezoelectric resonator for different values of $Z_2/Z_C$ ($Z_1 = 0$), and using the resultant curves as a basis for design. This procedure can be generalized for $Z_1$ finite, but it is not so convenient to work with the added variable this introduces. In such cases, it is better to use the KLM model of Fig. 1.4.12, or the Mason model of Fig. 1.4.4, first, to obtain some physical insight into the problem before resorting to numerical procedures.

Reeder and Winslow considered an air-backed transducer ($Z_1 = 0$) in contact with a solid substrate ($Z_2$ finite). They expressed the acoustic component $Z_a$ of the input impedance of the transducer in a normalized form, symmetric about the center frequency $f_0$, as follows:

$$Z_a = R_{a0}\left(\frac{f_0}{f}\right)^2 H_a(f) \tag{1.4.105}$$

We shall also find it convenient to define a second normalized quantity $M_a(f)$ that completely takes account of the variation of $Z_a$ with frequency. Therefore, we write

$$Z_a = R_{a0}M_a(f) \tag{1.4.106}$$

where

$$M_a(f) = \left(\frac{f_0}{f}\right)^2 H_a(f) \tag{1.4.107}$$

The radiation resistance at the resonant frequency $f = f_0$ ($\bar{\beta}_a l = \pi$) is defined by the relation

$$R_{a0} = \frac{2k_T^2 Z_C}{\pi^2 f_0 C_0 Z_2} \tag{1.4.108}$$

The parameters $H_a(f)$ and $M_a(f)$ are complex quantities. Thus we write

$$H_a(f) = H_r(f) + jH_i(f) \tag{1.4.109}$$

and

$$M_a(f) = M_r(f) + jM_i(f) \tag{1.4.110}$$

From Eq. (1.4.23), with $Z_1 = 0$,

$$H_r(f) = \frac{1}{4}\left(\frac{Z_2}{Z_C}\right)^2 \frac{[1 - \cos(\pi f/f_0)]^2}{1 + [(Z_2/Z_C)^2 - 1]\cos^2(\pi f/f_0)} \tag{1.4.111}$$

and

$$H_i(f) = \frac{1}{2}\frac{\sin(\pi f/f_0)\{1 + [1/2(Z_2/Z_C)^2 - 1]\cos(\pi f/f_0)\}}{1 + [(Z_2/Z_C)^2 - 1]\cos^2(\pi f/f_0)} \tag{1.4.112}$$

Figure 1.4.21 gives plots of $H_r(f)$ and $H_i(f)$ as functions of $f/f_0$ for different values of $Z_2/Z_C$. This normalization procedure is convenient because $H_r(f)$ and $H_i(f)$ are symmetric functions of $(f - f_0)$. Plots of $M_r(f)$ and $M_i(f)$ are given in Fig. 1.4.22.

When $Z_2 = Z_C$, then

$$H_r(f) = \sin^4\frac{\bar{\beta}_a l}{2} = \sin^4\left(\frac{\pi}{2}\frac{f}{f_0}\right) \tag{1.4.113}$$

Thus the 3-dB power points of $H_r(f)$ are at $f = 0.64f_0$ and $f = 1.36f_0$. The bandwidth is $\Delta f/f_0 = 0.72$. This result may be compared to the value of $\Delta f/f_0 = 0.79$, calculated for the bandwidth of $M_r$ with a frequency of maximum response at $f_M = 0.74f_0$ and with $\Delta f/f_M = 1.07$. Therefore, an estimate of the effective bandwidth of $H_r(f)$ gives a conservative estimate of the actual bandwidth, and a somewhat pessimistic estimate of $Q_a$, the acoustic $Q$.

By choosing $Z_2 << Z_C$, the bandwidth decreases when $Z_2/Z_C$ is decreased, as we have shown in Eq. (1.4.96) and can observe from Fig. 1.4.21(a). In this case,

$$H_r(f) \approx \left[\left(\frac{Z_C}{Z_2}\right)^2 \sin^2\pi\left(\frac{f - f_0}{f_0}\right) + 1\right]^{-1} \tag{1.4.114}$$

or

$$H_r(f) \approx \left[1 + \left(\frac{\pi(f - f_0)}{f_0}\frac{Z_C}{Z_2}\right)^2\right]^{-1} \tag{1.4.115}$$

Defining $Q$ as $f/\Delta f(3\text{ dB})$, the spacing $\Delta f(3\text{ dB})$ between the 3-dB points of $H_r(f)$ gives the effective acoustic $Q$, $Q_a$, of the resonator as

$$Q_a = \frac{1}{2}\left|\frac{f_0}{f(3\text{ dB}) - f_0}\right| = \frac{\pi Z_C}{2Z_2} \tag{1.4.116}$$

This result is the same as Eq. (1.4.94), which we derived using the KLM equivalent

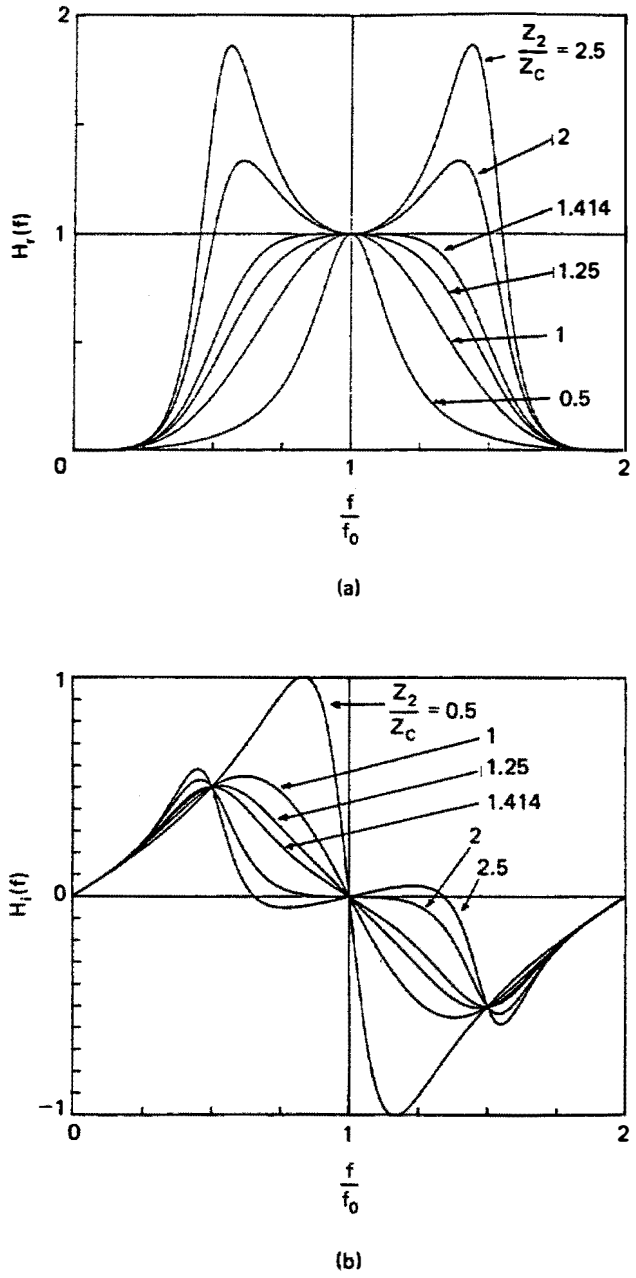


**Figure 1.4.21** Acoustic bandshape function $H_a(f)$ for a thin disk unbacked transducer, plotted as a function of normalized frequency. $Z_C$ and $Z_2$ are the characteristic mechanical impedances of the transducer medium and the medium in which the wave is being excited, respectively. (a) $H_r(f)$, real part of the bandshape function; (b) $H_i(f)$, imaginary part of the bandshape function.

circuit of Fig. 1.4.12. Note that this result also applies to $M_r(f)$, and hence $R_a(f)$, when $Z_2 << Z_C$. For $Z_2/Z_C = \sqrt{2}$, the exact acoustic response function $H_r(f)$ is maximally flat. Beyond this point, when $Z_2/Z_C > \sqrt{2}$, there are peaks on both sides of $f_0$.

The basic physical reason for the sharp response near $f/f_0 = 1$ is that when $Z_2 << Z_C$, the transducer exhibits a strong resonance when $l \approx \lambda/2$. When $Z_2/Z_C$ is very large, the peaks in $H_r(f)$ tend to occur at $f = 0.5f_0$ and $f = 1.5f_0$ because the reflection at $z = l$ tends to make the transducer resonant when its thickness is one quarter-wavelength or three-quarters of a wavelength.

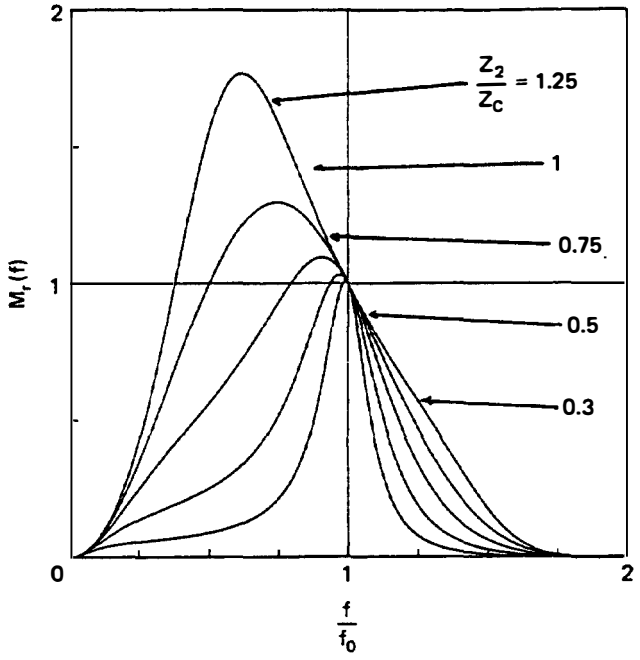


(a)

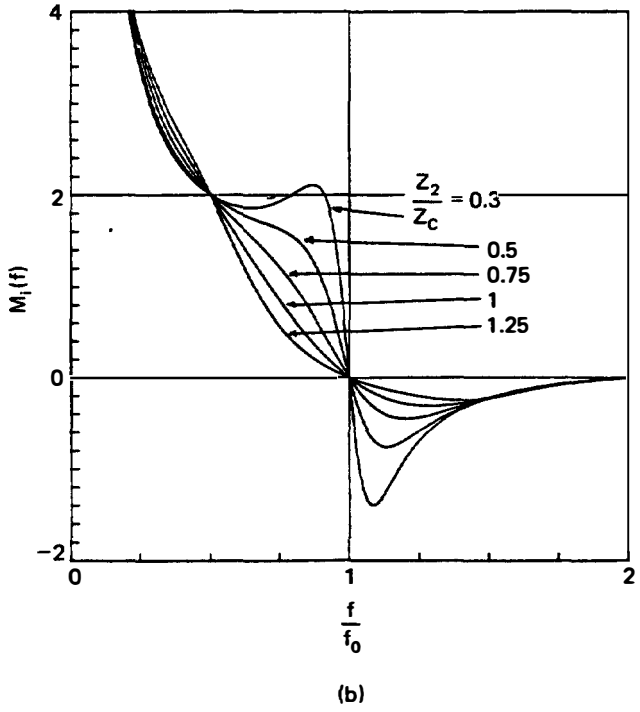


(b)

**Figure 1.4.22** Acoustic bandshape $M_a(f)$ function for a thin disk unbacked transducer plotted as a function of normalized frequency: (a) $M_r(f)$, real part of the bandshape function; (b) $M_i(f)$, imaginary part of the bandshape function.

**Example: $Z_1$ or $Z_2 >> Z_C$**

A zinc oxide thin-film air-backed transducer on a high-impedance substrate, such as sapphire, tends to resonate nearer $l = \lambda/4$ than $l = \lambda/2$. This gives broadband characteristics and leads to the use of thinner films, which is convenient because of the long sputter deposition times such films often require.

Furthermore, it follows from Eq. (1.4.112) or Figs. 1.4.21(b) and 1.4.22(b) that when $f = f_0/2$, then $H_i(f) = 0.5$ and $M_i(f) = 2$. So, at this frequency, the motional reactance is inductive and tends to cancel out the reactance of the series capacity. When $k_T^2/\pi = 1$ or $k_T^2 = 0.39$, the input impedance of the transducer is purely real at a frequency $f = f_0/2$. It may therefore be possible to make a PZT transducer, without external tuning, that can operate in an extensional mode ($k_{z3}^2 \approx 0.5$) and is well matched to a source with a real input impedance. At the same time, it is useful to choose the impedance $Z_2$ so that the real part of the transducer impedance is maximum at this frequency $f = f_0/2$.

It is also interesting to consider some practical examples for the situation when either $Z_1 > Z_C$ and $Z_2 < Z_C$ or $Z_1 < Z_C$ and $Z_2 > Z_C$. If a rigid backing is employed with a relatively low impedance front layer, the transmission line in the KLM model of Fig. 1.4.12 tends to resonate when it is a quarter-wavelength or three-quarters of a wavelength long and, by symmetry, the input impedance is the same as when $Z_1 = 0$ and $Z_2 > Z_C$. Thus the resonant frequency is halved. If the backing is perfectly rigid ($Z_1 = \infty$), the value of $R_{a0}$, with a given $Z_2$ at a center frequency $f = f_0/2$, is halved from the $R_{a0}$ value of the equivalent half-wavelength-long air-backed resonator. In this case, however, the frequency response is broader-band and the pulse response can be as narrow as that of a half-wavelength-long resonator with $Z_1 = Z_C$, like the one shown in Fig. 1.4.16(a) and (b).

A very important practical example of this phenomenon is the plastic piezoelectric material polyvinylidene difluoride ($PVF_2$), which has a longitudinal wave velocity of 2.2 km/s and an impedance of $3.92 \times 10^6$ kg/m$^2$-s, and thus can match reasonably well to water if used with a rigid backing such as brass, which has an impedance of $31 \times 10^6$ kg/m$^2$-s. This material has a low value of $k_T$ ($k_T = 0.11$), so its electrical efficiency is poor. However, very little power is lost at the acoustic mismatch into water. Thus it has outstanding broadband short-pulse performance as a receiving transducer exciting a high-impedance unmatched electrical load (see Probs. 6 and 7).

We can calculate the true response of a transducer by multiplying the response function $H_a(f)$ by $(f_0/f)^2$. This yields the true skewed response function $M_a(f)$, which is plotted in Fig. 1.4.22. It follows from Eqs. (1.4.107) and (1.4.115) that if $Z_2 < Z_C$, then

$$M_r(f) \approx \left(\frac{f_0}{f}\right)^2 \left[1 + \left(\frac{\pi(f - f_0)}{f_0}\frac{Z_C}{Z_2}\right)^2\right]^{-1} \tag{1.4.117}$$

Thus the response function for $M_r(f)$ or $R_a(f)$ is skewed and tends to peak at a lower frequency. We can obtain a similar result with the KLM model of Fig. 1.4.12 if we take account of how the transformer turns ratio varies with frequency.

It can be shown from Eq. (1.4.117) that if $(Z_2/Z_C\pi)^2 << 1$, the maximum

value of $R_a$ occurs when $f = f_M$, where $f_M$ is given by the relation

$$\frac{f_M}{f_0} \approx 1 - \frac{Z_2^2}{Z_C^2 \pi^2} \tag{1.4.118}$$

It follows from Eqs. (1.4.98) and (1.4.118), or from the derivation given in this section, that for optimum electrical matching from a constant-voltage zero-impedance source, $Z_2 = Z_C k_T \sqrt{2}$. This implies that

$$\frac{f_M - f_0}{f_0} = 1 - \frac{2k_T^2}{\pi^2} \tag{1.4.119}$$

at the point where $R_a$ is maximum.

Thus, when the criteria for electrical matching are satisfied for $k_T^2 = 0.25$ (PZT-5A) and $Z_2 = 0.7Z_C$, $R_a$ is maximum at 95% of the resonant frequency of the transducer. The result given in Eq. (1.4.118) is apparent in the theoretical curve of Fig. 1.4.22(a). Equation (1.4.119) implies that when a quarter-wavelength matching layer is designed for a transducer, it should be optimized for the frequency $f_M$, rather than for the shunt resonant frequency $f_0$ of the transducer.

The results of this analysis are identical to those that can be obtained with the KLM equivalent circuit of Fig. 1.4.12, in which the transformer response skews the response function. On the other hand, the KLM model provides a more general physical picture of the frequency behavior of the transducer which allows us to consider terminations at both its ends. We conclude that both the KLM model and the Reeder–Winslow model provide useful criteria for choosing the design parameters of a broadband transducer. In general, however, it is still necessary to make a final check of the design with numerical procedures. This is particularly important when electrical matching conditions must also be considered.

### 1.4.12 Some Examples of Transducer Design

The design criteria we have given in Secs. 1.4.10 and 1.4.11 lead to a good understanding of the optimum parameters required for efficient operation of a transducer with a large bandwidth. In practice, it is not always easy to obtain materials with the optimum values of $Z_1$ or $Z_2$, although this can usually be achieved by using one or more acoustic matching layers, each approximately a quarter-wavelength thick at the center frequency.

As we saw in Sec. 1.4.7, we expect optimum pulse responses when the back of the transducer is well terminated. More generally, Fourier transform theory leads to the conclusion that we can obtain a Gaussian-shaped pulse if the amplitude response of the transducer, as a function of frequency, is Gaussian, while at the same time its phase response is flat or varies linearly with frequency. A distortion in the phase response gives severe ringing in the pulse response. Such effects tend to show up when multiple matching layers are employed.

Figures 1.4.23–1.4.27 illustrate some examples of experimental results obtained with PZT-5A transducers. Figure 1.4.23 shows a longitudinal wave PZT-4 transducer with no matching layers, a lossy tungsten–epoxy backing of impedance $26 \times 10^6$ kg/m$^2$-s, and an acoustic $Q$ of value $Q_a = 2.05$. The transducer disk

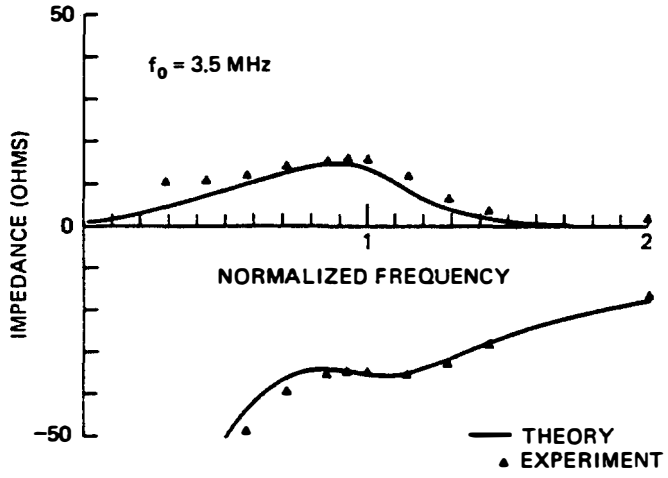


(a)

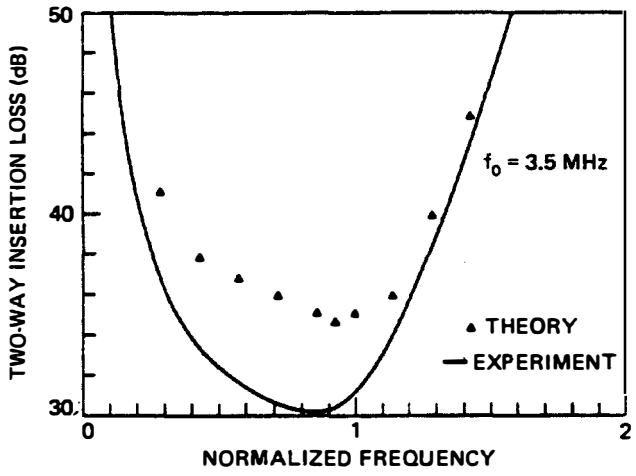


(b)


(c)

**Figure 1.4.23** Comparison of experimental results with theory for a PZT-4 transducer matched with a high-loss, high-impedance backing (solid curve, theory; dots, experimental results): (a) electrical impedance; (b) two-way insertion loss; (c) theoretical and experimental impulse responses. (After DeSilets et al. [10].)

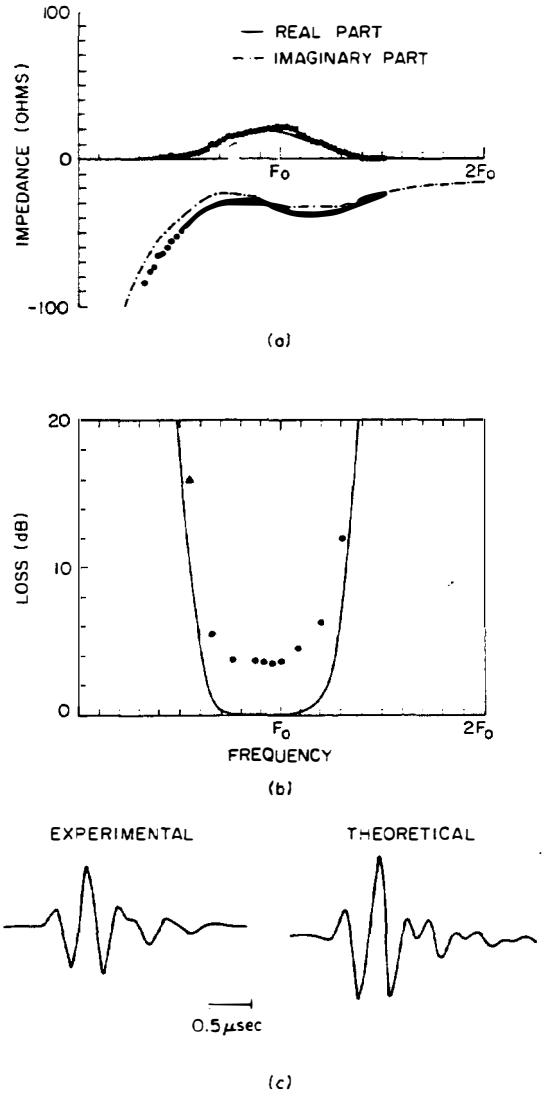


**Figure 1.4.24** Comparison of experiment with theory for a 19-mm-diameter, 3.4-MHz PZT transducer with matching layers of impedance, $2.45 \times 10^6$ kg/m$^2$-s and $8.91 \times 10^6$ kg/m$^2$-s, and no backing (solid curve, theory; dots, experimental results): (a) electrical impedance; (b) two-way insertion loss; (c) theoretical and experimental impulse responses.

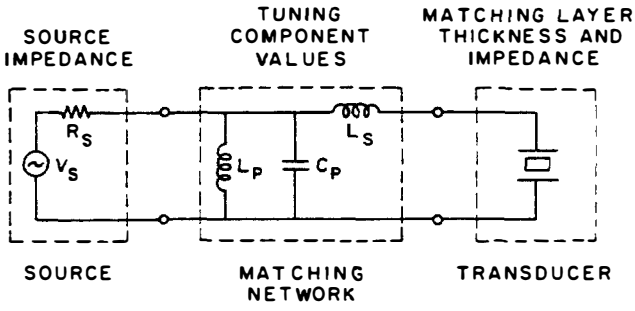


**Figure 1.4.25** Transducer and driving network to be optimized. (After Selfridge et al. [12].)

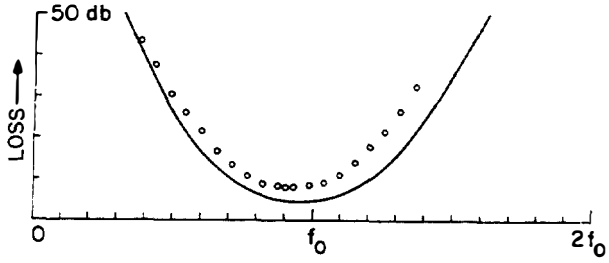


**Figure 1.4.26** Measured insertion loss compared with theory: solid curve, theory; circles, experimental results. (After Selfridge et al. [12].)

was 12.7 mm in diameter with a resonant frequency of 3.5 MHz; its important material parameters were $k_T^2 = 0.24$, $\varepsilon = 730\varepsilon_0$, and $Z_0 = 34 \times 10^6$ kg/m$^2$-s. The impedance, insertion loss, and impulse response were measured by determining the power into a matched 50-$\Omega$ electrical load after reflection from a perfect acoustic reflector. No electrical tuning was employed and a 50-$\Omega$ source was used. The distance between the transducer and the reflector was 3.0 cm.

In the impedance plot of Fig. 1.4.23(a), note the small value of the resistance compared to the reactance at the center frequency. (This would have led to a high $Q$, as well as a narrow bandwidth, if electrical tuning had been used.) The insertion-loss plot of Fig. 1.4.23(b) shows the very high loss and the broad, smooth

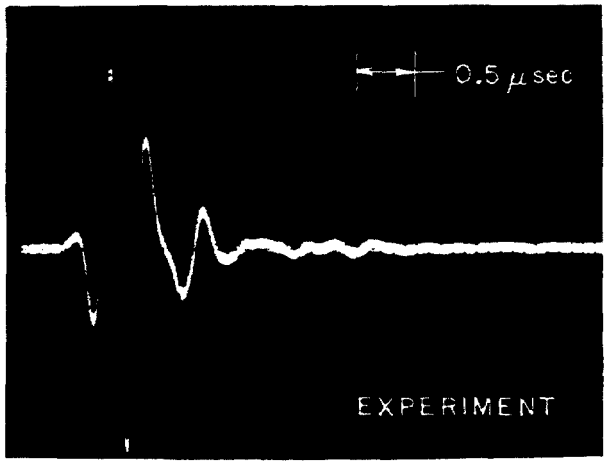


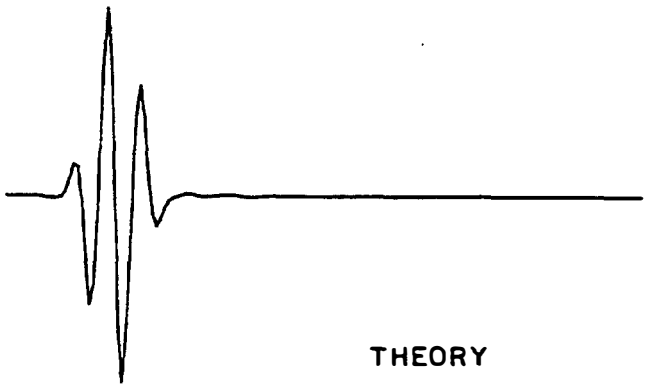


**Figure 1.4.27** Measured impulse response compared with theory. (After Selfridge et al. [12].)

bandshape characteristic of such transducers. The measured two-way insertion loss of 34.5 dB was about 3.3 dB worse than the theoretical value of 30.2 dB for a lossless transducer material; this loss can be attributed to the finite loss of the transducer material. Calculations of commercial transducers that account for loss, when present, in the transducer material and matching layers usually give excellent agreement with theory. The 3-dB bandwidth is 105%, so the very narrow impulse response that results remains the outstanding property. Note that the effective center frequency $f_M$, where $R_a$ is maximum, is lower than the resonance frequency $f_0$. With $Z_1 = 26 \times 10^6$ kg/m$^2$-s, we expect, from the simple formula of Eq. (1.4.118) with $Z_2$ replaced by $Z_1$, that $f_M/f_0 \approx 0.94$.

Figure 1.4.24 shows results for a transducer with two quarter-wave matching layers on an air-backed 19 mm PZT disk whose resonant frequency is 2.3 MHz. The transducer material parameters were $k_T^2 = 0.25$, $\varepsilon = 830\varepsilon_0$, and $\overline{Z}_0 = 31.6 \times 10^6$ kg/m$^2$-s. Two matching layers were made, one of silicon carbide–loaded epoxy with an impedance of $8.91 \times 10^6$ kg/m$^2$-s, the other of an epoxy with an impedance of $2.45 \times 10^6$ kg/m$^2$-s. These matching layers were designed, using criteria of Riblet [4] and DeSilets et al. [10], to give an approximate maximally flat response. Calculations indicated that the impedance presented by the matching layers at the transducer surface was $19.8 \times 10^6$ kg/m$^2$-s, leading to $Q_a = 2.5$. From Eq. (1.4.118), the frequency for $R_a$ to be maximum was reduced by 4%. These matching layers were therefore chosen to be a quarter-wave thick at 4% below the center frequency of the transducer. However, in the actual plates produced, the equivalent number for the epoxy layer was 5%. This 5% change in the thickness of the epoxy plate amounted to 12 μm, which illustrates the difficulty of fabricating these devices. A series inductor was used to tune the impedance to a real value at the center frequency, and an autotransformer was employed to obtain a value of 50 Ω.

The electrical impedance of the transducer was measured as a function of frequency; this is compared with the calculated values in Fig. 1.4.24(a). After electrical matching, the two-way insertion loss, when a signal is reflected from a perfect reflection as a function of frequency and impulse response, is compared to theory in Fig. 1.4.24(b) and (c). The measured tuned insertion loss was 3.5 dB at 2.3 MHz, and the 3-dB bandwidth was 79%, a considerably higher value than would be expected from the approximate value of $Q_a$, the acoustic $Q$. The impulse response was not as narrow as desirable, but as the calculation shows, we might have expected this from the rather square bandshape of this transducer design. We can attribute half the measured insertion loss of 3.5 dB to losses in the electrical components and diffraction of the acoustic beam from a piston radiator, as discussed in Chapter 3; the rest is due to loss in the ceramic material.

In practice it is difficult to design a transducer for optimum pulse response on the basis of a desired frequency response. As we saw in Fig. 1.4.24, the optimum frequency response is more like a Gaussian than a maximally flat response. Ideally, it is desirable to optimize the thickness and impedance of one or more matching layers, as well as the parameters of the electrical matching circuit, to obtain as short a pulse response as possible simultaneously with the maximum peak response.

Iterative techniques for such a design have been worked out by Chou et al. [13] and by Selfridge et al. [12]. The components to be used are specified and then adjusted iteratively in the theoretical design to optimize the length of the pulse response. A transducer made of high-quality Murata PZT ceramic, with $Q \approx 4000$, $\bar{V}_a = 4.72$ km/s, $k_T^2 = 0.24$, and impedance $39.6 \times 10^6$ kg/m$^2$-s, which uses one matching layer of epoxy to water and an epoxy backing of impedance $4 \times 10^6$ kg/m$^2$-s, has been designed by this technique. The matching circuit is shown in Fig. 1.4.25 [12]; its adjustable parameters are the matching layer thickness, the area of the transducer (or the input impedance), and the three tuning components $L_p$, $C_p$, and $L_s$. Figures 1.4.26 and 1.4.27 demonstrate the excellent agreement between theory and experiment, showing the smooth frequency response and the short pulse, respectively; the tuning circuit used values of $L_p = 5.7$ μH, $L_s = 4.1$ μH, $C_p = 332$ μF, and $R_s = 86\ \Omega$. As in the previous designs, there is a two-way loss in excess of theory, due to loss in the PZT, of approximately 2.5 dB. Note in Fig. 1.4.26 that the response in the frequency domain has approximately a Gaussian form. Interestingly, the optimum impedance and thickness of the matching layer were not those that we would arrive at by simple theoretical considerations; instead, they were $3.45 \times 10^6$ kg/m$^2$-s and $0.243\lambda$, respectively, at the center frequency. This impedance is far lower than the value we expect from a design for a maximally flat response (i.e., with $Z \sim 7 \times 10^6$ kg/m$^2$-s). The iterative technique provides a much-improved pulse response in comparison to the simpler concepts of quarter-wavelength matching discussed earlier.

## PROBLEM SET 1.4

1. A ceramic transducer made of PZT-5A, 1 cm square and 1 mm thick, is coated with a thin silver film on each side. The transducer is tested in air, and its impedance as a function of frequency is measured.
   (a) Work out the frequencies $f_0$ and $f_1$, for maximum and minimum impedance, respectively.
   (b) The transducer is now used to excite a longitudinal wave in an infinitely long aluminum bar by bonding it to the bar. Work out the impedance, including the series capacity at the resonant frequency $f_0$, and the efficiency of conversion of power from a generator with a 50-Ω impedance. Estimate the acoustic bandwidth of the transducer. Use the values of $c_{33}$, $k_T$, and $\varepsilon_{zz}^s$ given in Appendix B.
2. Suppose that the bar in Prob. 1 is not infinitely long but has a length of 2.5 mm. What would be the impedance looking into the transducer at a frequency $f_0$ under CW conditions? This impedance is purely reactive.
3. The transducer described in Prob. 1 is placed with its front surface in water.
   (a) Work out its impedance, including the series capacitance at the resonant frequency $f_0$, and the efficiency of conversion of power from a generator with a 50-Ω impedance.
   (b) Estimate the acoustic bandwidth and acoustic $Q$ of the transducer.
4. Consider a transducer terminated on its back surface by a perfect match $Z_1 = Z_C$. Suppose that the transducer is excited by a voltage pulse of the shape shown below, which increases in amplitude for a time $T_1$.

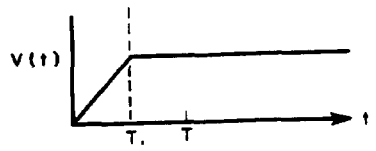


**(a)** Take the transit time through the transducer to be $T = l/V_a$ and $l$ to be the length of the transducer. Assume that the coupling coefficient $k_T^2 << 1$, so that the current $I$ passing through the transducer is $I \approx C_0 \partial V/\partial t$. By using the treatment of Sec. 1.4.7 for pulsed transducers, show that when $T_1 = T$, the transducer excites a triangular pulse of pressure or stress of base length $2T$, as shown below.

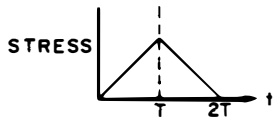


**(b)** Sketch the form of the output when $T_1 < T$.

**(c)** Sketch the form of the output when $T_1 > T$.

**5. (a)** Consider a receiving transducer terminated on its back surface by its own impedance. Suppose that the transducer is excited by an acoustic signal on its front surface ($z = -l/2$), whose velocity is $v_0 \exp(j\omega t)$. Find the output into an electrical load $R_L$. Assume that $k_T^2 << 1$. Thus the wave in the medium of the transducer is unaffected by the induced current in the electrical load.

**(b)** Now, with $R_L >> 1/\omega C_0$ for all frequency components of interest, use a Fourier or Laplace transform to derive the form of the output when the input signal is a very short velocity pulse of length $\tau << T$ (a $\delta$ function).

**(c)** What will the form of the output be with the same excitation when $R_L << 1/\omega C_0$?

**6.** Consider a transducer made of the plastic piezoelectric transducer material $PVF_2$ (polyvinylidene difluoride). This material is a plastic much like Teflon, and can be cut easily with a pair of scissors. It has a density of $1.78 \times 10^3$ kg/m$^3$, a longitudinal wave acoustic velocity of 2.2 km/s, and an acoustic impedance of $3.92 \times 10^6$ kg/m$^2$-s. Therefore, its impedance is far closer to the impedance of water ($1.5 \times 10^6$ kg/m$^2$-s) than to that of ceramics ($\sim 30 \times 10^6$ kg/m$^2$-s), so the impedance mismatch into water is not too severe. This transducer normally shows a very broadband characteristic, especially when used as a receiving transducer.

**(a)** Using the equivalent circuit or the expressions of Eq. (1.4.23), consider a $PVF_2$ transducer of length $l$ bonded to a brass backing material that you may regard as having infinite impedance (i.e., being perfectly rigid), which means that $v_1 = 0$ when the other side is terminated by a medium of impedance $Z_2$. Determine the input impedance of the transducer, and show that the motional impedance or acoustic impedance $Z_a$ is purely real when the material is a quarter-wavelength thick.

**(b)** Taking $Z_2 = 0$ (i.e., with the front surface looking into air), find an expression for the frequency $\omega_1$ where the electrical impedance of the transducer is zero. Following the derivation of Eq. (1.4.46), work out a lumped equivalent circuit like that of Fig. 1.4.9 for the rigidly backed transducer.

*Note.* The change in result for part (b) from Eq. (1.4.46) is minor. Basically, it requires changes by factors of 2.

7. For the brass-backed $PVF_2$ transducer described and illustrated in Prob. 6, work out the ratio $R = V_3/T_{F1}$, an important parameter when the device is used as a receiving transducer operating into a very high impedance circuit for which $I_3 = 0$. This result gives the voltage output due to a stress wave of stress $T_{F1}$ incident on the transducer. Find $R(\omega = 0)/R(\omega_0)$, where $\omega_0$ is the resonant frequency corresponding to the quarter-wavelength-long transducer. What is this ratio for a transducer operating in water?

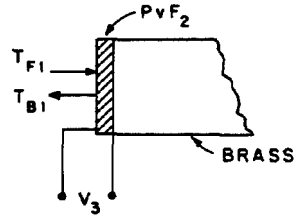


*Note.* In this situation, $|R|$ does not change very much with frequency, so the device is a broadband receiving transducer.

*Hint.* For this problem, consider the piezoelectric coupling to be small, so that the wave approaching the transducer has an amplitude $T_{F1}$. The reflection coefficient $\Gamma = T_{B1}/T_{F1}$ of this wave is dictated by the transducer length and the impedance of the piezoelectric material. Find the value of $v_1 = v_{F1} + v_{B1}$ at the $H_2O$–$PVF_2$ interface, and hence $V_3/T_{F1}$.

8. Consider a multiple transducer array terminated by an acoustic impedance $Z_C$ at each end, that is, the medium is infinite on each side and of the same impedance as the transducer medium, as illustrated below.

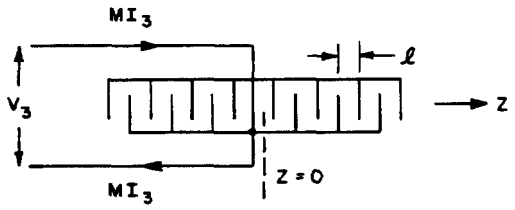


Suppose that each individual transducer is of length $l$. It has been shown that at $z > l/2$ ($z = 0$ at the center),

$$T_F(z) = -\frac{eI_3}{\varepsilon^S \omega A} e^{-j\bar{\beta}_a z} \sin \frac{\bar{\beta}_a l}{2}$$

**(a)** Now suppose that there are $M$ transducers stacked in a row, which are interdigitally connected so that the currents flowing into neighboring transducers are flowing in opposite directions, and that the total current flowing into this $M$-section transducer is $MI_3$. By using superposition (i.e., adding the contribution from each transducer in the correct phase when all transducers are excited by a current $I_3$ or $-I_3$), find the total stress at a plane $z$ where $z > Ml$. Add up the sum of the contributions

to $T(z)$ by using the relations

$$\sum_{0}^{M-1} e^{-jnx} = \frac{e^{-jMx} - 1}{e^{-jx} - 1}$$

$$= e^{-j(M-1)x/2} \frac{\sin (Mx/2)}{\sin (x/2)}$$

Determine the real power in the forward traveling wave excited at a plane $z$ outside the interdigital transducer by the total current $I$, by using the relation

$$P_F = A \text{ Re} \left( \frac{TT^*}{2Z_0} \right)$$

where $A$ is the area of the transducer.

Assuming, by symmetry, that the same amount of power is radiated in the backward direction from the left-hand side of the transducer, find the total power radiated by the transducer in terms of $I$. We may now determine the radiation resistance of this multiple element transducer as follows. If the current entering the transducer is $I$ and the voltage across it is $V$, the radiated power must be

$$P = \tfrac{1}{2} \text{ Re } (VI^*)$$

However, if $R_a$ is the radiation resistance and $jX_a$ is the reactance of the transducer,

$$P = \tfrac{1}{2} \text{ Re } (R_a + jX_a) II^*$$

$$= \tfrac{1}{2} R_a II^*$$

It follows that $R_a = 2P/II^*$. Using the expression for $P$ that you have already found, determine the radiation resistance of the transducer (the real part of its impedance). Show that $R_a$ is maximum when each transducer is a half-wavelength long.

You have now worked out a simple theory for the radiation resistance of an interdigital transducer, the type most often used for surface acoustic wave devices. Note that in most interdigital transducer theories (see Secs. 2.4, 2.5, and 4.2), the number of transducers is defined by the number of transducer pairs $N$. Here $M = 2N$; because $M$ can be an even or an odd integer, however, $N$ will not be an integer if $M$ is odd.

**(b)** From your result, consider an $M$-element transducer with $M$ large, so that you can write $\sin x \approx x$ but cannot approximate $\sin Mx$. Since for $y = \pi/2$, $(\sin y)/y$ corresponds to a 4-dB change from the maximum value of 1, find the bandwidth between 4-dB points of an $M$-element transducer.

**9.** Derive Eq. (1.4.23) from the KLM equivalent circuit.

**10.** **(a)** Derive the circuit of Fig. 1.4.11(a) directly from the Mason equivalent circuit of Fig. 1.4.4. You will need to write an expression for an admittance term $Y_a$ in the form of a series such as Eq. (1.4.42), keeping only one term corresponding to the lowest-order resonance.

**(b)** Assuming that $(Z_1 + Z_2) << Z_C$, derive the circuit of Fig. 1.4.11(b) from the Mason equivalent circuit of Fig. 1.4.4.

**11.** Derive the equivalent circuit of Fig. 1.4.20(a) using the methods described in the discussion of the schematic in Sec. 1.4.10 [see Eq. (1.4.95)].

**12.** Derive Eq. (1.4.118) from Eq. (1.4.117).

13. Use the equivalent circuit of Fig. 1.4.20(a) to prove Eq. (1.4.118). You will find it helpful to expand your expressions to first order in $\omega - \omega_0$.

## 1.5 TENSOR NOTATION AND CONSTITUTIVE RELATIONS FOR PIEZOELECTRIC AND NONPIEZOELECTRIC MATERIALS

### 1.5.1 Introduction

So far we have dealt mainly with one-dimensional forms for stress, strain, and the equation of motion in piezoelectric and nonpiezoelectric materials; we have also derived the theory of the thickness expander mode for a piezoelectric plate. The piezoelectric constitutive relations we have used throughout this chapter are particularly convenient when reduced to their one-dimensional forms [Eqs. (1.2.4) and (1.2.9)], because only one component of strain, the longitudinal component in the $z$ direction, is finite in a piezoelectric plate. For certain other situations, however, this form of the constitutive relations may be less convenient. Thus, in this section, we describe some alternative formulations [14, 15].

In all cases, whether referring to shear or longitudinal waves, we will describe wave interactions in a one-dimensional form. This is actually a correct and rigorous approach, provided that the propagation of the wave of interest is along an axis of symmetry of a crystal. However, to carry out quantitative calculations, we must state the equation of motion, Hooke's law, and the elastic and piezoelectric parameters of the crystal, and then reduce them to one-dimensional terms. *Tensor notation* will be introduced; to simplify the resulting equations, we also introduce *reduced subscript notation.* A detailed treatment of some of the notation used is given in Appendix A.

### 1.5.2 Mathematical Treatment

**Displacement and strain.** In general, the displacement is a vector **u** with three Cartesian components $u_x$, $u_y$, and $u_z$, each of which can be a function of the three Cartesian components $x$, $y$, and $z$ of the vector **r**. Thus, in general, **S** will be a tensor with nine components. For example,

$$S_{xx} = \frac{\partial u_x}{\partial x} \tag{1.5.1}$$

and

$$S_{xy} = \frac{1}{2}\left(\frac{\partial u_x}{\partial y} + \frac{\partial u_y}{\partial x}\right) \tag{1.5.2}$$

with $S_{xx}$, $S_{xy}$, $S_{yz}$, $S_{yx}$, $S_{yy}$, $S_{yz}$, $S_{zx}$, $S_{zy}$, and $S_{zz}$ defined similarly. For pure one-dimensional motion, however, we can represent **S** by only one component (e.g., $S_{xx}$ for one-dimensional longitudinal strain and $S_{xy}$ for one-dimensional shear strain). The symmetry of Eq. (1.5.2) shows that $S_{xy} = S_{yx}$.

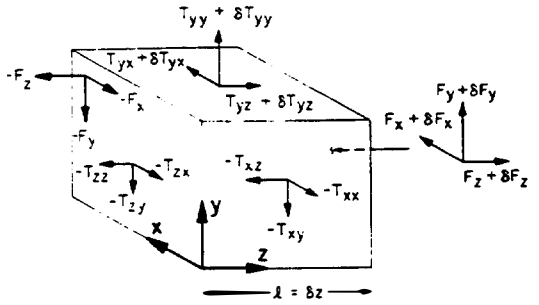


**Figure 1.5.1** Application of general stress components.

**Stress.** We now consider the stress on a cube of volume $\delta x\, \delta y\, \delta z$, illustrated in Fig. 1.5.1. The force applied to the left-hand surface $\delta x\, \delta y$ is called the traction **F**. The traction applied to this surface has three components: $-F_x$ and $-F_y$, both parallel to the surface, and $-F_z$, perpendicular to the surface. The traction applied to the opposite surface has components $F_x + \delta F_x$, $F_y + \delta F_y$, and $F_z + \delta F_z$. By carrying out a Taylor expansion to first order in $\delta z$, we see that this traction has components $F_x + (\partial F_x/\partial z)\, \delta z$, $F_y + (\partial F_y/\partial z)\, \delta z$, and $F_z + (\partial F_z/\partial z)\, \delta z$, where $\delta z$ is equivalent to the parameter $l$ used in the one-dimensional formulation of Sec. 1.1. We define the stresses on a surface perpendicular to the $z$ axis as follows:

$$\text{Shear stress:} \qquad T_{zx} = \frac{F_x}{\delta x\, \delta y} \tag{1.5.3}$$

$$\text{Shear stress:} \qquad T_{zy} = \frac{F_y}{\delta x\, \delta y} \tag{1.5.4}$$

$$\text{Longitudinal stress:} \qquad T_{zz} = \frac{F_z}{\delta x\, \delta y} \tag{1.5.5}$$

The first subscript of the tensor **T** denotes the coordinate axis normal to a given plane; the second subscript denotes the axis to which the traction is parallel. There are nine possible stress components:

$$\mathbf{T} = \begin{bmatrix} T_{xx} & T_{xy} & T_{xz} \\ T_{yx} & T_{yy} & T_{yz} \\ T_{zx} & T_{zy} & T_{zz} \end{bmatrix} \tag{1.5.6}$$

The terms $T_{xx}$, $T_{yy}$, and $T_{zz}$ are longitudinal stress components, while the terms $T_{xy} = T_{yx}$, $T_{xz} = T_{zx}$, and $T_{yz} = T_{yz}$ are shear stress components that are euqal in pairs, because internal stresses can give no net rotation of the body.

By analogy to our earlier simple derivation in Sec. 1.1, the force per unit volume in the $z$ direction is the net resultant of the forces per unit volume applied to an infinitesimal cube, that is,

$$f_z = \frac{\partial T_{zz}}{\partial z} + \frac{\partial T_{xz}}{\partial x} + \frac{\partial T_{yz}}{\partial y} \tag{1.5.7}$$

**Hooke's law and elasticity.** We write, for example, the relation between $T_{xx}$ and the applied strains $S_{xx}$ and $S_{yy}$ as

$$T_{xx} = c_{xxxx}S_{xx} + c_{xxyy}S_{yy} \tag{1.5.8}$$

and the relation between $T_{xz}$ and the applied strain $S_{xz}$ as

$$\begin{aligned} T_{xz} &= c_{xzxz}S_{xz} + c_{xzzx}S_{zx} \\ &= 2c_{xzxz}S_{xz} \end{aligned} \tag{1.5.9}$$

where $S_{xz} = S_{zx}$ and $c_{xzxz} = c_{xzzx}$, due to symmetry. In each case, the first two subscripts of the elastic tensor correspond to the subscripts for the stress tensor, and the last two subscripts correspond to those for the strain tensor.

It follows from Eq. (1.5.7) that the equation of motion in the $z$ direction is

$$\rho_{m0}\ddot{u}_z = \rho_{m0}\dot{v}_z = \frac{\partial T_{zz}}{\partial z} + \frac{\partial T_{xz}}{\partial x} + \frac{\partial T_{yz}}{\partial y} \tag{1.5.10}$$

with corresponding equations for the other components of $\ddot{\mathbf{u}}$ and $\dot{\mathbf{v}}$.

**Tensor notation.** A simpler notation, described more fully in Appendix A, can be used to denote the components of the vectors and tensors involved. We shall use the subscripts $i$, $j$, and $k$ to denote any one of the $x$, $y$, and $z$ axes. For example, $E_i$ is the $i$th component of the $E$ field. We write the electric displacement field in terms of the $E$ fields in the form

$$D_i = \varepsilon_{ij}E_j \tag{1.5.11}$$

More fully, this means that

$$D_i = \sum_j \varepsilon_{ij}E_j \tag{1.5.12}$$

or

$$\begin{aligned} D_x &= \sum_j \varepsilon_{xj}E_j = \varepsilon_{xx}E_x + \varepsilon_{xy}E_y + \varepsilon_{xz}E_z \\ D_y &= \sum_j \varepsilon_{yj}E_j = \varepsilon_{yx}E_x + \varepsilon_{yy}E_y + \varepsilon_{yz}E_z \\ D_z &= \sum_j \varepsilon_{zj}E_j = \varepsilon_{zx}E_x + \varepsilon_{zy}E_y + \varepsilon_{zz}E_z \end{aligned} \tag{1.5.13}$$

Here $j$ is a floating subscript over which summation is automatically implied, while the subscript $i$ denotes the required component of interest on the left-hand side of the equation.

As a further example, we write the electric field in terms of the scalar electric potential as follows:

$$E_i = \frac{-\partial\phi}{\partial x_i} \tag{1.5.14}$$

Here there is no floating subscript. Similarly, the tensors denoting stress and strain are $T_{ij}$ and $S_{ij}$, respectively. We write Hooke's law in the form

$$T_{ij} = c_{ijkl}S_{kl} \tag{1.5.15}$$

where $k$ and $l$ are floating subscripts indicating summation over $k$ and $l$, while $i$ and $j$ indicate the stress components required. Similarly, the equation of motion in tensor form is

$$\frac{\partial T_{ij}}{\partial x_j} = \rho_{m0}\ddot{u}_i \tag{1.5.16}$$

where $j$ is the floating subscript.

**Reduced subscript notation.** Because $T_{ij} = T_{ji}$ and $S_{ij} = S_{ji}$, there are actually only six independent tensor quantities. We can therefore simplify the notation even further. The subscripts $i$, $j$, and $k$ will be used to denote the tensor components of interest in what is called the *reduced form*. Hence $T_I$ is a component of the stress tensor, which replaces the longer unreduced notation $T_{ij}$, and $S_I$ is a component of the strain tensor, which replaces the longer unreduced notation $S_{ij}$.

Table 1.5.1 summarizes how this notation is used, taking the $E$ field vector, the strain tensor, and the stress tensor as examples. It also gives notation describing the stress and strain tensors in nonreduced form.

We can now write the full tensor form of the constitutive relations for a

**TABLE 1.5.1** TENSOR AND VECTOR COMPONENTS

| Stress or vector component | Example | Meaning |
|---|---|---|
| Electric field, $E_i$ | $E_x$ $(i = x)$ | $E$ field in $x$ direction |
| | $E_y$ $(i = y)$ | $E$ field in $y$ direction |
| | $E_z$ $(i = z)$ | $E$ field in $z$ direction |
| Strain, $S_I$ | $S_1$ $(I = 1) = S_{xx}$ | Longitudinal strain in $x$ direction |
| | $S_2$ $(I = 2) = S_{yy}$ | Longitudinal strain in $y$ direction |
| | $S_3$ $(I = 3) = S_{zz}$ | Longitudinal strain in $z$ direction |
| | $S_4$ $(I = 4) = 2S_{yz}$ | Shear strain, motion about $x$ axis; shear in $y$ and $z$ directions |
| | $S_5$ $(I = 5) = 2S_{zx}$ | Shear strain, motion about $y$ axis; shear in $x$ and $z$ directions |
| | $S_6$ $(I = 6) = 2S_{xy}$ | Shear strain, motion about $z$ axis; shear in $x$ and $y$ directions |
| Stress, $T_I$ | $T_1$ $(I = 1) = T_{xx}$ | Longitudinal stress in $x$ direction |
| | $T_2$ $(I = 2) = T_{yy}$ | Longitudinal stress in $y$ direction |
| | $T_3$ $(I = 3) = T_{zz}$ | Longitudinal stress in $z$ direction |
| | $T_4$ $(I = 4) = T_{yz}$ | Shear stress about $x$ axis |
| | $T_5$ $(I = 5) = T_{zx}$ | Shear stress about $y$ axis |
| | $T_6$ $(I = 6) = T_{xy}$ | Shear stress about $z$ axis |

**TABLE 1.5.2** EXAMPLES OF THE REDUCED TENSOR NOTATION

| Parameter | | |
|---|---|---|
| Reduced notation | Standard notation | Meaning |
| Elastic constant | | |
| $c_{IJ}$ | $c_{ijkl}$ | The ratio of the $I$th stress component to the $J$th strain component |
| $c_{11}$ | $c_{1111}$ | The longitudinal elastic constant relating longitudinal stress and strain components in the $x$ direction |
| $c_{44}$ | $c_{2323}$ | The shear elastic constant relating shear stress and strain components in the 4-direction (motion about $x$ axes) |
| $c_{12} = c_{21}$ | $c_{1122} = c_{2211}$ | $c_{IJ} = c_{JI}$ |
| Dielectric constant | | |
| | $\varepsilon_{ij}$ | The ratio of the $i$th component of displacement density to the $j$th component electric field |
| | $\varepsilon_{xx}$ | The dielectric constant relating $D_x$ and $E_x$ |
| | $\varepsilon_{xy}$ | *Note:* $\varepsilon_{ij}$ is generally finite; $\varepsilon_{ij} = \varepsilon_{ji} = 0$ if $i$, $j$, and $k$ are along symmetry axes of a crystal |
| Piezoelectric stress constant | | |
| $e_{Ij}$ | $e_{ikj}$ | The ratio of the $I$th stress component to the $j$th vector component of electric field |
| $e_{3z}$ | $e_{333}$ | The ratio of the longitudinal stress in the $z$ direction to the $E$ field in the $z$ direction |
| $e_{iJ}$ | $e_{ijk}$ | The ratio of the $i$ vector component of electric displacement density to the $J$th component of strain |
| $e_{Ij}$, $e_{Ji}$ | $e_{ijk} = e_{jki}$ | Note that $e_{Ij}$ is the transposed form of $e_{jI}$ |

piezoelectric material, which were given in one-dimensional form as Eqs. (1.2.4) and (1.2.9):

$$\begin{aligned} T_I &= c_{IJ}^E S_J - e_{Ij} E_j \\ D_i &= \varepsilon_{ij}^S E_j + e_{iJ} S_J \end{aligned} \tag{1.5.17}$$

To clarify the meaning of these expressions further, some more examples of the notation are given in Table 1.5.2.

When the material is not piezoelectric, we can write

$$T_I = c_{IJ} S_J \tag{1.5.18}$$

or, more fully,

$$\begin{bmatrix} T_1 \\ T_2 \\ T_3 \\ T_4 \\ T_5 \\ T_6 \end{bmatrix} = \begin{bmatrix} c_{11} & c_{12} & c_{13} & c_{14} & c_{15} & c_{16} \\ c_{21} & c_{22} & c_{23} & c_{24} & c_{25} & c_{26} \\ c_{31} & c_{32} & c_{33} & c_{34} & c_{35} & c_{36} \\ c_{41} & c_{42} & c_{43} & c_{44} & c_{45} & c_{46} \\ c_{51} & c_{52} & c_{53} & c_{54} & c_{55} & c_{56} \\ c_{61} & c_{62} & c_{63} & c_{64} & c_{65} & c_{66} \end{bmatrix} \begin{bmatrix} S_1 \\ S_2 \\ S_3 \\ S_4 \\ S_5 \\ S_6 \end{bmatrix} \tag{1.5.19}$$

Generally, there are 21 independent elastic constants ($c_{IJ} = c_{JI}$), but these reduce to far fewer independent terms in crystals with certain symmetries. In a cubic crystal, for instance, $c_{11} = c_{22} = c_{33}$, $c_{12} = c_{21} = c_{31} = c_{13} = c_{23} = c_{32}$, and $c_{14} = c_{15} = c_{16} = c_{24} = c_{25} = c_{26} = c_{34} = c_{35} = c_{36} = 0$. Thus there are only three independent constants: $c_{11}$, $c_{44}$, and $c_{12}$. If the material is isotropic, it can be shown that

$$c_{11} - c_{12} = 2c_{44} \tag{1.5.20}$$

With a piezoelectric material such as PZT, which is symmetrical about its $z$ axis, or isotropic in the $x$ and $y$ directions, we find that only $e_{z3}$, $e_{z1}$, $e_{z2}$, and $e_{x5} = e_{y4}$ are finite with $c_{44} = c_{55}$, $c_{11} = c_{22}$, $c_{11} - c_{12} = 2c_{66}$, and $\varepsilon_{xx} = \varepsilon_{yy}$. In this case, if we consider the longitudinal component of stress in the $z$ direction, in a large area plate in which there is no motion in the $x$ and $y$ directions, we see that $S_1 = S_2 = 0$.

It follows from Eq. (1.5.17) that†

$$\begin{aligned} T_3 &= c_{33}^E S_3 - e_{3z} E_z \\ D_z &= \varepsilon_{zz}^S E_z + e_{z3} S_3 \end{aligned} \tag{1.5.21}$$

Thus the values of $c$ and $e$ that we must use for longitudinal waves correspond to $c_{33}$ and $e_{3z}$, respectively.

In the same way, if we consider shear wave propagation along the $x$ axis of the material, we see that

$$\begin{aligned} T_5 &= c_{55}^E S_5 - e_{5x} E_x \\ D_x &= \varepsilon_{xx}^S E_x + e_{x5} S_5 \end{aligned} \tag{1.5.22}$$

because $E_x$ couples only to $T_5$.

Thus we can excite a shear wave in the 5-direction (motion about the $y$ axis or shear in the $x$ and $z$ directions) by using electrodes placed at $x = 0$ and $x = l$. This means that a piezoelectric transducer for shear waves can be constructed using a ceramic material "poled" in the $z$ direction. In this case, the appropriate elastic and piezoelectric stress constants in the one-dimensional theory are $c_{55}$ and $e_{x5}$, respectively.

Consider the expansion of a thin bar along its length, with the $E$ field in the same direction. As the bar is compressed in the $z$ direction, it will bulge in the $x$

†In the literature, the subscripts 1, 2, and 3 are often used instead of $x$, $y$, and $z$, respectively. For example, $\varepsilon_{zz}^S$ would be written as $\varepsilon_{33}^S$; $e_{z3}$ would be $e_{33}$ [16].

or $y$ direction; the restoring force in those directions is negligible. Thus we assume that $T_3$ is the only finite component of stress. In this case, it is more convenient to use constitutive relations stated with stress as the independent variable. These are written in the reduced subscript form as follows:

$$\begin{aligned} S_I &= d_{Ij}E_j + s^E_{IJ}T_J \\ D_i &= \varepsilon^T_{ij}E_j + d_{iJ}T_J \end{aligned} \tag{1.5.23}$$

Both $c^E_{IJ}$ and $s^E_{IJ}$ are reciprocal matrices; so are $c^D_{IJ}$ and $s^D_{IJ}$. The parameter $s$ is called the *compliance* and is often quoted in preference to $c$. The customary names and definitions of these parameters are given in Table 1 of a paper by Jaffe and Berlincourt [15].

Leaving out the subscripts, Eq. (1.5.23) reduces to a set of one-dimensional equations that are equivalent to Eqs. (1.4.4) and (1.4.9):

$$\begin{aligned} S &= dE + s^E T \\ D &= \varepsilon^T E + dT \end{aligned} \tag{1.5.24}$$

For a thin piezoelectric rod transducer of PZT poled in the $z$ direction, for example, this set of equations would be more convenient than Eqs. (1.4.4) and (1.4.9).

We define a piezoelectric coupling coefficient $k_{z3}$ as follows [16]:

$$k^2_{z3} = \frac{d^2_{z3}}{s^E_{33}\varepsilon^T_{zz}} \tag{1.5.25}$$

In general, $d_{iJ}$ is called the *transmitting constant* or *piezoelectric stress constant*. Often, in the literature, the parameter $k_{z3}$ in Eq. (1.5.25) is called $k_{33}$, the two nomenclatures being interchangeable (see the footnote on p. 80).

The acoustic velocity of a wave along a thin bar is normally lower than it is along a plate. When $E = 0$, for example, the acoustic velocity of an acoustic wave along a thin rod of PZT-5A is 2.62 km/s, while when $D = 0$, the stiffened velocity is increased by a factor of $(1 - k^2_{z3})^{1/2}$, to 3.71 km/s. Equivalently, we can write

$$s^D = s^E(1 - k^2_{z3}) \tag{1.5.26}$$

The $k_{z3}$ term defined here is used in the expressions for the impedance of a piezoelectric transducer [see, e.g., Eq. (1.4.23)], just as the parameter $k_T$ is used for a piezoelectric plate in Sec. 1.4.

Let us consider some other useful forms of the constitutive relations. When the transducer is used as a transmitter, we can obtain a good idea of its characteristics by using the constitutive relations given above. Alternatively, if it is used as a receiving transducer operating into a very high impedance (a common situation in low-frequency devices), we can assume that $D = 0$ (i.e., that the load impedance is much higher than the capacitive reactance of the transducer).

When the acoustic load at one surface of the transducer is specified and the impedance of the acoustic source is known, we can find the stress and strain component within the transducer in terms of the driving velocity or strain. However, it is often easier to specify the input stress to a receiving transducer. When

a severe mismatch exists, as it would using a piezoelectric receiving transducer in water, the stress or pressure at the transducer's surface may be a known or measurable quantity, for the transducer will tend to be rigid relative to the water, and the velocity at its surface will not be easily measurable or calculable. Thus, for low-frequency work, it is often convenient to write the constitutive relations with the known quantities as the dependent variables in the reduced subscript notation, that is,

$$\begin{aligned} E_i &= \beta_{ij}^T D_j - g_{iJ} T_J \\ S_I &= g_{Ij} D_j + s_{IJ}^D T_J \end{aligned} \tag{1.5.27}$$

If the current is small, as it would be with a high-impedance receiver, then $D = 0$, and the one-dimensional longitudinal wave equations for a plate transducer become

$$\begin{aligned} E &= gT \\ S &= s^D T \end{aligned} \tag{1.5.28}$$

The parameter $g$ is often called the *receiver constant* and is the only one required to determine the voltage output of the transducer with a given applied stress. By comparison with Eq. (1.5.24), we see that

$$g = \frac{d}{\varepsilon^T} \tag{1.5.29}$$

The constitutive relations can be written in yet another convenient form:

$$\begin{aligned} E_i &= \beta_{ij}^S D_j - h_{iJ} S_J \\ T_i &= -h_{Ij} D_j + c_{IJ}^D S_J \end{aligned} \tag{1.5.30}$$

In this case, the one-dimensional relations become

$$\begin{aligned} E &= -hS + \beta^S D \\ T &= c^D S - hD \end{aligned} \tag{1.5.31}$$

The parameter $h$ is called the *transmitting constant*; it determines the voltage required across the transducer to produce a given strain. We see from Eqs. (1.4.7), (1.4.8), and (1.5.31) that

$$h = \frac{e}{\varepsilon^S} \tag{1.5.32}$$

as we have shown in Sec. 1.4.2. Similarly, comparing the one-dimensional forms, we see that

$$\beta^S = \frac{1}{\varepsilon^S} \tag{1.5.33}$$

In practice, any one of these constitutive relations can be used; the choice entirely

a matter of convenience and custom. When one complete set of parameters is given, the others can be determined in terms of them, but to do so may require considerable algebraic manipulations.

## PROBLEM SET 1.5

1. **(a)** We have worked out the equivalent circuit of the in-line transducer by using the fact that $D$ is uniform in $x$, $y$, and $z$, while $E$ varies with $z$. Another important case is the *crossed-field transducer*, also known as the *length expander bar*, in which a thin strip of ceramic is coated with electrodes, with the crystal axes chosen so that when a potential is applied between the electrodes, the piezoelectric material expands parallel to them. This transducer is used to excite longitudinal or shear waves in hollow cylinders or thin strips. Analyze it, taking the $D$ and $E$ fields to be in the $z$ direction (i.e., perpendicular to the electrodes) and $v = u_x$ and $T = T_1$ to be in the $x$ direction. In this case, we assume that $T_3 = 0$ and $S_2 = 0$.

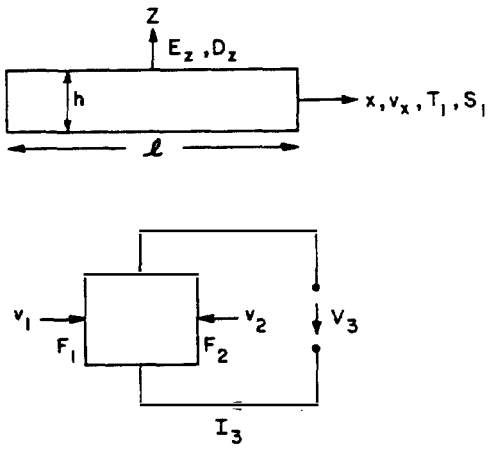


We assume that $T_1$, like $S_1$, varies with $x$, but not with $y$ or $z$. The length of the transducer is $l$, and the electrode spacing is $h$.

*Hint:* You will find it convenient to work in terms of $E$ rather than $D$. Take $E_x = 0$ so that as $\nabla \times \mathbf{E} = 0$, $\partial E_z/\partial x = 0$ (i.e., $E_z$ and $\phi$ are independent of $x$). Now, however, $D_z$ will vary with $x$.

**(b)** Show that the Mason equivalent circuit of the transducer is just like that of the in-line transducer illustrated in Fig. 1.4.4, except that it lacks a negative capacity. Using the three-port concept, state what coefficients with what subscripts are required to specify the parameters of the transducer when it is a ceramic material such as PZT-5H poled in the $z$ direction.

2. Work out the KLM equivalent circuit for the crossed-field transducer described in Prob. 1.

## REFERENCES


1. B. A. Auld, *Acoustic Fields and Waves in Solids*, Vol. 1. New York: John Wiley & Sons, Inc., 1973.
2. S. Ramo, J. R. Whinnery, and T. Van Duzer, *Fields and Waves in Communication Electronics*. New York: John Wiley & Sons, Inc., 1965.
3. R. E. Collin, "Theory and Design of Wide-Band Multisection Quarter-Wave Transformers," *Proc. IRE*, 43, No. 2 (Feb. 1955), 179–85.
4. H. J. Riblet, "General Synthesis of Quarter-Wave Impedance Transformers," *IRE Trans. Microwave Theory Tech.*, MTT-5, No. 1 (Jan. 1957), 36–43.
5. J. L. Altman, *Microwave Circuits*. Princeton, N.J.: D. Van Nostrand Company, 1964.
6. J. A. Stratton, *Electromagnetic Theory*. New York: McGraw-Hill Book Company, 1941.
7. M. Redwood, "Transient Performance of a Piezoelectric Transducer," *J. Acoust. Soc. Am.*, 33, No. 4 (Apr. 1961), 527–36.
8. M. Onoe, H. F. Tiersten, and A. H. Meitzler, "Shift in the Location of Resonant Frequencies Caused by Large Electromechanical Coupling in Thickness-Mode Resonators," *J. Acoust. Soc. Am.*, 35, No. 1 (Jan. 1963), 36–42.
9. R. Krimholtz, D. A. Leedom, and G. L. Matthaei, "New Equivalent Circuits for Elementary Piezoelectric Transducers," *Electron. Lett.*, 6, No. 13 (June 25, 1970), 398-99.
10. C. S. DeSilets, J. D. Fraser, and G. S. Kino, "The Design of Efficient Broad-Band Piezoelectric Transducers," *IEEE Trans. Sonics Ultrason.*, SU-25, No. 3 (May 1978), 115–25.
11. T. M. Reeder and D. K. Winslow, "Characteristics of Microwave Acoustic Transducers for Volume Wave Excitation," *IEEE Trans. Microwave Theory Tech.*, MTT-17, No. 11 (Nov. 1969), 927–41.
12. A. R. Selfridge, R. Baer, B. T. Khuri-Yakub, and G. S. Kino, "Computer-Optimized Design of Quarter-Wave Acoustic Matching and Electrical Matching Networks for Acoustic Transducers," *1981 Ultrason. Symp. Proc.*, (IEEE), 81-CH1689-9, Vol. 2, 644–48.
13. C. H. Chou, J. E. Bowers, A. R. Selfridge, B. T. Khuri-Yakub, and G. S. Kino, "The Design of Broadband and Efficient Acoustic Wave Transducers," *1980 Ultrason. Symp. Proc.*, (IEEE), 80CH1602-2, Vol. 2, 984–88.
14. J. F. Nye, *Physical Properties of Crystals: Their Representation by Tensors and Matrices*, corr. rpt. of 1st ed. (1957: rpt. Oxford: Clarendon Press, 1960).
15. H. Jaffe and D. A. Berlincourt, "Piezoelectric Transducer Materials," *Proc. IEEE*, 53, No. 10 (Oct. 1965), 1372–86.
16. "IRE Standards on Piezoelectric Crystals: Measurements of Piezoelectric Ceramics, 1961," *Proc. IRE*, 49, No. 7 (July 1961), 1161–69.